Fundamentals and Utilization of Solid/ Liquid Phase Boundary Interactions on functional surfaces

László Mérai[1], Ágota Deák[1], Imre Dékány[1,*], László Janovák[1,*]

[1]Department of Physical Chemistry and Materials Science, University of Szeged, H-6720, Rerrich Béla tér 1, Szeged, Hungary

[*] Corresponding authors. Tel.: +36 62 544 210; Fax: +36 62 544 042.

E-mail address: i.dekany@chem.u-szeged.hu (I. Dékány)

E-mail address: janovakl@chem.u-szeged.hu (L. Janovák)

Abstract

The affinity of macroscopic solid surfaces or dispersed nano- and bioparticles towards liquids plays a key role in many areas from fluid transport to interactions of the cells with phase boundaries. Forces between solid interfaces in water become especially important when the surface texture or particles are in the colloidal size range. Although, solid-liquid interactions are still prioritized subjects of materials science and therefore are extensively studied, the related literature still lacks in conclusive approaches, which involve as much information on fundamental aspects as on recent experimental findings related to influencing the wetting and other wetting-related properties and applications of different surfaces.

The aim of this review is to fill this gap by shedding light on the mechanism-of-action and design principles of different, state-of-the-art functional macroscopic surfaces, ranging from self-cleaning, photoreactive or antimicrobial coatings to emulsion separation membranes, as these surfaces are gaining distinguished attention during the ongoing global environmental and epidemic crises.

As there are increasing numbers of examples for stimulus-responsive surfaces and their interactions with liquids in the literature, as well, this overview also covers different external stimulus-responsive systems, regarding their mechanistic principles and application possibilities.

Keywords: *wetting, stimulus-responsive, liquid manipulation, oil-water separation, antimicrobial*

Contents of paper

1. Introduction

It cannot be questioned, that the interactions of solids and liquids are ubiquitous and fundamental to the actual shape of our world, and all living organisms in it, even including us, humans. Basically, the interactions of different organic molecules and the abundant water made all known forms of life possible.

In biological systems, the most abundant water acts as a medium and a metabolite, which practically determines which functions the different organic molecules could take, based on their interactions towards water [1]. For example, the 3D-structure and overall function of proteins is influenced by the interactions among the amino-acid sidechains and the polar, aqueous medium [2], while certain amphiphilic or hydrophobic molecules (e.g. phospholipids, lipids) are inherently suitable for forming a self-assembled water-repellent barrier to contain all necessary life functions in a living cell and to provide its integrity [3,4].

While these molecular interactions determine how life works on a sub-microscopic scale, they also affect macroscopic and microscopic properties, enough to think about how the capillary phenomena promotes water and nutrient transport in plants or blood circulation in animals [5].

In the case of designing synthetic materials, which are intended to interact with liquids (even in the presence of biomolecules), the same interactions should be taken into consideration to achieve a desired functionality.

The wetting of solid surfaces by liquids is a well-developed and formulated area of interfacial science and of high importance [6-10]. Despite the solid theoretical background of this field, some functional applications are still limited, while others are being discovered (or rediscovered) for emerging problems, such as environmental remediation [11,12], power saving [13] or healthcare issues [14,15].

As today's literature is rich in functional surfaces, such as antimicrobial- or self-cleaning coatings, it is becoming more and more vital to understand their mechanism-in-action and application possibilities to create more advanced solutions and to improve existing ones.

In the light of this, in the beginning of this review, a generalizing approach is used to present the main influencing factors on the wetting of solid surfaces, that is followed by the introduction of different functional surfaces and how wetting properties affect their performance in scenarios, like coating, decontamination, oil-water separation, and even interactions with bio(macro)molecules and living cells. As the most important and abundant liquid in our environment is water, – non-surprisingly – most literature examples are tailored

around influencing the water-wettability of surfaces, therefore these approaches are prioritized in this review, as well.

2. Factors influencing the wetting of solid surfaces

2.1. General quantification of wettability

The affinity of macroscopic solid surfaces towards liquids is practically quantified by the contact angle (Θ) [7], which is the angle between the macroscopic plain of the solid surface and the tangential of the contour line of the liquid drop, drawn towards the three-phase (solid, liquid and gas/vapour) connection point. As **Fig. 1 a)** shows, the affinities towards liquids can be categorized according to contact angle values. The Θ value can range from 0 to 180°, which means in case Θ-s, smaller than the intermediate 90°, the surface is considered well wetted by the liquid (*lyophilic*, e.g., hydrophilic), while over 90°, the surface is non-well-wetted (*lyophobic*, e.g., hydrophobic). In the case of extreme spreading of the liquid ($\Theta < 10°$), the surface is called *superlyophilic* (e.g., superhydrophilic), while in the case of extremely low spreading ($\Theta > 150°$), the surface is *superlyophobic* (e.g., superhydrophobic).

The value of Θ is dependent on the magnitude of free energies (or interfacial tensions) at the interface of the connecting phases. This relation in the case of a plain solid surface, energetically homogenous, non-reactive phases and mechanical equilibrium (static system) is described by Young's equation, which is represented by **Fig. 1 b**): $\gamma_{SG} - \gamma_{SL} - \gamma_{LG} = \cos\Theta$ (**Eq. 1**) While the interfacial tension between the solid- and gas-phases (or surface free energy, γ_{SG}) contributes to the spreading of the liquid drop and the increase of S/L-contact area, it is counteracted by the S/L-interfacial tension (γ_{SL}). The (static equilibrium) Θ value is defined by their relation towards L/G-interfacial tension (γ_{LG}). The static Θ is usually measured via the conventional sessile-drop technique [16-18].

However, usually in a non-equilibrium state, so Θ can take different values in a range between characteristic upper- and lower limits (depending on the drop deposition circumstances and the evaporation) at a certain temperature, which limits respectively are the advancing- (Θ_A) and receding contact angle values (Θ_R) (**Fig. 1 c**)) . These are the so-called dynamic contact angles and can be studied upon the movement of liquids at S/L-interfaces [19-21]. Θ_A is mainly correlated to the strength of cohesion within the liquid phase, while Θ_R is associated with the strength of S/L-adhesion. Their difference (Θ_R-Θ_A) is noted as contact angle hysteresis, which can also be an indicator of surface wettability [22]. A common determination technique is the Wilhelmy-method [23], while dynamic contact angles can also be determined e.g., via carefully

increasing or decreasing the droplet volume in a conventional sessile drop experimental setup [16].

Another common quantification value of wetting is the sliding angle (s.a.) [24], which is the angle for a macroscopically plain surface to be tilted at to make the contacting liquid moving downwards by its own weight (**Fig. 1 c**)). In the case of superlyophobic surfaces, this angle is usually denoted as roll-off angle (r.o.a.), as the liquid does not spread on the surface upon contact [25]. The more wettable surfaces have higher sliding angles, meaning it requires more contribution from gravitational force (F_g is proportional to sin s.a.) to counteract the force of S/L-adhesion. During rolling, the Θ_A can be observed at the front end of the moving drop, while Θ_R at the rear end, therefore the determination of dynamic contact angles is also possible by capturing images of sliding droplets [26] (**Fig. 1 c**)).

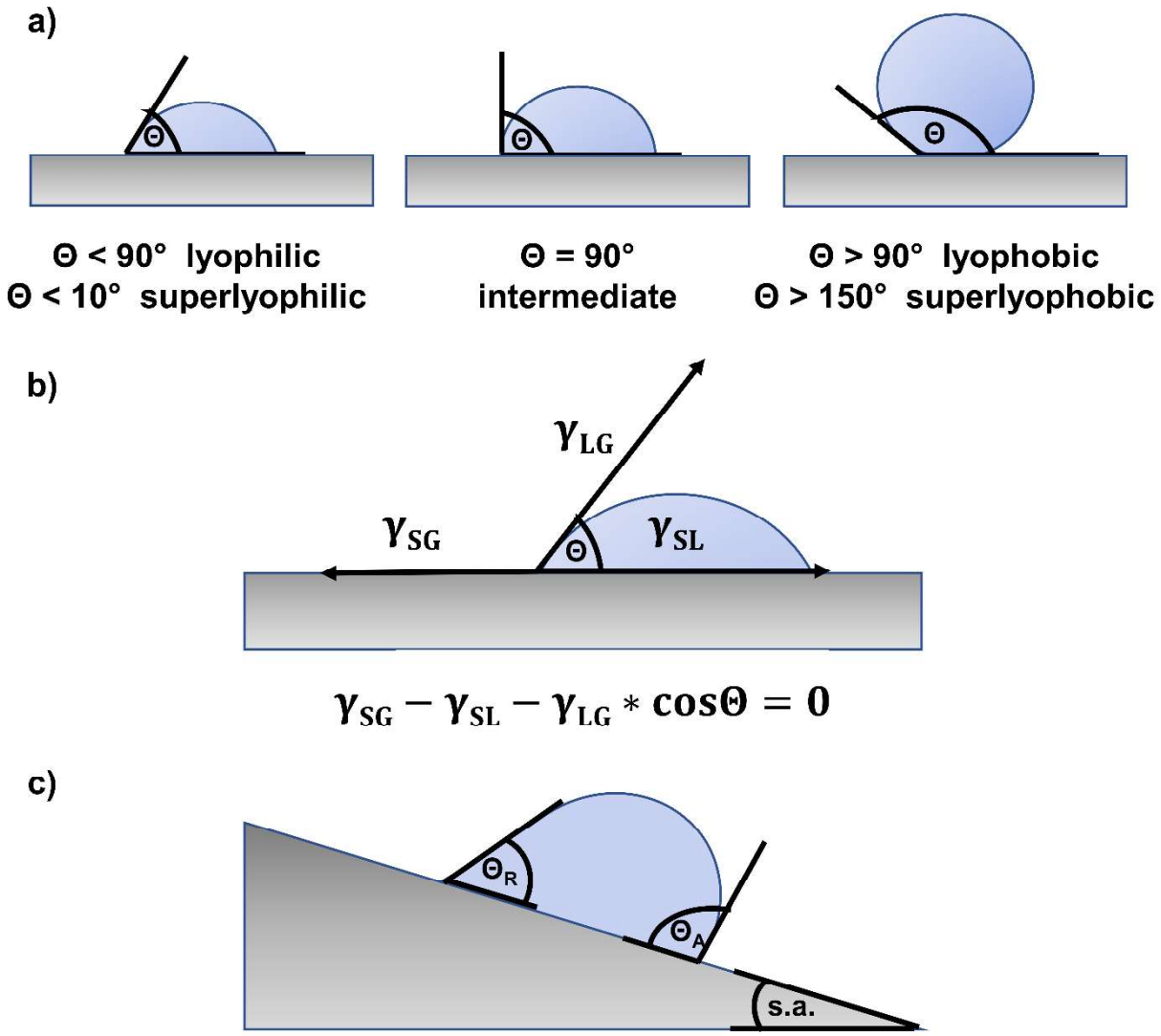

Figure 1. Different wetting characteristics of smooth solid surfaces, categorized according to contact angle values **a)** visual representation of the Young-equation **b)** and representation of the sliding angle **c)**

The wetting of solids is generally described by the above parameters, which can be traced back to three main factors (or group of factors): the surface texture (rough, smooth etc. surfaces) [27], the surface chemistry (starting materials, functional groups at the S/L-interface) [28] and external stimuli (such as light, temperature, magnetic field etc.) [29]. Besides wetting characteristics, the first two factors influence other physical- and chemical properties, such as responsivity to external stimuli, or antimicrobial- and photocatalytic effect, as well: these together can define the overall surface functionality in S/L-systems.

2.2. The role of surface texture

2.2.1. Classification of surface texture

The application of the previously presented (**Fig. 1 b)**) formalism of contact angle determination is limited by the assumption that the wetted solid surface is perfectly flat, which rarely occurs in real-life scenarios. The macroscopic- (curvature) and microscopic- or submicroscopic texture (roughness) can influence the wetting properties: while in the case of macroscopic inhomogenities, the magnitude of L/S-contact area influences the overall force of adhesion between solid and liquid, in the case of (sub)microscopic irregularities, the wetting is also driven by capillary action [28]. The distortions from Young's equation in the wetting of rough surfaces is usually explained by two main wetting models: in the case of Wenzel-type surfaces [30], the liquid fills the available space between surface protrusions, leading to increased contact area and adhesion, while in the case of Cassie-Baxter-type surfaces [31], the surface irragularities are not penetrated by the liquid. As a third wetting state, the so-called impregnating Cassie-state is usually acknowledged: these surfaces behave similarly to Cassie-Baxter surfaces (similar c.a. and s.a. values) towards droplets, although, the liquid fills surface texture, as well [32]. However, in practical scenarios, these models are mostly inaccurate due to the possible multiscale roughness (e.g. hierarchical micro- and nanoroughness) or irregularities, therefore these initial modes of wetting were put into question and were enhanced over the years [33], besides new concepts of liquid-phobicity were created [32] (**Fig. 2**).

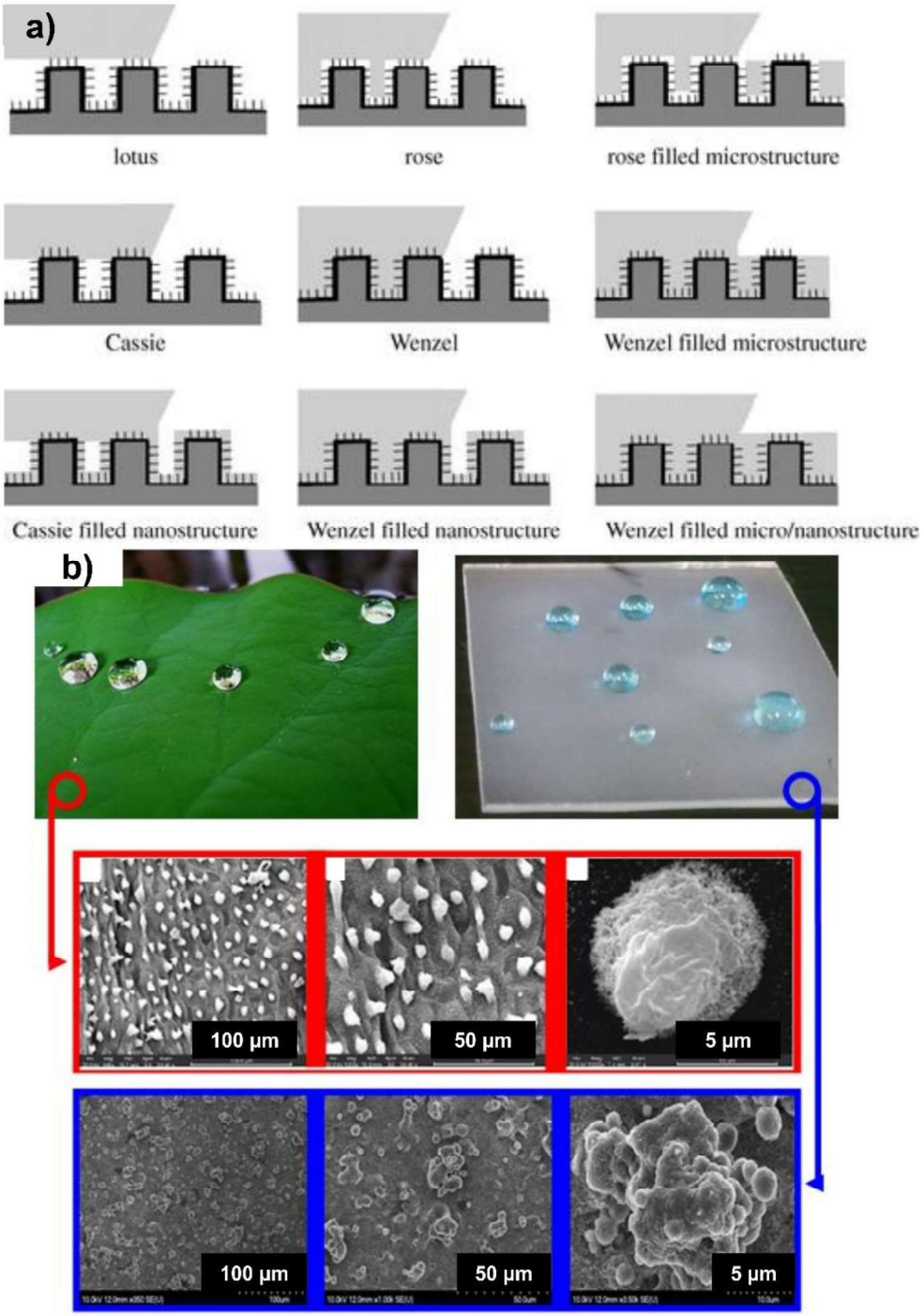

Figure 2. Schematic representation of nine wetting scenarios for a surface with hierarchical roughness [32] **a)** Photographs and SEM images of a natural (lotus leaf) and a biomimetic artificial superhydrophobic surfaces [34] **b)**

A common example is the rose petal – lotus leaf comparison [32]. Both are inherently hydrophobic and have hierarchical roughness, however, the water can penetrate the microgrooves between surface protrusions of rose petals, leading to higher contact area,

adhesion, and s.a. values, while the rough texture of lotus leaf is impenetrable to water (Cassie-state), which results in lower contact area (0.6% of the solid surface), adhesion and s.a. values. Transitions between the modes of liquid-phobicity are also possible [35], as in the case of certain surfaces, the liquid partially penetrates surface protrusions, indicating e.g., the so-called metastable Cassie-characteristics [36]. Beside rose petal and Cassie significant wetting state Depending on the position of the three-phase contact line (or TPCL) other rose petal-like intermediate wetting-regimes also exist in cases when the liquid phase can only enter one scale (micro- or nano-) of the surface texture [37] (**Fig. 2**).

However, it is important to note, that at S/L/Air systems practically water is the only liquid to show such behaviour, thanks to its relatively high surface tension (72 mN/m at 25 °C), while in the case of S/L/L-interfaces, other liquids (e.g. oil droplets on an underwater oleophobic surface, under water [37,38]) can display similar characteristics, as well.

Despite Wenzel- and Cassie-Baxter models are becoming outdated, they still referred to present the fundamental aspects of wetting. The depiction of the two models can be seen in **Fig. 2**. As in these cases, the macroscopically observable cantact angle is non-identical to the Young-contact angle (Θ), it is usually denoted as apparent contact angle (Θ_{app}). While the Wenzel-model ($\Theta_{app} = r \times \cos\Theta$ (**Eq. 2**)) only adds a roughness-factor (r) to the Young-equation, the Cassie-Baxter model ($\Theta_{app} = r \times f \times \cos\Theta + f - 1$ (**Eq. 3**)) introduces the fraction of wetted solid surface area (f). It is important to note, that at full fractional wetting (f=1), this equation transforms into the Wenzel-equation (**Eq. 2**).

The r roughness factor can be determined via measuring contact angles on smooth and roughened surfaces of the same solid or in case it is not possible, by laser scanning confocal microscopy [39] or by profilometric methods [40]. The first protocol also allows the determination of the roughness-dependent wetting characteristics, via the the Wenzel-Cassie-Baxter phase diagram diagram [41,42], in which the cosine values of Θ and Θ_{app} are compared. In conclusion, upon creating rough surfaces with extreme liquid-repellent character, the Cassie-type behaviour is preferred as it provides the lowest possible adhesion and contact angle hysteresis [32].

2.2.2. Utilization and elaboration of surface texture

As in the example of lotus leaf and rose petal from the previous chapter, the first attempts to understand the role of surface roughness began with studying the superhydrophobic surfaces (Θ>150°) in nature, which became available after the appearance of electron microscopy [43,44]. Researchers found out, that the extreme wetting behaviour is the result of dual-scale

micro- and nanoroughness. In the case of lotus leaf, the microstructures are protrusions of the plant epidermis, while the nanostructures are vax crystals, excreted by the leaf. While rose petals also have similar surface texture, the spatial arrangement and shape of its protrusions allows the penetration of water into the microstructure.

The function of superhydrophobicity in nature is to provide self-cleaning character: as the water droplets roll off the surface, they also wash away contaminants. Non-surprisingly, this phenomenon inspired various manmade solutions to enhance surfaces with self-cleaning property [45,46].

As it was mentioned before, roughness also increases surface area. On the other hand, the actual S/L contact area and therefore the adhesion is highly influenced by the surface structure and the ability of the liquid to penetrate it. As a result of this, surface roughness can amplify the initial wetting character of a surface towards a liquid, however, it can also increase adhesion as it is shown by the natural example of the gecko skin [47,48].

The desired surface roughness can be elaborated via both additive- (bottom-up) and destructive (top-down) techniques. The available bottom-up techniques include spray-coating [49], spin-coating [50], solvent-precipitation [51], film-casting [52], chemical vapor deposition [53], physical deposition [54], electrochemical deposition [55], hydrothermal [56], or templating methods [57], in-situ polymerization [58], or even 3D-printing [59] while top-down approaches utilize chemical- [60] and laser-/plasma-etching [61,62]. Despite top-down techniques in general offer better controllability over surface roughness with higher reproducibility, bottom-up approaches are still more popular as they are cheaper, easier to apply, and offer higher scalability. Although, the advanced examples of rough surfaces for wetting-related functional applications are composites (consisting of a matrix-/support- and one or more roughening filler materials) [63,64], monolithic systems also can be prepared by top-down techniques [65], filtrate deposition [51], foam-sintering [66] or templating methods [67].

The main weak point of a roughened surface is the vulnerability of the texture to mechanical damage. This can be overcome by the right choice of durable raw materials (e.g., metals [65], brittle inorganics [68]) or by utilizing self-healing behaviour to regain the damaged roughness [69-72].

The self-healing character can be achieved via incorporating a „repairing agent” in the matrix material, which could be e.g. a reactive monomer, that renews the surface polymer layer upon damage [73] or by other external stimuli, such as temperature [74].

Another crucial disadvantage of rough hydrophobic surfaces is their capability to droplet pinning as a result of mechanical damage or faulty preparation [75]. The pinned droplets can

then act as condensation seeds, which limits the overall applicability in such scenarios as anti-fouling, anti-corrosion or anti-icing. To overcome this hindrance, one may choose to prepare so-called slippery liquid-infused porous surfaces (or SLIPS), which contain a lubricating liquid in their surface structure [75]. This lubricant have to be chemically inert and be immiscible with the test liquid, while it spreads on the solids and wets it with higher affinity than the test liquid. To achieve this, for example, pairing silicones with silicone oils are preferred, which both show phobic character towards water [76]. Besides SLIPS in general may provide increased anti-icing [77,78], anti-corrosion [78] or anti-fouling performances [76], the slippery liquid reduces drag and friction [79], provide self-healing ability [80], low contact angle hysteresis [81] and can contribute to the uniform evaporation of test liquids [82].

2.3. The role of surface chemistry

2.3.1. Physicochemical interactions

As it was discussed before, surface roughness can amplify the inherent -phobic or -philic interactions towards liquids, however, the origin of these interactions lies within the chemical composition of a surface, and the liquid, as well.

According to the Young equation (**Fig. 1 b), Eq. 1**), the wettability of a solid surface by a liquid depends on the relation of interfacial tensions, which are influenced by the overall chemical and physical interactions at the surface. These interactions are mostly governed by the hydrogen-bonding and the van der Waals forces, which are the following, in the order of increasing magnitude: London-type dispersive interaction, induced dipole-dipole interaction, dipole-dipole interaction and charge-dipole interaction. In the case of a given liquid, the dominant interaction is determined by the surface functionalities. In general, the apolar surface groups (in the absence of considerable dipole moment or dipole moment-inducing capability) contribute to the dominance of the two weaker interactions, leading to lower surface free energy (γ_{SG}) and higher contact angles, while in the case of polar surfaces the stronger hydrogen bonding, dipole-dipole or dipole-induced dipole interactions can dominate, leading to higher surface free energy and lower contact angles [83].

On the other hand, the γ_{LG} value of a liquid depends mostly on the same interactions in the bulk phase, as well [84]. For instance, water has γ_{LG} of 72 mN/m at 25 °C due to the stronger dipole-dipole interactions and hydrogen bonds between water molecules, while apolar organic liquids, such as diethyl ether has lower surface tension (20.1 mN/m at 25 °C). An extreme example is mercury, having an exceptionally high γ_{LG} of 485.5 mN/m at 25 °C due to the strong

metallic bonds in the bulk liquid, which results in the well-known non-wetting characteristics of the liquid metal. In the case of ionic liquids [85] and magnetic fluids [86], electromagnetic interactions can also affect spreading on different surfaces. To reduce γ_{LG} and γ_{SL} values of liquids and therefore to increase wettability, one can apply surfactant materials [87], which provide increased spreading.

The mentioned decrease of γ_{SL} values is achieved through surfactant adsorption on solids, which is influenced by surface chemistry [88]. As charged surfaces tend to adsorb species with the opposite charge, and they are difficult to remove due to electrostatic interactions, surfactants are commonly used to neutralize surface charge and promote hydrophobic- & oleophilic character [89]. However, in the case of multilayer adsorption the surface becomes charged again [90]. On the contrary, neutral surfaces tend to become charged because of the adsorption of ionic surfactants from aqueous phase (weaker physisorption) [91]. In this instance, multilayer adsorption is not preferred as the charged functional groups repel each other. Besides surfactants, the γ_{SL} values are tunable through the adsorption of many other chemical species, including polymers, biopolymers, or ions [92].

The presence of reactive surface functionalities also influences wettability. Oxygene-deficient materials, such as UV-treated TiO_2 may promote the dissociative chemisorption of water, leading to superhydrophilic behaviour [93].

2.3.2. Approaches towards surface free energy

In the case of liquids, the γ_{LG} values are easy to obtain directly via tensiometric methods, however, the interfacial energies at the boundaries of solid surfaces are more implicit quantities. The several existing determination methods of γ_{SG} values are based on contact angle or adhesion force measurements [94]. As the surface free energy can get contribution from many interaction types, there is no universally applicable approach: the existing models utilize different parameters to suit different needs. For example, the Zisman method [95] is simple and quick, while the surface free energy term in its equation is single component and can only deal with dispersive interactions, therefore the successful application is practically restricted to hydrophobic (low surface energy) polymer surfaces and provides a so-called critical surface tension value that is similar but not equal to the actual γ_{SG}. On the contrary, there are two-component methods to deal with polar (or non-dispersive) interactions beside dispersive forces, such as the Owens-Wendt-Rabel & Kaelble [96], or Wu methods [97], but these usually require more contact angle measurements.

The main drawback of the widespread models is their inability to deal with surface roughness and its effect on wettability. To overcome this limitation, e.g. the model of E. Chibowsky can be applied, which is based on contact angle hysteresis [98], according to the following equation: $\gamma_s^{tot} = \gamma_l \times (1 + \cos\Theta_{adv})^2 / (2 + \cos\Theta_{rec} + \cos\Theta_{adv})$ (**Eq. 4**), where the total surface free energy of a solid (γ_s^{tot}) can be determined knowing the respective advancing- (Θ_{adv}) and receding contact angles (Θ_{rec}) of a probe liquid with known surface tension (γ_l). The most popular determination methods of surface free energy are displayed in **Table 1.**

Model	Information	Minimum no. of liquids	Application	Related references
Zisman	Critical surface tension	2	Non-polar solids	[95,99]
Fowkes	Disperse parts of surface free energy	2	Non-polar systems	[100,101]
Extended Fowkes (Owens-Wendt)	Disperse, polar and hydrogen parts of surface free energy	3	Specific questions of surface properties	[102-104]
OWRK	Disperse and polar parts	2	universal	[96,102,105,106]
Wu1 (harmonic mean)	Disperse and polar parts of surface free energy	2 (at least 1 polar liquid)	low energy systems	[79,97]
Wu2 (geometric harmonic mean)	Disperse and polar parts of surface free energy	2 (at least 1 polar liquid)	high energy systems	[107]
Acid-Base Theory (Good-van Oss-Chaudhury)	Disperse, acid and base parts of surface free energy	3	Specific questions of surface properties	[108,109]
Schultz	Disperse and polar parts of surface free energy	2 (at least 1 polar liquid)	High or low energy systems	[110,111]
Good and Girifalco	surface free energy	1	Low energy systems	[112,113]
Equation of State (Neumann)	surface free energy	1	universal	[101,114,115]
Chibowsky	surface free energy	1	universal	[73,98]

Table 1. Popular surface free energy determination methods and their scope of application

2.4. The role of external stimuli

2.4.1. The significance of stimulus-responsivity

Besides the role of surface chemistry and roughness in wetting scenarios is well-emphasized in the literature, less attention is paid to the effect of external stimuli in this context, however, the so-called stimulus-responsive materials have been attracting increased attention at other fields [116,117].

The stimulus-responsivity is the ability of a system to alter its physical and/or chemical properties upon exposure to external influence, e.g. temperature- and pH-change, light or magnetic field, ionic strength etc. This feature – non-surprisingly – is dependent on the surface chemistry and can lead to the development of intelligent materials. The significance of this scientific field has already been acknowledged by giving the Nobel Prize in chemistry to Sauvage, Stoddart, and Feringa back in 2016 „for the design and synthesis of molecular machines".

There are examples for stimulus-responsive materials even in our everyday life: enough to mention liquid crystal displays (LCD) and windows with adjustable transmittance [118,119]. Moreover, numerous drug formulations exploit stimulus-responsivity in order to achieve the controlled release of different active pharmaceutical ingredients (APIs) in a specific target organ and/or at a specific rate [120]. Most examples are pH- or thermoresponsive release systems, where the release is controlled by the pH- or temperature regulated swelling of the drug carrier [121], however, cases of magnetic field-responsivity are also known, which property could be elaborated through the addition of different magnetic particles, such as magnetite (Fe_3O_4) or maghemite (Fe_2O_3) [122]. Stimulus-responsivity also opened new perspectives at the field of analytics, where the responsivity serves as a core mechanism in sensing physical quantities, such as pH and temperature [123] and at microfluidics, where these surfaces are used as miniaturized actuators to create and maintain fluid motion via mechanical response or via the altered surface wetting characteristics [124,125].

While in the case of 3D systems, there are approaches to influence properties such as swelling degree, bulk density, shape, size [126], optical properties or degree of dispersion, in the case of 2D materials, surface properties are the subject of stimuli-responsiveness. These include surface functionality, charge excess and roughness [127,128]: manipulating these by external stimuli leads to the reversible change of wetting properties [129-131].

In the followings, the most popular surface-types with stimuli-responsive character are presented, grouped according to the affecting stimuli.

2.4.2. Photoresponsivity

A well-known case of photoresponsive wetting behaviour belongs to the initially slightly hydrophilic and oleophilic TiO_2, that becomes amphiphilic (upon UV-illumination. This transition is achieved as the UV-illumination creates oxygen-vacancies (conversion of Ti^{4+} sites to Ti^{3+}) on the surface, which promotes the dissociative chemisorption of water and therefore increased water adhesion [93]. As this water sorption takes place (even in humid atmosphere), the wetting character slowly returns to its original state. This property of TiO_2 is mainly utilized in antifogging systems [132], however, in such cases, the reversibility of the wetting character is an issue that is needed to be overcome. Recently, fruitful studies were conducted towards superhydrophilic TiO_2 without the need of UV-activation [133].

The photoresponsive wetting character in most cases of recent publications is attributed to the presence of the so-called photoswitches, which are molecules with double-bonds, capable of reversible cis-trans isomerization upon near-UV- or VIS irradiation [134,135]. As these cis-trans isomer pairs have different configurations and dipole moments, the free energy of the interfacial layer changes through isomerization (different functionalities are present at the S/L-phase boundary). The photoswitches can be utilized in various scenarios, such as light-controlled catalytic processes [136] or drug delivery [137], adsorption [138], or even supramolecular [139] and particle assemblies [140]. Applying periodic isomerization cycles, rotary motion is also achievable: due to this possibility, these compounds are also called molecular machines.

The aromatic diazo compounds (e.g. azobenzene) are popular photoswitches due to the achievable broad contact angle ranges and decent chemical stability [141]. As these molecules have conjugated electron system (colourful compounds), the wavelengths required for the isomerization and wetting transitions usually fall within the visible range.

The most common ways of photoswitch immobilization are forming disulfide bonds (e.g. on gold substrates [141]) or using polypodal linker groups [142].

However, there are drawbacks to overcome related to photoswitch-decorated surfaces, for example, the possible photodegradation [143] and the difficulties in achieving a surface coverage or complete control, sufficient for considerable wetting transitions. The preparation of photoswitch-decorated surfaces is usually an at least two-step process: at first, the elaboration of the base or substrate, then the subsequent binding of the photoswitches takes place [141]. It is also important to note, that the operation of such surfaces requires (near)monochromatic light

sources, however, a crucial drawback of the application of such photoresponsive surfaces is the multistep preparation procedure.

2.4.3. Thermoresponsivity

Wetting itself is dependent on the relation of interfacial tensions, which themselves are inherently temperature-dependent quantities, the changes in temperature only have a minimal effect on the observable Θ values. The so-called thermoresponsive systems undergo physical- and/or chemical changes upon increasing or decreasing their temperature [144,145]. The termoresponsive character implies that these wetting alterations exceed the temperature-dependency of γ in magnitude.

A common way to elaborate thermoresponsive wetting characteristics is the application of poly(N-isopropyl acrylamide) (pNIPAAm). The pNIPAAm polymer chains are miscible with water at room temperature, but these systems undergo phase separation over ~32 °C due to entropy-driven precipitation (intramolecular hydrogen bonds become dominant) [146]. This lower critical solution temperature (LCST) can be tuned to fulfil the requirements of scenarios by adjusting the molecular mass and its dispersity or by copolymerization of NIPAAm with other monomers. The application of pNIPAAm offers versatility as its chains can be bound and grafted to different substrates, such as silicon [147], glass [122], or polymers [148], while their mass can have monodispersed distribution if living polymerization methods, such as atomic transfer radical polymerization (ATRP) or Reversible addition−fragmentation chain-transfer (RAFT) are applied [148,149]. This monodispersity is essential to provide the narrowest possible temperature-range for the solution-dissolution processes, while the copolymerization or endcapping with other monomers can tune LCST values, as well [149].

The thermoresponsive feature of pNIPAAm is utilized in many ways: one can find pNIPAAm-based drug release systems [150] and analytical applications [151], but there are pNIPAAm-utilizing approaches at the field of catalysis, as well [152,153]. Thermoresponsive polymers can also be utilized in carrying out catalytic reactions, as enablers of thermal separation of modified catalysts from reaction mixtures [154].

Jia and their co-workers coated photoreactive Cu_2O nanoparticles coated with pNIPAAm molecules, which gave the particles thermoresponsive photocatalytic behaviour during methyl-orange photodegradation experiments [155]. According to the proposed mechanism, not only the wetting of the coated particles is influenced, but the diffusion of the degradable model

pollutant towards the catalyst surface also becomes hindered over the LCST, which can influence the reaction rates, as well.

Despite the topic of thermoresponsive photocatalytic particles is somewhat covered in the literature, there are less examples for macroscopic thermopresponsive photocatalytic surfaces. In one of our previous works [156], such coatings were prepared on pNIPAAm-grafted PDMS basis, with temperature- and composition-dependent wetting and photoreactivity. The visible light-photoreactivity of the surfaces could be attributed to the 15 wt.% Ag-TiO_2 photocatalyst nanoparticle content and was also proven to be temperature-responsive in the 25-50 °C temperature range and visible light-photoreactivity (blue LED-light, λ= 405 nm) at the S/L-interface during methylene-blue (MB) degradation tests (**Fig. 3 A**). This behaviour can clearly be attribute to the temperature-induced changes in wettability (achieved contact angles ranged from 50.7 to 108.9°). As it was determined applying the theory of Chibowsky [98], the surface free energy of the pNIPAAM-decorated coatings was significantly lower over the LCST (switched from 42.12 mJ/m^2 to 8.22 mJ/m^2 upon heating up from 25 °C to 50 °C), while the free energy of the ungrafted coatings remained similar upon increasing the temperature (from 7.54 mJ/m^2 to 4.71 mJ/m^2 (**Fig. 3 B**).

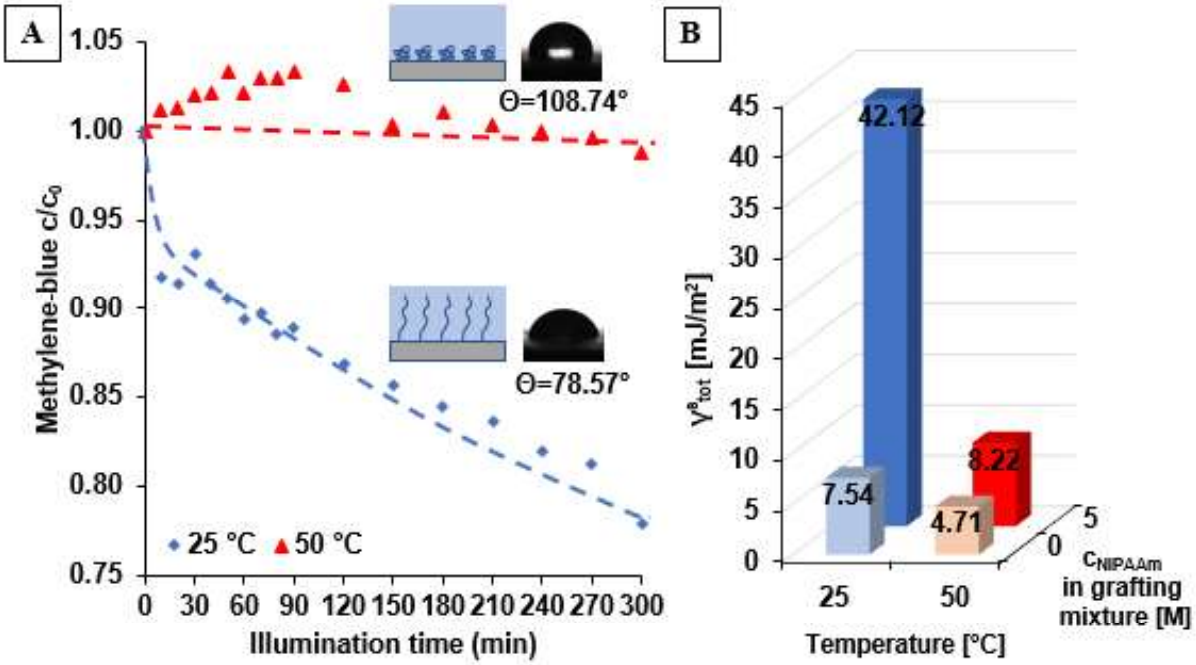

Figure 3. Schematic representation of the wetting and photocatalytic efficiency of pNIPAAM-grafted Ag-TiO_2/PDMS composite coatings; methylene-blue (c_0= 6.25 μM) relative concentration vs. illumination time (λ=405 nm) **A** and the calculated surface free energy values of the composites as a function of temperature and grafting NIPAAm monomer concentration **B** [156]

The pNIPAAm-containing surfaces with thermoresponsive wetting can also be used for cell attachment-detachment purposes: the adhesion is preferred over the LCST, while at lower temperatures the decoiled surface-soluble polymer chains hinder cell adhesion by their sterical hindrance [144].

Although, pNIPAAm dominates the field, other considerable, but still less popular thermoresponsive polymers with LCST are Pluronics, elastin-like polypeptides (ELP) and poly(*N*-vinylcaprolactam) (PNVCL) are also applied in medical-related scenarios [144]. It is also worth to mention, that zwitterionic polymer-water systems with upper critical solution temperatures (UCST) also exist, however, their relevance is even lower due to the difficulties of their application in physiological conditions [144,157].

Overall, the utilization of thermoresponsive wetting property is preferable and extensively studied at the scale of colloidal- and nano systems, while there are less examples with this property from among macroscopic surfaces. As these wetting transitions are affected by heat transfer, in the case of macroscopic surfaces, the difficulties of implementing a heating-

cooling cycle (insufficient heating- and/or cooling power, thermal conductivity, volume of the overall system, convection etc.) may result in delayed response, which means limited capabilities and reversibility [158,159]. The application of these surfaces may be limited by the high cost of raw materials (e.g., NIPAAm monomer, living polymerization catalysts), as well.

2.4.4. Magnetoresponsivity

Although, many magnetic surfaces with superhydrophobic properties ($\Theta \geq 150°$) are known, including magnetic sponges for water-oil separation [160] and coatings for electromagnetic shielding [161], magnetic field-induced wettability transitions are still less studied than systems with other responsivities. While liquid manipulation by magnetic field is achievable through dispersing particulate magnetic materials in the liquid itself [162], the enhancement of solid surfaces with magnetic fillers is a more advantageous alternative as in this case the properties of the wetting liquid remain unchanged.

The so-called magnetorheological elastomers offer altered mechanical properties and are deformable in the presence of external magnetic field. Lee et al. [163] and Sorokin et al. [164] dispersed iron microparticles in doctor blade-casted poly(dimethylsiloxane) (PDMS) films. The incorporated particles then align in the direction of the external magnetic force-field lines to form needle-like surface texture, resulting in increased roughness and hydrophobicity. As these surfaces mostly consist of uncured PDMS or contain high amounts of plasticizer to achieve broad wettability ranges, their application is limited due to their sticky and plastic character. A different type of magnetic coatings utilizes magnetic strains or pillars to alter wetting conditions [165]. These strains can be prepared via dispersing magnetic particles (e.g., magnetite, iron, etc.) in uncured polymer matrices, and the following exposure of the composite to an external magnetic field. Depending on the field-strength and direction, latter results in the formation of elongated magnetic polymer strains. These strains can be bent or stiffened by adjusting the direction and strength of the magnetic field, which therefore alters the surface structure and the wetting properties real-time.

In the paper of Yang et al., the magnetic pillars of carbonyl iron and PDMS were presented: these systems were elaborated during magnetic field-assisted spray-coating [166]. When no magnetic field was present, the pillars had random orientation and could be bent by the impacting water droplets, increasing the S/L contact surface and adhesion, resulting in decreased contact angles. However, when a magnetic field is introduced perpendicularly to the substrate surface, the pillars stiffened and pinned the drops, which meant decreased contact area

and adhesion, therefore seemingly more hydrophobic character. Due to stimulus-responsivity, these coatings can even be applied as liquid manipulation tools: by the help of a magnet, the water droplets can be picked up and released, that makes lossless liquid transportation and handling achievable. In a previous study of our research group [167], we enhanced such systems with another, photocatalytic functionality through the addition of Ag-TiO_2 photocatalyst nanoparticles: as a result, besides the tuneable wetting properties (Θ=57-164°) the photocatalytic efficiency at S/L-interface (methylene-blue decomposition, λ_{LED}=405 nm) was proven to be adjustable by the external magnetic field, as well. Besides the tuneable photocatalytic activity, the catalyst-roughened photocatalytic pillars were capable of droplet catch and release (**Fig. 4**)

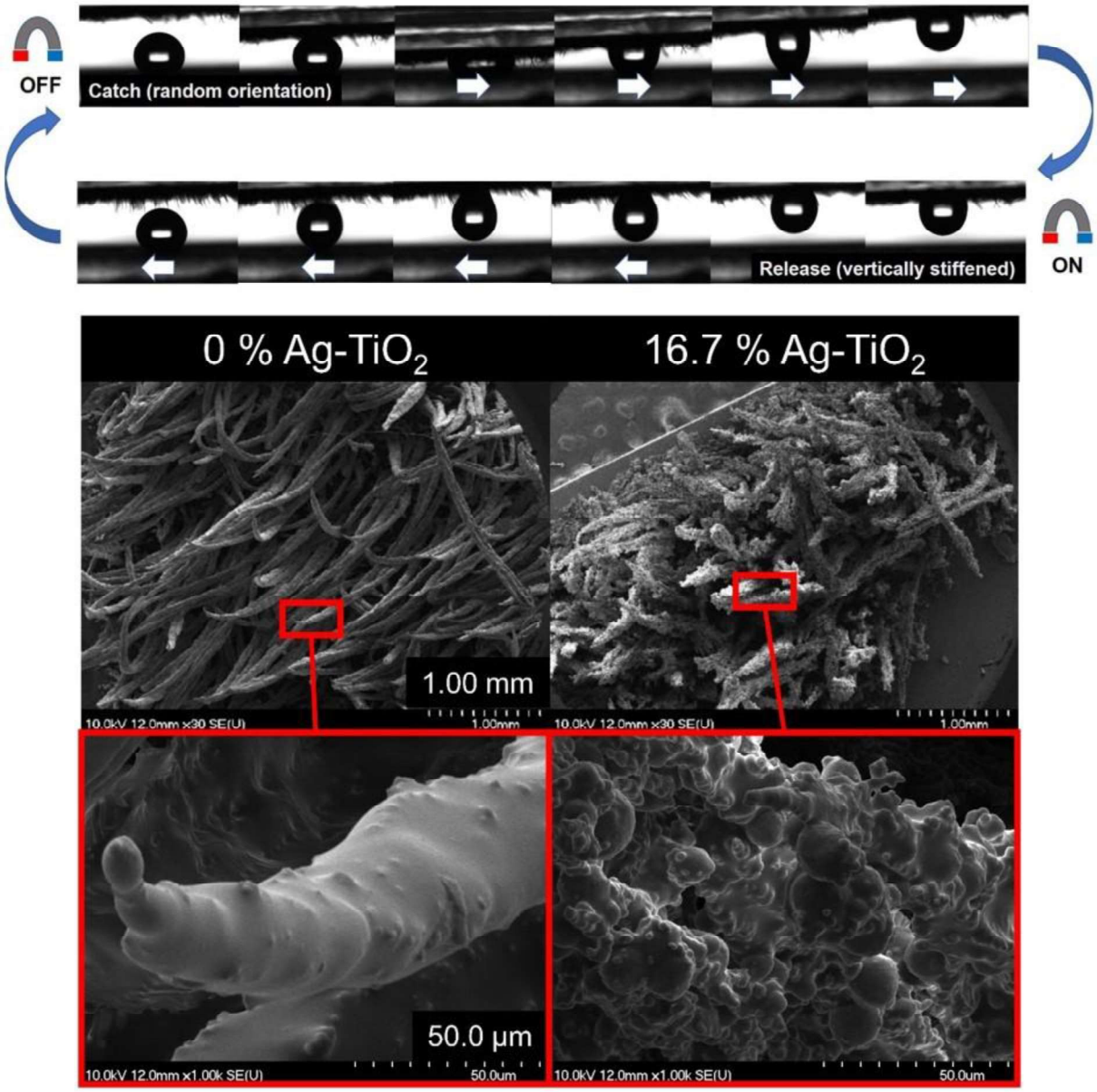

Figure 4. CCD images of water droplet catch and release from a superhydrophobic surface by magnetic pillar coatings with 16.7 wt.% Ag-TiO_2 content (top) and SEM images of the magnetic pillars with 0 and 16.7 wt.% nominal Ag-TiO_2 content) (bottom) [167]

The application of these magnetoresponsive systems may be preferred as they are capable of spontaneous response, the ingredients are relatively cheap, and they are easy-to-prepare as spray-coating or film casting are scalable and quick techniques. However, the vulnerability of the polymer strains and the many affecting factors (e.g. density, height, thickness of the pillars) may limit their application, alongside the fact that these coatings are macroscopically three-dimensional structures.

2.4.5. Electroresponsivity

The application of electric field for wettability alteration is generally limited to the utilization of the electrowetting-phenomenon. During electrowetting, the contact angle of a liquid on a solid is decreased through charge polarization: the attraction of the liquid to the oppositely charged surface results in the overcompensation of the interfacial tension, which leads to lower contact angles and increased wetting [168,169].

Most novel approaches towards electrowetting belong to the group of EWOD-surfaces (ElectroWetting On Dielectrics) [170] which utilize a conductive lower layer (e.g., metals), covered by an insulating upper layer (e.g., PTFE [171]) to inhibit charge recombination. With the oppositely charged liquid, this system practically acts as a charge-condenser. As these surfaces are electrically controlled, their response is fast, which promotes the reversibility of switching between different wetting states. As in EWOD-systems, both oppositely charged electrodes can be placed under an insulating layer, the use of electrowetting phenomenon became a viable alternative of actuation in microfluidic channels made of initially insulating materials, such as PDMS [172].

As the curvature of the wetting liquid droplets change upon being introduced to external electric field, the electrowetting can be utilized in the creation of tuneable liquid microlenses [173] and pixels [174], as well.

There are examples for combining electrowetting and slippery surfaces, which can lead to more uniform droplet spreading and evaporation [82], while in the case of rough surfaces, electrowetting can lead to transitions between wetting states (e.g. Cassie-Baxter-to-Wenzel transition) [175].

2.4.6. pH-responsive wetting

As it was mentioned before, wetting in general is not only influenced by the properties of solids but the chemistry of the liquid, as well. A surface therefore can be called respondent to the properties of liquid, if the occurring wettability changes overcompensate the differences between interfacial tensions. This can be achieved through implementing changes in surface chemistry. An obvious and simple mean of this is the utilization of weak electrolyte functional groups, such as amino- (especially tertiary amino-) or carboxyl-groups, which can bear electric charge, depending on the pH of the liquid phase [176, 177]. As net surface charge increases

affinity towards polar and polarizable solvents, the protonated and deprotonated surface species offer different wettability conditions.
To achieve such transitions, polyelectrolites, such as amino-functionalized polyacrylates [178] or proteins are excellent candidates [179].

pH-responsive surfaces have already made their way towards their application in oil-water separation scenarios [178,180]. The copolymer-amino-functionalized silica composite (spray)coated filter papers of Jiang et al. [180] with pH-responsive wetting were able to achieve both superhydrophilic and superhydrophobic character (Θ: 0-160°) below and above pH=7 thanks to the amino groups of the 2-(Dimethylamino) ethyl methacrylate (DMAEMA) monomer. The samples were capable of reversible transitions upon pH change and of keeping the obtained wetting character after the removal of the bulk liquid phase. The modified filters were applied in oil-water separation with high efficiency, where the contact angle was proportional, and the separation efficiency was inversely proportional to the roughening agent (silica) loading.

A similar approach is made by Chi et al. [181], however, they applied 2-Vynilpiridine (2VP) as pH-responsive monomer, fluorinate hydrophobic silica as roughening agent and the coating was applied to polyester fabric by dip-coating. At pH=10, the coating showed omniphobic character, however, the superhydrophobic behaviour turned to superhydrophilic at pH=1, making o-v separation possible. The surfaces turned out to be anti-oil-fouling, while the superhydrophilic-superoleophobic state was also proven to be hygroscopic and anti-static.

pH-responsivity can also be utilized in antibacterial applications, as negative surface charge (above pH=7) promotes bacterial adhesion. Song et al. prepared dodecanethiol and 11-mercaptoundecanoic acid functionalized silver-covered copper mesh [182], which possessed superhydrophobicity and low bacterial adhesion at pH=7, while showing decreased hydrophobicity, better adhesivity and antimicrobial activity (due to the presenting silver content) at pH=9. These surfaces were effective against both Gram-positive (*S. aureus*) and Gram-negative (*E. coli*) bacteria.

As one can see, pH-responsivity is mainly linked to the presence of weak electrolyte functional groups, which are abundant in nature. Biomolecules such as proteins can exhibit pH-responsive wetting, as well. In the light of this, Liu et al. prepared films of amphoteric and amphiphilic soy protein microfibrils on different substrates and examined the release rate of the incorporated methylene-blue (MB) at different pH values [179]. Their study concluded that the

cumulative release of the cationic dye is higher at lower pH value, indicating the effect of sidechain protonation on intermolecular electrostatic interactions.

2.4.7. Mechanoresponsivity

Another promising way of wettability regulation is the utilization of mechanical stimuli to alter surface texture [183]. In most of the literature examples of this feature, elastomeric matrix materials, such as PDMS [184,185] are applied to promote reversible transitions. To produce uniform response, these surfaces possess highly ordered structure, which can be elaborated via destructive methods, such as photo- or plasma etching [186].

PDMS surfaces with micrometric or sub-micrometric waviness are common examples: Zhao et al. prepared wavy, fluorosilylated PDMS surfaces, which achieved reversible wetting transitions against water in the Θ=138°-120° range (0-100 % stress ration) with excellent reversibility [187].

However, as mechanical strains may cause cracks and irreversible deformations in these surfaces, the pool of starting materials is somewhat limited. Rhee et al. demonstrated the differences between an elastic, fluorinated, wavy PDMS surface and an oxygen plasma-treated PDMS layer with brittle SiO_x-like surface layer. Latter was found out to be prone to cracking, resulting in decreased contact angle range and reduced capability for reversible operation upon anisotropic stretching [186].

Overall, the main disadvantage of these surfaces is their need for microfabrication equipment, however, the roughness-influenced wetting transitions can only be achieved through mechanical responsivity. Parra-Barranco et al. deposited TiO_2 on PDMS. The resulting surfaces with hierarchical roughness were responsive to stretching and bending, being able to turn on and off rose petal-like behaviour and regulate the roll-off of water and diiodomethane [186].

There are bright examples for mechanical responsivity among the slippery liquid-infused surfaces (or SLIPS), in case of which the lubricant can be reversibly pumped in and out of a porous surface through applying mechanical stimuli [188]. As the coverage of the S/L-interface by lubricant influences contact area and adhesion, it regulates wettability, as well.

2.4.8. Multistimulus- responsivity

While each of the presented external stimuli are eligible to offer wetting-related functionalities on their own, their combinations towards more sophisticated systems is trending among materials scientists [189-192]. The elaboration of responsiveness to two stimuli is the most common [193], however, there are increasing numbers of surfaces responsible to three different stimuli [194]. Although, a significant portion of the related literature approaches multistimulus-responsive systems as shape-changing 3D objects, such as hydrogels [195,196] with controllable swelling, drug-release systems [197] or mechanical actuators [198,199], studies focused on wettability alteration of macroscopic systems are also numeorus [193,198,199].

In these scenarios, both the surface chemistry and the surface morphology can be the subject of stimuli-responsiveness. In such an example for light-and temperature-responsive surfaces, donor acceptor Stenhouse adduct (DASA) photoswitch-functionalized hydroxypropyl cellulose nanoparticle films were capable of light-induced hydrophilization [193]. The elevated temperature were then able to melt the surface structure, irreversibly leading to a smoother but moderately hydrophobic character.

As an example for solely surface morphology-controlled wettability transitions, in the study of Wang et al. [199] the authors prepared self-assembled micropillars of PDMS and carbonyl iron in external magnetic field. As the pillar-decorated composites were then subjected to magnetic field and mechanical strain, the angle of inclination of the pillars and the distance between them could be changed, respectively, which led to the changes in apparent contact angle of hexadecane droplets in the 150-38° contact angle range.

In an another approach, Zhang et al. [200] prepared surfaces on the basis of pH-responsive poly(2-(diisopropylamino)ethyl methacrylate (PDPAEMA)-modified temperature-triggered shape memory polymer (SMP), being capable of superhydrophilic-superhydrophobic transitions.

However, the solely surface chemistry-dependent approaches towards multistimulus-responsive wetting can only achieve smaller contact angle ranges. Alkan et al. created temperature- (polyethilene glycol based copolymer), redox-state (ferrocene-moieties) and pH-dependent (amino-groups) wetting character for electrocatalytic purposes [194]. The contact angles on the modified surfaces were found out to be in the 48-81° range, depending on the conditions.

Another example for fully surface chemistry-dependent wetting (and triple stimuli-responsiveness) is the work of Zhou et al. [190] the authors achieved contact angle transitions in the hydrophilic regime with the magnitude of ~10° with the prepared temperature-, pH- and fructose concentration-dependent biointerfaces. The authors also found correlation between the wetting properties and the adhesion of ovalbumin model protein and bacterial and mammal cells to the surfaces, which later were enchanced with antimicrobial functionalities (quaterner ammonium groups) to create a hold-release cycle of antimicrobial operation.

Despite wetting character is an obvious and easy-to-study physical property of stimuli-responsive macroscopic surfaces, it is still overlooked in many published works.

3. Wetting-related applications of functional surfaces

3.1. Self-cleaning surfaces

3.1.1. Utilization of extreme wetting characters

As it was discussed in previous chapters, the lotus leaves possess self-cleaning behaviour thanks to their inherently hydrophobic character and hierarchical surface roughness [44,45]. As nature already achieved its best, most scientific approaches try to mimic, improve and utilize this texture [201-203]. These biomimetic superhydrophobic surfaces made their way towards commercial application as wallpaints or antifouling coatings [204], but superhydrophobic surfaces have increasing usage in anti-corrosion [205] or anti-icing [206] scenarios, as well.

Although, the self-cleaning behaviour of superhydrophobic surfaces is more well-known, superhydrophilic surfaces are also considered to be self-cleaning [207,208], as water usually has higher affinity to the surface than contaminants, being able to practically wash them away. The elaboration of such surfaces is based on similar principles: as surface roughness introduces increased contact area to inherently hydrophilic surfaces, the adhesion between the solid and water increases, while the contact angle decreases. As superhydrophilic character promotes uniform spreading of water, such surfaces are also applied in antifogging scenarios [209], where they provide increased optical transmittance in humid conditions (swimming glasses, mirrors etc.).

3.1.2. Photoreactive surfaces

As the global environmental problems urge the development of greener, chemical-less means of environmental remediation, semiconductor photocatalysts and their composites gained increased attention. These materials are capable of generating reactive, oxidative radicals (such as $^{\cdot}OH$, $O_2^{\cdot -}$ or $^{\cdot}OOH^-$ in aqueous media) upon illumination [210]. The formed radicals are then responsible for the decomposition of organic species [51,73,211], even complete oxidation (or mineralization) is possible. At the S/L-interface, the effectivity of photocatalytic surfaces against specific compounds depends on several factors, such as temperature, wavelength and intensity of the incident light, the affinity of the solid surface towards the liquid medium and its contaminants is also crucial [212,213]. The most important and most studied medium in this context is water, in which the formed reactive radicals generally have very short lifetime (up to a few μs half-life) available to oxidize contaminants. This means, that the adsorption of the oxidizable species, and the wetting of the surface by the medium – which influences the radical formation rate itself - are both critical parameters.

The ability of pohotocatalysts to decompose contamination implies, that the self-cleaning character of surfaces can be enhanced through the addition of photocatalyst materials. In the case of superphilic/-phobic characters, the aimed surface roughness can be elaborated by applying inorganic photocatalyst particles as roughening agents [73,211].

To achieve this feature, in our previous studies [73,211] we prepared spray-coated composite coatings of a hydrophobic fluoropolymer (poly(perfluorodecyl-acrylate) or pPFDAc), a hydrophilic polyacrylate (poly(2-hydroxyethyl acrylate) or pHEA) and visible-light active plasmonic Ag-TiO_2 photocatalyst nanoparticles ($d_{prim.}$=50 nm). The wettability and photoreactivity of the prepared coatings were proven to be adjustable by both the nanoparticle loading (roughening agent) and the matrix composition (fluoropolymer : polyacrylate mass : mass ratio). In the case of both polymers, the extreme wetting characters were achieved at 80 wt.% photocatalyst loading (**Fig. 5 A and B**).. At this nanoparticle content, changing the ratio of the matrix polymers could result in wide range of wettability, from superhydrophilic (Θ=0°) to superhydrophobic (Θ=150.9°) (**Fig. 5 B**). Non surprisingly, as it was calculated applying the theory of Chibowsky [98], the surface free energy values of the initial smooth polymer films were changed upon roughening, resulting in increased (in the case of the polyacrylate) and decreased (in the case of the fluoropolymer) values (**Fig. 5 B**). These wetting and surface free energy alterations also resulted in composition-dependent photoreactivity. As **Fig. 6** shows, the coating more hydrophilic composition produced higher concentrations of reactive radicals

[214] at the S/L interface upon UV-illumination, while the more hydrophobic coatings were proven to me more effective in decomposing EtOH (g) at the S/G-interface upon visible light-illumination (λ_{LED}=405 nm).

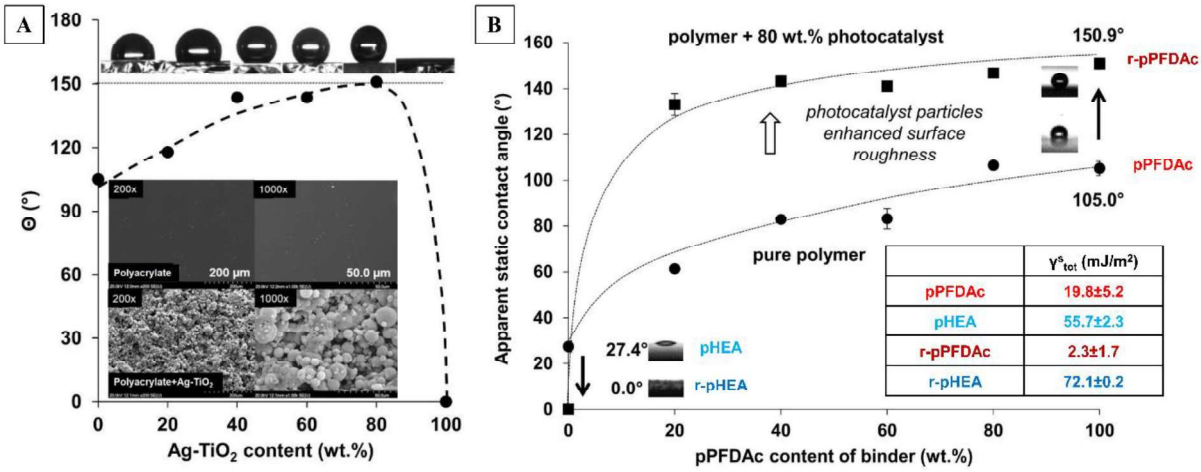

Figure 5. Measured Θ-values on Ag-TiO_2/pPFDAc hybrid layers as a function of Ag-TiO_2 content (the dashed line is a guide to the eyes) [73] and SEM images of the prepared smooth pPFDAc fluoropolymer layer (top) and the 80 wt% Ag-TiO_2 containing pPFDAc thin layers with different magnifications (bottom) [211] **A** measured apparent static initial water contact angles on pure polyacrylate thin films and Ag-TiO_2 photocatalyst-roughened polyacrylate hybrid layers (r-) as a function of the hydrophobic pPFDAc content of the copolymer matrix (T = 25±0.5 °C) [211] beside the determined total apparent surface free energy (γ^s_{tot}) values of initial (smooth) and roughened (r-) polyacrylate thin layers [211] **B**

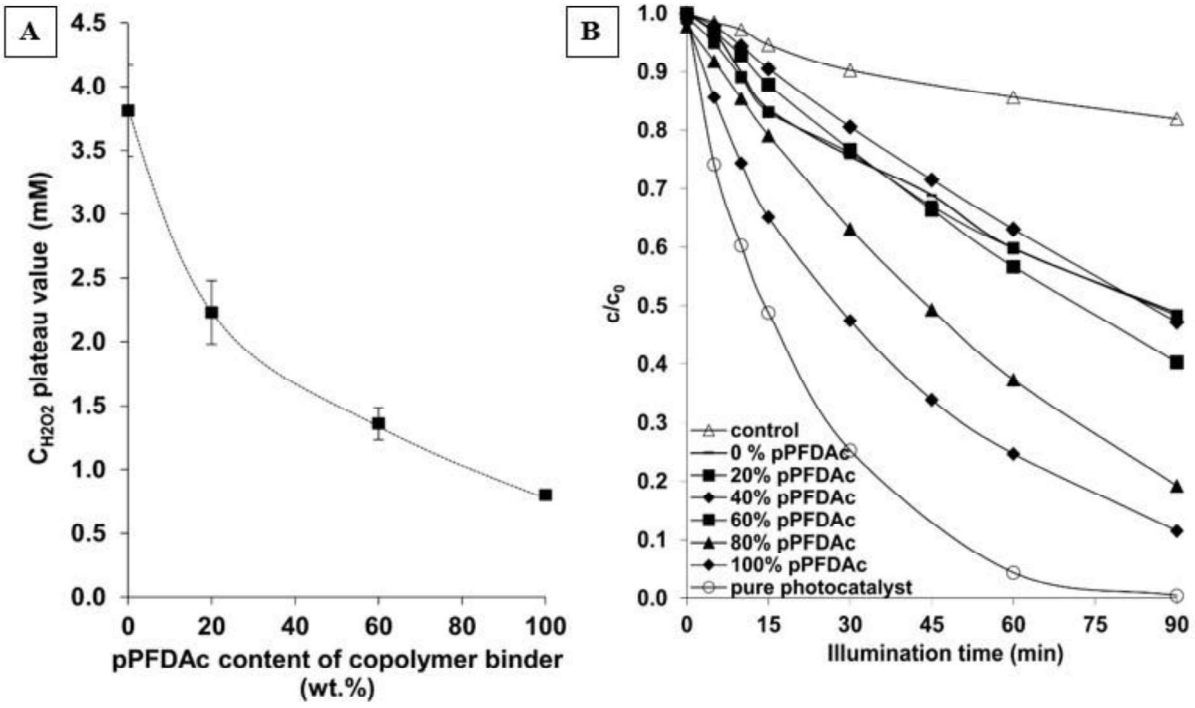

Figure 6. Evolution of ROS on roughened (r-) pPFDAc and pHEA hybrid layers upon blue LED illumination (λ = 405 nm), the measured maximum H_2O_2-equivalent radical concentrations as a function of the pPFDAc content of the polymer matrix **A** [214] and characterization of EtOH (g) (c_0=0.36 mM) decomposition on Ag-TiO_2/polyarcrylate hybrid layers under LED light illumination (λ = 405 nm) as the function of illumination time (the legends refer to the composition of the polymer matrix) [211]

There are examples for monolythic photocatalytic surfaces with extreme wetting, such as roughened semiconductor polymer surfaces, as well. In our previous study [51], hierarchically structured, semiconductor polymer poly(3-hexyltiophene) (P3HT) surfaces were prepared through solvent-precipitation and filtrate deposition to achieve superhydrophobicity and visible light-photoreactivity. The roughness and wettability (Θ=100-150°) of the prepared surfaces was proven to be adjustable by changing the ratio of solvents (toluene and dimethyl formamide) and the time of sonication. Although, a similar monolythic surface does not require particulate inorganic semiconductor materials, more examples of composite surfaces can be found in the literature. As it was represented by our previously presented works, semiconductor photocatalyst particles (eg. ZnO, TiO_2) are preferably immobilized in different polymer matrices, such as fluoropolymers [73,211,214,215], PDMS (both leading to hydrophobic or

superhydrophobic character) [73,216,217], or even hydrophilic polyacrylates to achieve superhydrophilicity [211]. To reach the optimal wetting character, one must consider the inherently hydrophilic nature of semiconductor oxides and their possible surface coverage by the matrix material, as e.g. in the case of superhydrophobic surfaces, even a few percent surface coverage with the binding (matrix) material can lead to superhydrophobic behaviour [73,218]. As this surface coverage – and the roughness, as well – mostly depend on the matrix : filler ratio and the preparation technique, the proper selection of these two is crucial. Among preparation techniques, spray- [73,211,214-218] or spin-coating [219] and casting methods (e.g. doctor blade) [216,220] are the most worthy to mention, however one can choose to apply microfabrication techniques [221] or templating methods [222], as well.

As wettability is in close relation with the adsorption affinity of the surface towards the different photocatalytic substrates and the medium, the photocatalytic activity can be fine-tuned by setting the wettability [73,211]. It is also proven, that hydrophilic surfaces in general produce reactive radicals in higher concentrations, while the wettability can also affect the photocatalytic activity at not just S/L but at the S/G interfaces, as well. The alredy mentioned UV-photoinduced superhydrophilicity of TiO_2 can influence photoreactivity, as well. On TiO_2 surfaces exposed to air (S/G interface), this superhydrophilicity facilitates the adsorption of a thin water layer (S/G/L interface), which contributes to the complete oxidation (mineralization) of hydrophilic volatile organic compounds (VOCs) [223].

In the case of photoreactive composite surfaces, it should also be taken into consideration, that the immobilization of photocatalyst particles results in lower reactive surface area, which should be taken into account when considering overall photocatalytic effectivity. If the immobilizing matrix also consists of decomposable material(s), the wettability and photoreactivity of these surfaces may change overtime, which can lead to the diminishing of extreme-wetting character, as well [218,224]. This diminish can be overcome by enhancing the surface with self-healing character or by the right choice of durable matrix materials.

In our previous study [73] we applied dodecyl-trichlorosilane-infused PDMS/silicone oil oleogel matrices in photocatalytic coatings to render them self-healing. Our coatings were proven to be superhydrophobic at 25 wt.% Ag-TiO_2 photocatalyst content, while they were able to regain their superhydrophobicity multiple times after the complete removal of the upper coating layer.

Photoreactivity (and wetting) can also be regulated by external stimuli: pNIPAAm-based temperature-responsive macroscopic surfaces [216] and particles or megnetoresponsive systems [217] are both available to prepare. In our previous studies we enhanced

thermoresponsive pNIPAAm-grafted PDMS caotings and Fe/PDMS composite grass coatings with visible light-active Ag-TiO_2 photocatalyst nanoparticles. Besides stimulus-responsive wetting, the resulting systems showed stimulus-responsive photocatalytic activity at the S/L interface, as well.

As the overall outcome of photocatalytic reactions is influenced by the temperature and the wavelength and/or intensity of the incident light, the effects of these factors should be studied independently aside the stimulus-responsive character.

Although, this chapter entirely focused on photocatalysis, the same principles apply for other catalytic surfaces, as their activity at S/L-interfaces may be dependent on their affinity towards the liquid medium and the catalytic substrates, as well [225].

3.1.3. Antimicrobial surfaces

Besides getting rid of harmful organic compounds, the neutralization of pathogen microorganisms is also of high priority. Recently, the spreading of antibiotics-resistant bacteria is causing an increasing number of healthcare problems, such as untreateble nosocomial infections, therefore the emphasis is getting to be put on preventive measures. A viable route of infection prevention is the application of different antimicrobial surfaces, which can eliminate pathogens and inhibit their multiplication [226-228].

The antimicrobial effect of these surfaces can be achieved in multiple ways. A general classification scheme distinguishes anti-adhesive, contact-active and biocide-releasing (organic biocide or metal ions) surfaces [229-232]. All three types are affected by wetting properties in terms of effectivity.

The anti-adhesive antimicrobial surfaces usually possess superhydrophobic character, which comes in pair with low surface energy [233]. This hinders the adsorption of proteins, therefore the adsorption of microbial cells, as well. The preferred materials for the elaboration of such surfaces are fluoropolymers and other fluorinated species [234], while the provision of adequate surface roughness is also crucial [235,236]. On the other hand, zwitterionic (and therefore more hydrophilic) polymer surfaces are also effective as these are capable of preventing the specific adsorption of cellular proteins [237].

Moreover, these surfaces can also belong to the group of contact-active surfaces as positive surface charge (e.g. from quaternary ammonium groups [238] or poly(guanidines) [239]) promotes the desintegration of phospholipide membranes of the attached cells [240].

As anti-adhesive surfaces are meant to repel microbes, contact-active surfaces are meant to utilize the opposite scenario, therefore the higher surface energy and increased wettability are essential for their functional operation. Contact-active antimicrobial character is mostly elaborated by applying raw materials such as cationic polymers (with amino or quaternary ammonium groups) [238-240], by binding antimicrobial peptides [241] to surfaces. The adhesivity towards bacteria is generally a pH-dependent parameter, which is well observable in the case of inorganic oxides, such as TiO_2.

In a previous publication of our research group [235], bacterial attachment (Gram− *E. coli*, and *P. aeruginosa*; Gram+ methicillin-resistant *S. aureus* (MRSA)) to TiO_2 and plasmonic Ag-TiO_2 photocatalyst nanoparticles and their aggregates were investigated during surface charge titrations. As the charge titration curves of **Fig. 7** show, at pH= 4.5 (below point-of-zero-charge, which is around pH=5.2) the photocatalyst particles possess net positive charge, while the bacteria are negatively charged. Knowing the specific surface charge of both the bacteria and the particles, upon the titration of the bacterial suspension with the nanoparticle suspension, the adhered amounts of bacteria could also be determined. In our latest cooperative study [242], the examined photocatalysts, immobilized in polyacrylate matrix showed virucidal character against alfaherpesvirus upon visible light-illumination, as well, which projects the applicability of these surfaces against other high-risk patthogenes, such as coronaviruses.

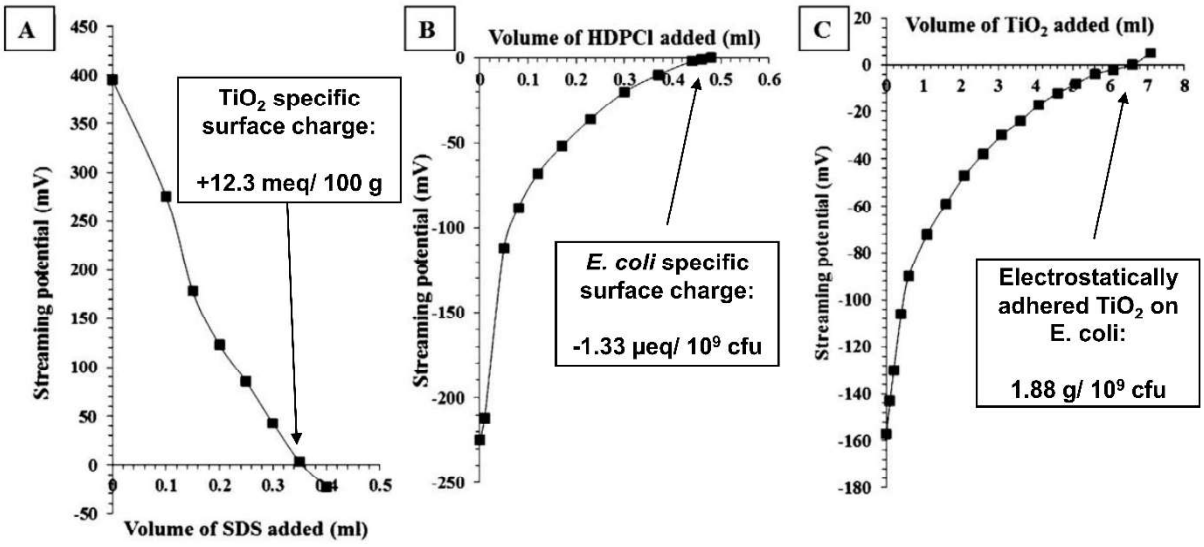

Figure 7. Determination of the specific surface charge values for TiO_2 **A**, for *E. coli* bacteria **B** and the amount of the adhered TiO_2 on the surface of *E. coli* at the electrostatic charge compensation point **C**. In all cases the pH was 4.5 and the standard error is 2.0%. [235]

The already described photoreactive surfaces [51,73,167,217,218] can fall into the category of biocide-releasing, surfaces, as well, due to their ability to produce reactive oxidative radicals. Moreover, bacteriotoxic metal ions (e.g. Ag^{+}, Cu^{2+}) may leach from metal-containing plasmonic photocatalyts (such as Ag-TiO_2), contributing to the elimination of Gram-positive and –negative bacteria [243-245]. Other biocide-releasing surfaces can consist of Lewis-acid metal oxides, such as MoO_3 or WO_3, which can exert their activity through in-situ generation of H_3O^{+} from moisture [246-248]. The rate of biocide-release from biocide-releasing surfaces is non-surprisingly dependent on the L/S contact area, which is a function of wettability.

While surface roughness is crucial in the provision of adequate wetting and bacterial adhesion, it should also be taken into consideration that – except in the case of contact-active surfaces – a surface preferrably should be rendered unable to exert retention on bacterial detachment. In general, smooth surfaces show the least retention, while surfaces with macroscopic and/or microscopic trenches have larger available space for bacterial adhesion [230,249]. Because of this, surfaces with hierarchical- or nanoroughness are preferred as they offer the least possible contact area.

3.2. Oil-water separation

Although, photocatalytic surfaces and membranes are effective to neutralize oily contaminants at lower concentrations (up to a few hundred or thousand mg/l), the removal of higher oil content from oil-water systems still remain a challenging task [250]. Beside the ability to minimize the harmful environmental impact of oils [251], the o/w-separation technologies have distinguished importance in the petrol industry, as well [252].

As most of the mineral oil reserves are depleting, the oil recovery requires so-called enhanced oil recovery (EOR) technologies, which in their most effective approaches means the injection of aqueous solutions of surfactants and/or polymers to mobilize the remaining oil content of reservoirs [253]. This results in the formation of stable emulsions, which are difficult to separate: the industrial o/w-emulsion separation is usually carried out by direct chemical means (salting out), which results in increased environmental impact [254]. In the last few years, a broad variety of functional porous surfaces (membranes and sieves) were tested and applied in o-w-separation [252,255]. Some of them even made their way to industrial

application, but mainly in water treatment, restricted to scenarios where the oily- and aqueous phases do not form stable dispersions and where the oil content is low.

Stable dispersions (emulsions) usually contain surfactants in higher concentrations, which counteracts the mechanism-of-action of separation surfaces. The physical o-w-separation via porous bodies is generally driven by the different wettability (different γ_{LG} and γ_{SL}) of the surface towards the two phases: the wetting phase can pass through the porous media and accumulate at the other side, while the non-wetting phase suffers retention [252]. As surfactants reduce interfacial tension, this driving force diminishes with their increasing concentration [256]. Another influencing factors on the effectivity of separation are the drop size of the dispersed phase and the pore diameter. If the porous medium is expected to exert retention on the dispersed phase, the pore diameters should be lower than the drop diameter, otherwise no retention occurs. As the presence of surfactants may reduce drop size (even below d<1 μm) by providing higher degree of dispersion, and may contribute to membrane fouling through adsorption [257,258], as well, they have triple effect on the separation efficiency.

Regarding wetting characters, the porous o-w-separation systems have three main types: superhydrophobic (oleophilic & permeable to oil) [259], superhydrophilic (underwater oleobhobic & permeable to water) [260] and amphyphilic (underwater oleophobic or under oil hydrophobic & permeable to both phases depending on the wetting media) [261]. A special subgroup of the latter are the so-called Janus-membranes, which are bifunctional as both of their sides have different wetting characters [262].

Examples for superhydrophobic separation systems utilize the inherent wetting properties materials such as hydrophobized (mostly fluorinated) silica nanoparticles [263], alginates [264], poly(phenylene sulfide) (PFS) [265], carbon nanotubes and PDMS [266], while the wetting character of superhydrophilic systems can be attributed to for example cthitosan [267,268], poly(vinyl alcohol) (PVA) [269], cellulose derivatives [270], polydopamine [63], silica [270], alumina [271] or titania [272] particles and graphene oxide [63]. Regarding the preparation of amphyphilic membranes, responsive materials such as pNIPAAm and NIPAAm copolymers are quite popular [273], while Janus membranes are usually prepared through the one-side oxidative treatment of originally hydrophobic membranes [262].

Although, the membranes themselves have inherent roughness, originated from theit porous nature, the provision of further surface micro- and nanostructures is practically unavoidable in order to create the desired extreme wetting character. Similarly to the surfaces of previously mentioned fields of applications, the roughness can be a result of particulate

material content [250,272], or the preparation methods, such as solvent-precipitation [263], hydrothermal treatment [274] or chemical deposition [55].

In general, surfactantless o-w-mixtures are easier-to-separate even via surfaces with broader pores, like modified sieves [55,275], while the separation of emulsions (with lower drop sizes) require membranes with narrower pores [276].

A trending membrane material is poly(vinilydene difluoride) (PVDF) [263,277], which is chemically stable, possess excellent heat resistance (up to 375 °C) and tensile strength and hydrophobic character. However, the practical application of PVDF-based membranes is still limited by the high cost of the raw material.

The emulsion separation efficiency can be enhanced by for example the elaboration of surface charge, which promotes the adsorption of oppositely charged surfactant molecules and the solubilized oil (and therefore promotes coalescence), or by prewetting the membranes with one of the phases.

In an example, Li et al. [278] deposited cationic polidomamine-based copolymer on the inner surface of polypropilene membrane tubes to form a hydrophilic layer. Both inner and outer sides of prepared Janus-type membranes were then prewetted with aqeous and organic phases respectively. The resulting systems were able to separate anionic surfactant-stabilized emulsions during continous flow operation as the charged inner layer of the tubes directed the oppositely charged oily solubilizates towards the hydrophobic outer layer.

As in the case of all other membranes or porous systems, the o-w-separating surfaces can suffer fouling, as well. In the case of charged surfaces, one must consider the charge of the stabilizing surfactants, as they promote fouling on surfaces with the opposite charge. The fouling can be hindered by minimizing adhesion and/or by enhancing the surfaces with self-cleaning charater. Latter can be created by the addition of photocatalyst to the system, which can act as roughening agent to promote extreme wettability, as well. Wang et al. prepared TiO_2 containing poly(acrylnitrile) based composite membranes for O/W separation [279]. The TiO_2 content in this instance was applied to photodegrade foulants and therefore to increase membrane lifetime.

Emulsion separation at a smaller scale can also be performed applying microfluidic systems [280-282], however, these process emulsions at a very low capacity and therefore restricted to everyday laboratory applications.

Despite the many successfull laboratory scenarios, most of the published separation systems cannot pass through the expenditure barrier of industrial applications, therefore

attempts exploiting cheaper raw materials and preparation techniques will be prioritized in the near future.

3.3. Microfluidics and liquid manipulation

As miniaturisation is ganining ground in nanotechnology, analytics (Lab-on-a-chip or LOC) [283], emulsification [284] or demulsification [280-282], flow chemistry [285] and other applications, the implementation of manipulating extremely small liquid volumes becomes more and more important.

Considering the dimensions of microfluidic channels, wettability-driven capillary interactions have crucial contribution to the overall liquid flow and can define a flow character, as well [286,287]. The most common, easy-to-process raw materials are silicones [288,289], especially PDMS [288], polyacrilates [284] and cellulose [290,291]. It is a common practice to hydrophilize the inherently hydrophobic silicone surfaces via oxidative treatment, however, these surfaces slowly transform back to hydrophobic overtime as the diffusion of lower molecular weight silicone species towards the interface proceeds [288].

Recently, the cellulose- or paper-based microfluidic systems gained increased attention as a result of their cheapness (does not require special preparation conditions, such as cleanroom etc.) [290-292]. As these systems are disposable, they already made their way towards healthcare applications as test kits (e.g. commercial pregnancy tests) [293,294]. The paper itself is porous and hydrophilic, thanks to the –OH group containing fibrous cellulose content, which provides excellent water-wettability and therefore being capable of liquid transport, solely based on capillarity. Thanks to the presence of –OH groups, paper is easy-to-functionalize, e.g. through silanization [290] or plasma deposition [291] to obtain microchannels with varied wettabilities. Li et al. modified paper through fluorosilanization and subsequent oxygen plasma treatment [290]. Depending on the time of plasma treatment, all four possible modes of oil- and watter wettability could be achieved (omniphobic, omniphilic, hydrophobic & oleophilic and hydrophilic and oleophilic).

In microfluidics, channel wettability has a key role in handling nonmiscible liquids (e.g. o-w-systems), as the right choice of wetting pattern can not just direct, but even mix or separate the liquid components.

To direct liquid flows autonomously, one can elaborate a wetting gradient pattern along the channel, such as in Shchedrina et al.'s study [295]. The researchers prepared gradient

wetting on stainless steel surfaces, solely by influencing microstructure via nanosecond laser pulses.

Männel et al. created 3D-printed polyacrylate microchannels with patterned wettability and applied them to prepare o/w and w/o emulsions, and even double emulsions [284] (**Fig. 8**). Wu et al. applied plasma coating, patterning and etching to prepare polymer microchannels with patterned wettability on various substrates. The resulting channel systems were able to direct, mix and separate flows of water and oil [281]. Recently, other materials such as graphene oxide or PDMS were applied for wettability patterning, as well [282].

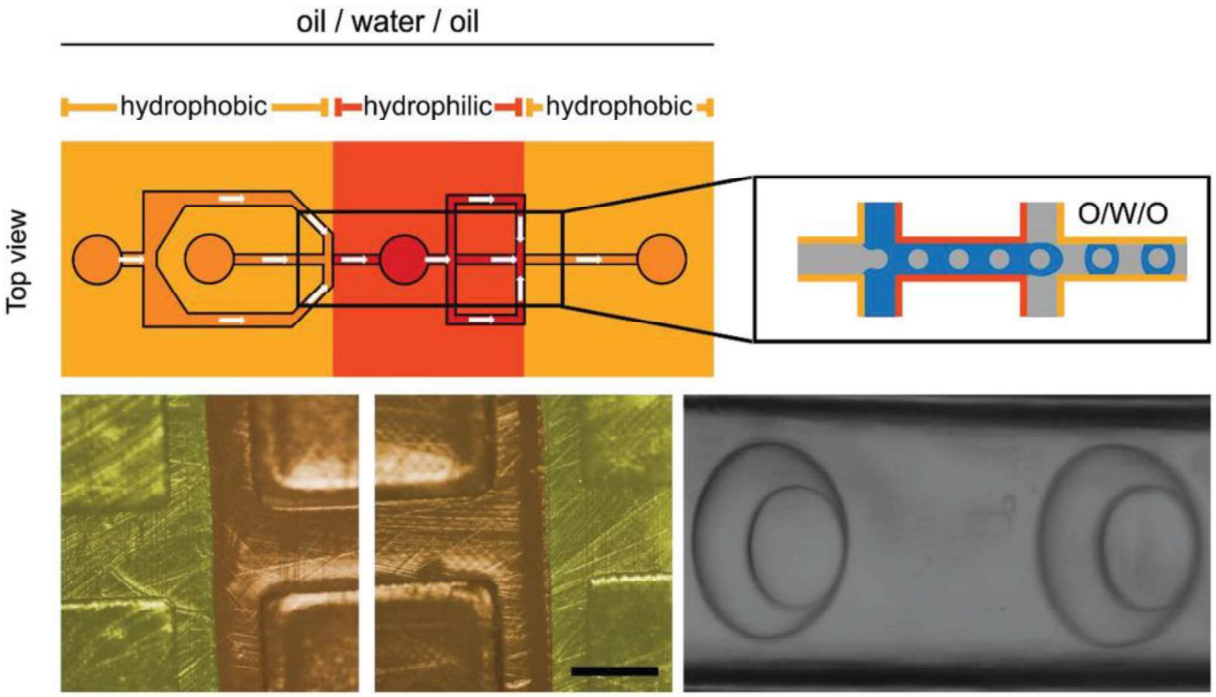

Figure 8. Schematic of a double emulsion device made via printing from two different materials with individual wettability. By manufacturing a surface pattern that is hydrophobic–hydrophilic–hydrophobic, O/W/O double emulsions can be formed inside the planar microchannels. In the lower row, a bright-field microscopy image of both junctions is shown. The hydrophobic material is colored in light-yellow and the hydrophilic material in reddish. The successful formation of double emulsions is followed inside the tubing of the outflow port (bottom right: Bright-field microscopy image of two double emulsion droplets). The scale bar denotes 300 µm. [284]

As it was mentioned before, the different stimulus-responsive surfaces with tunable wetting offer viable alternatives for flow actuation at the sub-mm scale and for droplet manipulation (merging, transportation), as well. Among all possible stimuli, electrowetting applications are superior and the most widespread, thanks to the excellent miniaturizeability and fast response [296-299]. Moreover, applying photoconductor & semiconductor materials, light-controlled optoelectrowetting microfluidic devices are also implementable. Recently, Loo et al. prepared such devices, capable of quick droplet manipulation with light intensity- and frequency-dependent operation speed [296]. An another interesting concept utilizes azobenzene photoswitch-modified liquid crystal polymer surfaces to create propagating surface waves, that are capable of driving liquid flow. In the study of De Jong et al. the authors describe the theoretical basis of such systems and their capability to create and maintain peristaltic flow, liquid slug transport, and free-standing droplet transport [298].

3.4. Analytical applications

Although, most of the presented microfluidic surfaces can be applied for liquid flow generation in miniaturized analytical systems, the operation of sensing elements can also be based on or be affected by wetting properties [300,301].

The most popular, low detection limit wetting-based approach towards sensing and liquid analysis is the application of modified quartz crystal microbalances (QCM) [302-306]. The QCM sensing itself is based on detecting the changes in the resonance frequency of a quartz crystal. Upon coming in contact with liquid droplets, the resonance frequency will highly be influenced by the S/L-contact area, which is proportional to the wettability. As dissolved chemical species affect interfacial tensions, the rate and/or extent of spreading can be correlated with their concentration. Applying this principle, even the analysis of multicomponent biological samples, such as urine is possible. For this purpose, Esmeryan and Chaushev prepared soot-coated QCMs, which were able to distinguish human urine samples with different pH, protein, urea and uric acid contents [306].

Hu et al utilized superhydrophobic surfaces in creating triboelectric nanogenerator drop sensors, which can be applied in healthcare environment to monitor infusion speed [307].

It was shown earlier, that surfaces with patterned wettability can be utilized in microfluidic liquid manipulation, however, they may make sensing elements, as well. He et al. prepared superhydrophobic adhesive tapes through the deposition of fluoroalkylsilanized silica

particles [308]. The authors then etched suprheydrophilic spots to the surface via oxygen plasma treatment in which they immobilized a colorimetric indicator: the resulting patterned surfaces were then able to collect droplets of aqueous, heavy metal ion-containing (Cr(VI), Cu(Ⅱ) and Ni(Ⅱ)) solutions. As the ions competed the indicator for binding sites, the color intensity-change of the droplet could be correlated with their concentrations.

In aqueous medium, sensing elements are usually exposed to chemical changes (corrosion, dissolution etc.), adsorption of unwanted chemical species and the adhesion of microorganisms (fouling), which all can influence their operation [309]. To overcome these effects, sensing elements can also be made superhydrophobic [309]. Lin et al. prepared Cassie-Baxter-type superhydrophobic strain sensors [310]. As the authors presented in their manuscript, the wetting character contributed to the sensor durability and antiadhesivity towards bacteria in aqueous environment.

In the case of oxygen sensors, the oxygen consumption of the adhered bacteria can lead to false measurements. To surpass this issue, Melnikov et al. modified oxygen biosensors with low bacterial adhesion applying fluorosurfactant-modified nanodiamonds as roughening agent [311].

It is a common practice to render electrochemical sensors hydrophilic by applying suitable polymers, such as poly(ethylene glycol) (PEG) in order to prevent fouling with hydrophobic organics in aqueous media. This can be achieved both via physical- (coating) and chemical modifications (grafting) [309].

The operation of a sensing element can be based on stimulus-responsive wetting, as well. In an example, Gao et al. prepared pH-responsive superwettable surfaces on the basis of organosilane-modified ((3-[2-(2-amino ethylamino) ethylamino] propyl trimethoxy silane (AEPTMS) and octyl trimethoxy silane (OTMS)) [312]. Due to superhydrophobic-superhydrophilic transitions, pH, urea, and glucose were specifically detected just by naked-eye. From the glucose oxidase catalyzed reaction, the pH of the examined solution was decreased by the produced gluconic acid. So, upon the growing concentration of glucose, the value of water contact angle was decreased. This system allowed non-invasive diagnosis of diabetes in urine and saliva on by visible water contact angle variations (**Fig. 9**).

It is also possible to apply slippery sufaces for sensing purposes. The oil-swollen organogels of Gao et al. were capable of achieving sliding speeds and sliding angles based on the length of DNA strain, contained in a water droplet [313].

In conclusion, wettability can be utilized many ways in analytical scenarios, and due to its vast influence over the outcome of the sensing process, it should be taken into consideration upon developing new methods and devices, as well.

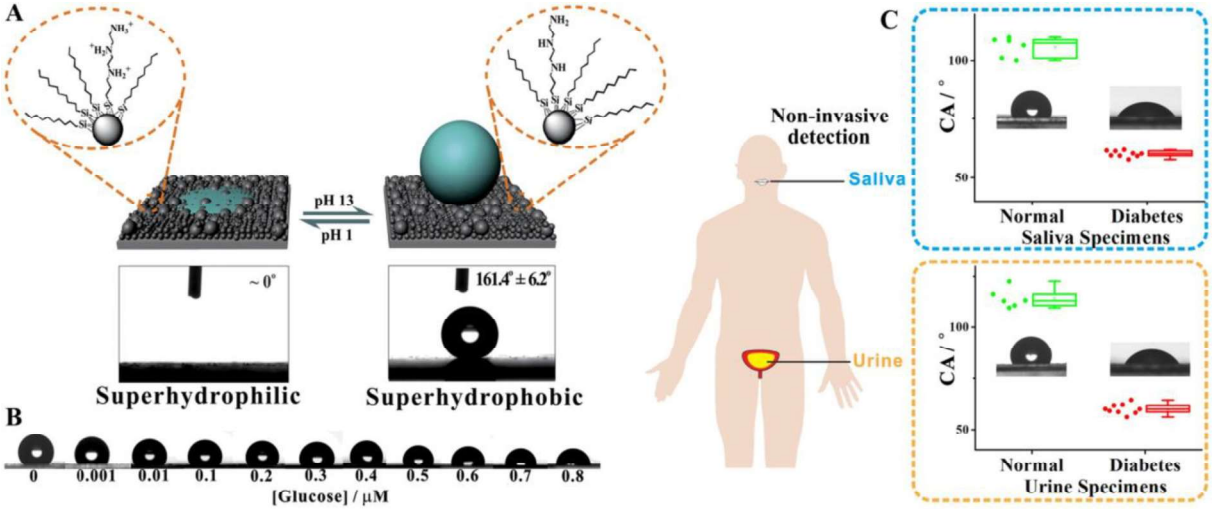

Figure 9. Working principle of the switching of the pH-responsive superwetting surface properties is shown, where a CA of water droplet decreased to ~0° at pH 1 and increased to 161.4° ± 6.2° at pH 13. **A** Wetting states of droplets with different concentrations of glucose within the linear range. **B** Corresponding to hydrophobicity, and those from patients with diabetes decreased to nearly 50°, indicating the hydrophilicity of the surface. **C** Non-invasive detection of saliva and urine obtained from nine patients with diabetes and six normal people illustrating that the CA can be employed to distinguish between samples of people with diabetes and normal people. **D** [301]

3.5. Moisture collection

As we have seen in the case of microfluidic systems, the application of surfaces with wettability gradients or patterned wettability [314] are highly preferred in creating, controlling and maintaining liquid flow. An another popular field of application is moisture (dew or fog) collection, where these patterned surfaces have dual functionality: the lyophilic surface domains act as seeds of condensation and provide area for drop coalescence, while the presence of lyophobic or superlyophobic domains promotes directed drop-rolloff after the sum of gravitational and mechanical forces on the droplets overcompensates adhesion [315]. In a case when a droplet is only influenced by downward gravitational pull on a flat surface, the following equation applies upon the initiation of droplet movement: $m \times g \times \sin\alpha = \gamma_{LG} \times (\cos\Theta_R - \cos\Theta_A) \times w$ (**Eq. 5**), in which m is the droplet mass, g is the gravitational acceleration,

α is the angle of the inclination of the surface, γ_{LG}, Θ_R and Θ_A respectively are the surface tension, the advancing and the receding contact angles of the liquid, while w stands for the width of the droplet. As this equation shows, surfaces with lower contact angle hysteresis generally offer increased renewability [315], as smaller droplets can roll off and form again during continuous condensation, however, real life scenarios are more complex. Among the other influencing factors, the most noteworthy are the heat transfer [316], the area-to-area ratio of lyophobic and lyophilic domains and their patterns [317], the surface roughness [318,319], besides the macroscopic shape of the moisture collecting surface is also crucial [320]. The speed of condensation is generally higher (due to drop growth-facilitating aerodynamical conditions) on macroscopic edges or fibers [321-323], therefore the most popular commercial moisture collection systems utilize different nets or meshes as condensation surfaces [324,325]. Another crucial parameter is the liquid transportation capability [315]. The driving force (F) of liquid transportation on a wettability-patterned harvesting surface is described by this equation:

$$F = \gamma_{LG} \times (\cos\Theta_1 - \cos\Theta_2) \quad \textbf{(Eq. 6)}$$

, where Θ_1 and Θ_2 are the contact angles of two neighbouring wetting domains. Several scenarios utilize Laplace pressure gradient to facilitate liquid transportation, by applying conical- or cylindrical-shaped channels [317], as well.

The preferred low contact angle hysteresis is achievable both by elaborating rough superlyophobic domains [314,318,319], or by applying slippery surfaces (as biomimetic models of pitcher plants) [326,327], however, in this case the collected liquid may get contaminated with the lubricant. The more emphasized superlyophobicity (like in the case of lotus leaves) can lead to decreased drop sizes, which thanks to the higher surface area-to-volume ratio results in faster evaporation, therefore in lower collection efficiency [328,329]. However, the more lyophilic surfaces promote coalescence and adhesion, besides improving film-forming capability, as well, which latter can also lead to increased heat transfer and faster evaporation in some cases [328]. Taking these considerations into account, the proper patterning of surface wettability becomes even more important in reaching an optimally high liquid collection efficiency.

Aside the principles, practical moisture collection research is solely focused on water (especially Atmospheric Water Harvesting, or AWH), as clean water in some areas of the world are inaccessible by any other means [330]. Despite the importance of this field and the high number of studies, it is difficult to objectively compare the water collection efficiencies of different surfaces to each other, as harvesting (fogging or dewing) and other experimental conditions and surface parameters (such as relative humidity, temperature, air flow rates,

inclination, shape etc.) can vary. Therefore, to comply with the rest of this review, in the followings, the influence of different wettability conditions will be discussed through a few literature examples.

Nioras et al. studied the water collection ability of different plain and plasma-etched rough, and hydrophobized plexiglass surfaces. Their study concludes, that the increased time of plasma treatment (and therefore the oncreased roughness) and the concomittant hydrophobization results in increased hydrophobicity, decreased contact angle hysteresis and increased collection efficiency both under fogging and dewing conditions [316].

Seo and coworkers compared the water collecting efficiency of different modified and slippery liquid-infused copper tube surfaces [320]. The authors came to the conclusion, that the water collection efficiency could be increased by decreasing the viscosity of the silicone oil lubricant, In this study the authors also point out the main difference between the dew and fog collecting scenarios: in the case of foggy conditions, the droplet collection on the surface is mainly the result of the droplets' collisions with the surface, regardless of its wettability, while in the case of dew harvest, the overall wettability matters more as primary condensation seeds are vital.

Bai et al. used fluoroalkylsilanes (FAS) to hydrophobize superhydrophilic spin-coated TiO_2 particle coatings, then applied UV-photolytography to produce different superhydrophilic patterns on them [317] (**Fig. 10**). According to their results, the star-shaped patterns - especially the 5-pointed star patterns - collected more water than circle-shaped patterns, thanks to the Laplace pressure difference. However, upon increasing the number of branches in the star pattern, the hydrophilic domains may overlap, leading to higher adhesion and therefore less efficient droplet transport.

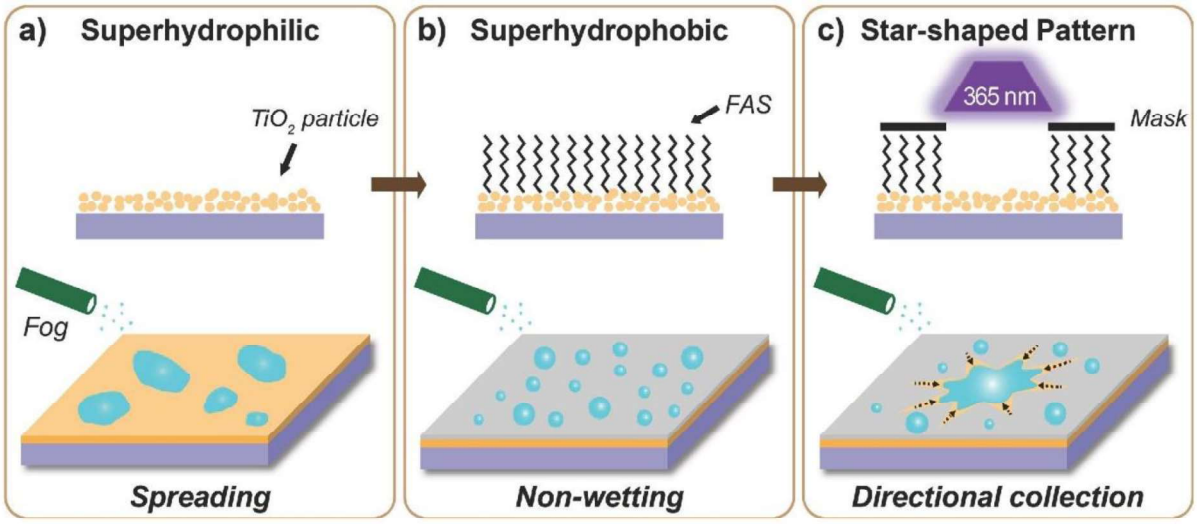

Figure 10. Schematic illustration of the fabrication process of bioinspired surfaces with star-shaped wettability patterns. **a)** Superhydrophilic surface composed of TiO_2 nanoparticles, where fog droplets spread (the bottom). **b)** Superhydrophobic surface modified with FAS showing non-wetting property to fog droplets (the bottom). **c)** Bioinspired gradient surface with a star-shaped wettability pattern. It is realized by illuminating the FAS-modified film under UV light with a photomask. The fog droplets would be collected directionally toward the star-shape region, which is more wettable (the bottom). [317]

Nature also inspires water collection surface research [331], as there are several – mainly desert – species (e.g. Namib desert grass (*Stipagrostis sabulicola*) and cactus (*Opuntia microdasys*) with unique fog or dew collecting capabilities. For example, the surfaces of Ghurera and Bushan mimicked the fog harvesting mechanism of the Namid desert beetle (*Stenocara gracilipes*) [328]: in their study, hydrophilic domains on hydrophobized silica micro- (d=10 μm) and nanoparticle (d=7 nm) coatings were elaborated via UV-photolitography. According to the authors' findings, the nanoparticle coatings provided more efficient water collection, thanks to the larger overall condensation surface area.

As the presented examples show, the research area of liquid collection is already well-developed, however, there are a few limitations ahead of the literature examples to overcome in order to become applicable in real life scenarios. These limitations include the vulnerability and foulability of rough surfaces, beside the fact, that some popular raw materials (such as fluorinated species and lubricants) may cause contamination.

4. Conclusions

As the presented examples show, the utilization of different surface wetting characters is widespread and more and more sophisticated functional systems and their applications are gaining ground, especially at the field of microfluidics and analytics. The existing functional surfaces may offer new and sustainable solutions to emerging healthcare or environmental problems, however, there are still many limitations left to overcome, including the vulnerability of rough structures, or cost-efficiency and scalability issues, which are interesting subjects of future research.

Regarding the scalability issues, as well, the application of chemical and especially the physical deposition methods in the elaboration of functional surfaces may lead to inhomogenous and/or irregularly patterned distribution of surface functionalities and therefore non-uniform wetting and wetting-related properties. These surfaces also subjected to the desorption of the functionalizing agents. Therefore, this aspect must be dealt with when conducting related research, including both the preparative and the respective analytical scenarios.

Although, the field of liquid manipulation and microfluidics are rapidly developing, these considerations are of even higher importance when we deal with smaller overall S/L contact areas. This not surprisingly implies the superiority of microfabrication techniques over common chemical and physical preparation methods (both additive and destructive), which is on the other hand leads to the above mentioned production scaling issues.

Another concerns may rise from the toxicity of raw materials, applied in best available techniques of functional surface elaboration. For example, although, the low surface free energy superhydrophobic surfaces are preferably achieved through the applications of different fluorinated polymers, these and their by- and decomposition products may cause environmental and healthcare issues due to their persistency. Therefore, their feasible substition in functional surfaces is also of high importance. This consideration especially applies to antimicrobial or other healthcare applications, where the harmfullness towards humans and other advanced lifeforms should be minimized. This can be achieved by lowering the use of biocidal agents (e.g. organic biocides or noble metal cations) and raw materials (e.g. cationic polymers) besides putting the emphasis on the elaboration of anti-adhesive character. The generation of reactive oxidative radicals via photocatalyst content may have bigger perspectives, as these systems offer antimicrobial scenarios with lesser impact on the environment and human health as these

radicals have low lifetime and therefore the biocidal effect is practically surface-localized both at the S/L and at the S/G interfaces, as well.

Regarding the oil-water separation surfaces, the separation of surfactantless mixtures is well manageable with the best available technologies, however, - despite the proposed industrial benefits are tempting - the development of economical systems, being capable of handling surfactant-containing emulsions on a larger scale still means a challenge.

As the full potential in this field of materials science is yet-to-be-exploited, the development and utilization of surfaces with wetting-related functionalities will inevitably reach further milestones with the constant development of microfabrication techniques (especially 3D-printing), with the more and more sophisticated approaches towards stimulus-responsiveness and as researches address the main, mentioned drawbacks of the existing systems.

Acknowledgements

The paper was prepared with the professional support of the Doctoral Student Scholarship Program of the Co-operative Doctoral Program of the Ministry of Innovation and Technology financed from the National Research, Development and Innovation Fund. The authors are also very thankful for the financial support from the Hungarian Scientific Research Fund (OTKA) K 132446 and FK 142437. This paper was also supported by the János Bolyai Research Scholarship of the Hungarian Academy of Sciences.

References

[1] Frenkel-Pinter M, Rajaei V, Glass JB, Hud N V., Williams LD. Water and Life: The Medium is the Message. J Mol Evol 2021;89:2–11. https://doi.org/10.1007/s00239-020-09978-6

[2] Farhadi T. Advances in protein tertiary structure prediction. Biomed Biotechnol Res J 2018;2:20. https://doi.org/10.4103/bbrj.bbrj_94_17

[3] van Meer G, Voelker DR, Feigenson GW. Membrane lipids: where they are and how they behave. Nat Rev Mol Cell Biol 2008;9:112–24. https://doi.org/10.1038/nrm2330

[4] Li J, Wang X, Zhang T, Wang C, Huang Z, Luo X, et al. A review on phospholipids and their main applications in drug delivery systems. Asian J Pharm Sci 2015;10:81–98. https://doi.org/10.1016/j.ajps.2014.09.004

[5] van Honschoten JW, Brunets N, Tas NR. Capillarity at the nanoscale. Chem Soc Rev 2010;39:1096. https://doi.org/10.1039/b909101g

[6] Chang H, Liu B, Zhang Z, Pawar R, Yan Z, Crittenden JC, et al. A Critical Review of Membrane Wettability in Membrane Distillation from the Perspective of Interfacial Interactions. Environ Sci Technol 2021;55:1395–418. https://doi.org/10.1021/acs.est.0c05454

[7] Kaplan WD, Chatain D, Wynblatt P, Carter WC. A review of wetting versus adsorption, complexions, and related phenomena: the rosetta stone of wetting. J Mater Sci 2013;48:5681–717. https://doi.org/10.1007/s10853-013-7462-y

[8] Gharabaghi M, Aghazadeh S. A review of the role of wetting and spreading phenomena on the flotation practice. Curr Opin Colloid Interface Sci 2014;19:266–82. https://doi.org/10.1016/j.cocis.2014.07.004

[9] Lu G, Wang X-D, Duan Y-Y. A Critical Review of Dynamic Wetting by Complex Fluids: From Newtonian Fluids to Non-Newtonian Fluids and Nanofluids. Adv Colloid Interface Sci 2016;236:43–62. https://doi.org/10.1016/j.cis.2016.07.004

[10] Li S, Huang J, Chen Z, Chen G, Lai Y. A review on special wettability textiles: theoretical models, fabrication technologies and multifunctional applications. J Mater Chem A 2017;5:31–55. https://doi.org/10.1039/C6TA07984A

[11] Wang Z, Elimelech M, Lin S. Environmental Applications of Interfacial Materials with Special Wettability. Environ Sci Technol 2016;50:2132–50. https://doi.org/10.1021/acs.est.5b04351

[12] Goh PS, Naim R, Rahbari-Sisakht M, Ismail AF. Modification of membrane hydrophobicity in membrane contactors for environmental remediation. Sep Purif Technol 2019;227:115721. https://doi.org/10.1016/j.seppur.2019.115721

[13] Wang J, Wang H, Xie J, Yang A, Pei A, Wu C-L, et al. Fundamental study on the wetting property of liquid lithium. Energy Storage Mater 2018;14:345–50. https://doi.org/10.1016/j.ensm.2018.05.021

[14] Shin S, Seo J, Han H, Kang S, Kim H, Lee T. Bio-Inspired Extreme Wetting Surfaces for Biomedical Applications. Materials (Basel) 2016;9:116. https://doi.org/10.3390/ma9020116

[15] Khan MF, Luong N, Kurian J, Brook MA. Superwetting comonomers reduce adhesion of E. coli BL21. Chem Commun 2017;53:3050–3. https://doi.org/10.1039/C6CC09984J

[16] Drelich J. Guidelines to measurements of reproducible contact angles using a sessile-drop technique. Surf Innov 2013;1:248–54. https://doi.org/10.1680/si.13.00010

[17] Schuster JM, Schvezov CE, Rosenberger MR. Influence of Experimental Variables on the Measure of Contact Angle in Metals Using the Sessile Drop Method. Procedia Mater Sci 2015;8:742–51. https://doi.org/10.1016/j.mspro.2015.04.131

[18] Albert E, Tegze B, Hajnal Z, Zámbó D, Szekrényes DP, Deák A, et al. Robust Contact Angle Determination for Needle-in-Drop Type Measurements. ACS Omega 2019;4:18465–71. https://doi.org/10.1021/acsomega.9b02990

[19] Eral HB, 't Mannetje DJCM, Oh JM. Contact angle hysteresis: a review of fundamentals and applications. Colloid Polym Sci 2013;291:247–60. https://doi.org/10.1007/s00396-012-2796-6

[20] Jafari M, Jung J. Direct Measurement of Static and Dynamic Contact Angles Using a Random Micromodel Considering Geological CO2 Sequestration. Sustainability 2017;9:2352. https://doi.org/10.3390/su9122352

[21] Aliabadi M, Konrad W, Stegmaier T, Arnim V, Kaya C, Liu Y, et al. A novel method for measuring dynamic contact angles of fibers with spindle- knots. J Appl Polym Sci 2021;138. https://doi.org/10.1002/app.50673

[22] Gao L, McCarthy TJ. Contact Angle Hysteresis Explained. Langmuir 2006;22:6234–7. https://doi.org/10.1021/la060254j

[23] Volpe C Della, Siboni S. The Wilhelmy method: a critical and practical review. Surf Innov 2018;6:120–32. https://doi.org/10.1680/jsuin.17.00059

[24] Hasegawa M, Endo H, Morita K, Sakaue H, Kimura S. Behavior of Sliding Angle as Function of Temperature Difference between Droplet and Superhydrophobic Coating for Aircraft Ice Protection Systems. Aerospace 2021;8:219. https://doi.org/10.3390/aerospace8080219

[25] Gonzales J, Kurihara D, Maeda T, Yamazaki M, Saruhashi T, Kimura S, et al. Novel Superhydrophobic Surface with Solar-Absorptive Material for Improved De-Icing Performance. Materials (Basel) 2019;12:2758. https://doi.org/10.3390/ma12172758

[26] Huhtamäki T, Tian X, Korhonen JT, Ras RHA. Surface-wetting characterization using contact-angle measurements. Nat Protoc 2018;13:1521–38. https://doi.org/10.1038/s41596-018-0003-z

[27] Gong Y, Xu J, Buchanan RC. Surface roughness: A review of its measurement at micro-/nano-scale. Phys Sci Rev 2018;3. https://doi.org/10.1515/psr-2017-0057

[28] Jothi Prakash CG, Prasanth R. Approaches to design a surface with tunable wettability: a review on surface properties. J Mater Sci 2021;56:108–35. https://doi.org/10.1007/s10853-020-05116-1

[29] Li C, Li M, Ni Z, Guan Q, Blackman BRK, Saiz E. Stimuli-responsive surfaces for switchable wettability and adhesion. J R Soc Interface 2021;18:20210162. https://doi.org/10.1098/rsif.2021.0162

[30] Zeng Q. Size matching effect on Wenzel wetting on fractal surfaces. Results Phys 2018;10:588–93. https://doi.org/10.1016/j.rinp.2018.07.010

[31] McHale G. Cassie and Wenzel: Were They Really So Wrong? Langmuir 2007;23:8200–5. https://doi.org/10.1021/la7011167

[32] Bhushan B, Nosonovsky M. The rose petal effect and the modes of superhydrophobicity. Philos Trans R Soc A Math Phys Eng Sci 2010;368:4713–28. https://doi.org/10.1098/rsta.2010.0203

[33] Bormashenko E. Physics of solid–liquid interfaces: From the Young equation to the superhydrophobicity (Review Article). Low Temp Phys 2016;42:622–35. https://doi.org/10.1063/1.4960495

[34] Cao F, Guan Z, Li D. Preparation of material surface structure similar to hydrophobic structure of lotus leaf. J Wuhan Univ Technol Sci Ed 2008;23:513–7. https://doi.org/10.1007/s11595-007-4513-8

[35] Giacomello A, Meloni S, Chinappi M, Casciola CM. Cassie–Baxter and Wenzel States on a Nanostructured Surface: Phase Diagram, Metastabilities, and Transition Mechanism by Atomistic Free Energy Calculations. Langmuir 2012;28:10764–72. https://doi.org/10.1021/la3018453

[36] Sarkar A, Kietzig A-M. Design of a robust superhydrophobic surface: thermodynamic and kinetic analysis. Soft Matter 2015;11:1998–2007. https://doi.org/10.1039/C4SM02787F

[37] Liu S, Zhou Z, Zhou S, Cui J, Wang Q, Zhang Y, et al. Fabrication of acrylamide decorated superhydrophilic and underwater superoleophobic poly(vinylidene fluoride) membranes for oil/water emulsion separation. J Taiwan Inst Chem Eng 2019;95:300–7. https://doi.org/10.1016/j.jtice.2018.07.015

[38] Anis SF, Lalia BS, Hashaikeh R, Hilal N. Hierarchical underwater oleophobic electro-ceramic/carbon nanostructure membranes for highly efficient oil-in-water separation. Sep Purif Technol 2021;275:119241. https://doi.org/10.1016/j.seppur.2021.119241

[39] Hongru A, Xiangqin L, Shuyan S, Ying Z, Tianqing L. Measurement of Wenzel roughness factor by laser scanning confocal microscopy. RSC Adv 2017;7:7052–9. https://doi.org/10.1039/C6RA26897H

[40] Li C, Zhang J, Han J, Yao B. A numerical solution to the effects of surface roughness on water–coal contact angle. Sci Rep 2021;11:459. https://doi.org/10.1038/s41598-020-80729-9

[41] De Nicola F, Viola I, Tenuzzo LD, Rasch F, Lohe MR, Nia AS, et al. Wetting Properties of Graphene Aerogels. Sci Rep 2020;10:1916. https://doi.org/10.1038/s41598-020-58860-4

[42] Lopes DM, Ramos SMM, de Oliveira LR, Mombach JCM. Cassie–Baxter to Wenzel state wetting transition: a 2D numerical simulation. RSC Adv 2013;3:24530. https://doi.org/10.1039/c3ra45258a

[43] Garg P, Ghatmale P, Tarwadi K, Chavan S. Influence of Nanotechnology and the Role of Nanostructures in Biomimetic Studies and Their Potential Applications. Biomimetics 2017;2:7. https://doi.org/10.3390/biomimetics2020007

[44] Zhang Y, Wu H, Yu X, Chen F, Wu J. Microscopic Observations of the Lotus Leaf for Explaining the Outstanding Mechanical Properties. J Bionic Eng 2012;9:84–90. https://doi.org/10.1016/S1672-6529(11)60100-5

[45] Li J, Wang G, Meng Q, Ding C, Jiang H, Fang Y. A biomimetic nano hybrid coating based on the lotus effect and its anti-biofouling behaviors. Appl Surf Sci 2014;315:407–14. https://doi.org/10.1016/j.apsusc.2014.07.147

[46] Xu Q, Zhang W, Dong C, Sreeprasad TS, Xia Z. Biomimetic self-cleaning surfaces: synthesis, mechanism and applications. J R Soc Interface 2016;13:20160300. https://doi.org/10.1098/rsif.2016.0300

[47] Riedel J, Vucko MJ, Blomberg SP, Schwarzkopf L. Skin hydrophobicity as an adaptation for self- cleaning in geckos. Ecol Evol 2020;10:4640–51. https://doi.org/10.1002/ece3.6218

[48] Stark AY, Mitchell CT. Stick or Slip: Adhesive Performance of Geckos and Gecko-Inspired Synthetics in Wet Environments. Integr Comp Biol 2019;59:214–26. https://doi.org/10.1093/icb/icz008

[49] Shen Y, Wu Z, Tao J, Jia Z, Chen H, Liu S, et al. Spraying Preparation of Eco-Friendly Superhydrophobic Coatings with Ultralow Water Adhesion for Effective Anticorrosion and Antipollution. ACS Appl Mater Interfaces 2020;12:25484–93. https://doi.org/10.1021/acsami.0c06074

[50] Meena MK, Sinhamahapatra A, Kumar A. Superhydrophobic polymer composite coating on glass via spin coating technique. Colloid Polym Sci 2019;297:1499–505. https://doi.org/10.1007/s00396-019-04560-z

[51] Janovák L, Dernovics Á, Mérai L, Deák Á, Sebők D, Csapó E, et al. Microstructuration of poly(3-hexylthiophene) leads to bifunctional superhydrophobic and photoreactive surfaces. Chem Commun 2018;54:650–3. https://doi.org/10.1039/C7CC07671A

[52] Wang H, Sun F, Wang C, Zhu Y, Wang H. A simple drop-casting approach to fabricate the super-hydrophobic PMMA-PSF-CNFs composite coating with heat-, wear- and corrosion-resistant properties. Colloid Polym Sci 2016;294:303–9. https://doi.org/10.1007/s00396-015-3772-8

[53] Guo X-J, Xue C-H, Sathasivam S, Page K, He G, Guo J, et al. Fabrication of robust superhydrophobic surfaces via aerosol-assisted CVD and thermo-triggered healing of superhydrophobicity by recovery of roughness structures. J Mater Chem A 2019;7:17604–12. https://doi.org/10.1039/C9TA03264A

[54] Li A, Wang G, Ma Y, Zhao C, Zhang F, He Q, et al. Study on preparation and properties of superhydrophobic surface of RTV silicone rubber. J Mater Res Technol 2021;11:135–43. https://doi.org/10.1016/j.jmrt.2020.12.074

[55] Wang F, Lei S, Xu Y, Ou J. Green Approach to the Fabrication of Superhydrophobic Mesh Surface for Oil/Water Separation. ChemPhysChem 2015;16:2237–43. https://doi.org/10.1002/cphc.201500138

[56] Wang G, Song D, Qiao Y, Cheng J, Liu H, Jiang J, et al. Developing super-hydrophobic and corrosion-resistant coating on magnesium-lithium alloy via one-step hydrothermal processing. J Magnes Alloy 2021. https://doi.org/10.1016/j.jma.2021.08.002

[57] Qing Y, Long C, An K, Hu C, Liu C. Sandpaper as template for a robust superhydrophobic surface with self-cleaning and anti-snow/icing performances. J Colloid Interface Sci 2019;548:224–32. https://doi.org/10.1016/j.jcis.2019.04.040

[58] Liu Z, Pang X, Wang K, Lv X, Cui X. Superhydrophobic Coatings Prepared by the in Situ Growth of Silicone Nanofilaments on Alkali-Activated Geopolymers Surface. ACS Appl Mater Interfaces 2019;11:22809–16. https://doi.org/10.1021/acsami.9b07990

[59] Dong Z, Vuckovac M, Cui W, Zhou Q, Ras RHA, Levkin PA. 3D Printing of Superhydrophobic Objects with Bulk Nanostructure. Adv Mater 2021;33:2106068. https://doi.org/10.1002/adma.202106068

[60] Wang C, Yao T, Wu J, Ma C, Fan Z, Wang Z, et al. Facile Approach in Fabricating Superhydrophobic and Superoleophilic Surface for Water and Oil Mixture Separation. ACS Appl Mater Interfaces 2009;1:2613–7. https://doi.org/10.1021/am900520z

[61] Liu M, Li M-T, Xu S, Yang H, Sun H-B. Bioinspired Superhydrophobic Surfaces via Laser-Structuring. Front Chem 2020;8. https://doi.org/10.3389/fchem.2020.00835

[62] Du K, Jiang Y, Liu Y, Wathuthanthri I, Choi C-H. Manipulation of the Superhydrophobicity of Plasma-Etched Polymer Nanostructures. Micromachines 2018;9:304. https://doi.org/10.3390/mi9060304

[63] Li F, Yu Z, Shi H, Yang Q, Chen Q, Pan Y, et al. A Mussel-inspired method to fabricate reduced graphene oxide/g-C 3 N 4 composites membranes for catalytic decomposition and oil-in-water emulsion separation. Chem Eng J 2017;322:33–45. https://doi.org/10.1016/j.cej.2017.03.145

[64] Badica P, Batalu ND, Burdusel M, Grigoroscuta MA, Aldica G, Enculescu M, et al. Antibacterial composite coatings of MgB2 powders embedded in PVP matrix. Sci Rep 2021;11:9591. https://doi.org/10.1038/s41598-021-88885-2

[65] Kim J-H, Mirzaei A, Kim HW, Kim SS. Facile fabrication of superhydrophobic surfaces from austenitic stainless steel (AISI 304) by chemical etching. Appl Surf Sci 2018;439:598–604. https://doi.org/10.1016/j.apsusc.2017.12.211

[66] Marlena J, Tan JKS, Lin Z, Li DX, Zhao B, Leo HL, et al. Monolithic polymeric porous superhydrophobic material with pneumatic plastron stabilization for functionally durable drag reduction in blood-contacting biomedical applications. NPG Asia Mater 2021;13:58. https://doi.org/10.1038/s41427-021-00325-9

[67] Gong D, Long J, Jiang D, Fan P, Zhang H, Li L, et al. Robust and Stable Transparent Superhydrophobic Polydimethylsiloxane Films by Duplicating via a Femtosecond Laser-Ablated Template. ACS Appl Mater Interfaces 2016;8:17511–8. https://doi.org/10.1021/acsami.6b03424

[68] Wang X-Y, Zhang C, Sun S, Kalulu M, Chen L, Zhou X, et al. Durable superhydrophobic coating based on inorganic/organic double-network polysiloxane and functionalized nanoparticles. Colloids Surfaces A Physicochem Eng Asp 2019;578:123550. https://doi.org/10.1016/j.colsurfa.2019.06.016

[69] Ma J, Porath LE, Haque MF, Sett S, Rabbi KF, Nam S, et al. Ultra-thin self-healing vitrimer coatings for durable hydrophobicity. Nat Commun 2021;12:5210. https://doi.org/10.1038/s41467-021-25508-4

[70] Xiang S, Liu W. Self- Healing Superhydrophobic Surfaces: Healing Principles and Applications. Adv Mater Interfaces 2021;8:2100247. https://doi.org/10.1002/admi.202100247

[71] Yuan G, Liu Y, Ngo C-V, Guo C. Rapid fabrication of anti-corrosion and self-healing superhydrophobic aluminum surfaces through environmentally friendly femtosecond laser processing. Opt Express 2020;28:35636. https://doi.org/10.1364/OE.400804

[72] Shen Y, Wu Y, Shen Z, Chen H. Fabrication of Self-healing Superhydrophobic Surfaces from Water-Soluble Polymer Suspensions Free of Inorganic Particles through Polymer Thermal Reconstruction. Coatings 2018;8:144. https://doi.org/10.3390/coatings8040144

[73] Mérai L, Varga N, Deák Á, Sebők D, Szenti I, Kukovecz Á, et al. Preparation of photocatalytic thin films with composition dependent wetting properties and self-healing ability. Catal Today 2019;328:85–90. https://doi.org/10.1016/j.cattod.2018.10.015

[74] Tu K, Wang X, Kong L, Guan H. Facile preparation of mechanically durable, self-healing and multifunctional superhydrophobic surfaces on solid wood. Mater Des 2018;140:30–6. https://doi.org/10.1016/j.matdes.2017.11.029

[75] Villegas M, Zhang Y, Abu Jarad N, Soleymani L, Didar TF. Liquid-Infused Surfaces: A Review of Theory, Design, and Applications. ACS Nano 2019;13:8517–36. https://doi.org/10.1021/acsnano.9b04129

[76] Wei C, Zhang G, Zhang Q, Zhan X, Chen F. Silicone Oil-Infused Slippery Surfaces Based on Sol–Gel Process-Induced Nanocomposite Coatings: A Facile Approach to Highly Stable Bioinspired Surface for Biofouling Resistance. ACS Appl Mater Interfaces 2016;8:34810–9. https://doi.org/10.1021/acsami.6b09879

[77] Juuti P, Haapanen J, Stenroos C, Niemelä-Anttonen H, Harra J, Koivuluoto H, et al. Achieving a slippery, liquid-infused porous surface with anti-icing properties by direct deposition of flame synthesized aerosol nanoparticles on a thermally fragile substrate. Appl Phys Lett 2017;110:161603. https://doi.org/10.1063/1.4981905

[78] Long Y, Yin X, Mu P, Wang Q, Hu J, Li J. Slippery liquid-infused porous surface (SLIPS) with superior liquid repellency, anti-corrosion, anti-icing and intensified durability for protecting substrates. Chem Eng J 2020;401:126137. https://doi.org/10.1016/j.cej.2020.126137

[79] Kim SJ, Kim HN, Lee SJ, Sung HJ. A lubricant-infused slip surface for drag reduction. Phys Fluids 2020;32:091901. https://doi.org/10.1063/5.0018460

[80] Rao Q, Lu Y, Song L, Hou Y, Zhan X, Zhang Q. Highly Efficient Self-Repairing Slippery Liquid-Infused Surface with Promising Anti-Icing and Anti-Fouling Performance. ACS Appl Mater Interfaces 2021;13:40032–41. https://doi.org/10.1021/acsami.1c09491

[81] Chang C-C, Wu C-J, Sheng Y-J, Tsao H-K. Anti-smudge behavior of facilely fabricated liquid-infused surfaces with extremely low contact angle hysteresis property. RSC Adv 2016;6:19214–22. https://doi.org/10.1039/C5RA27699C

[82] Armstrong S, McHale G, Ledesma-Aguilar R, Wells GG. Evaporation and Electrowetting of Sessile Droplets on Slippery Liquid-Like Surfaces and Slippery Liquid-Infused Porous Surfaces (SLIPS). Langmuir 2020;36:11332–40. https://doi.org/10.1021/acs.langmuir.0c02020

[83] Rupp F, Gittens RA, Scheideler L, Marmur A, Boyan BD, Schwartz Z, et al. A review on the wettability of dental implant surfaces I: Theoretical and experimental aspects. Acta Biomater 2014;10:2894–906. https://doi.org/10.1016/j.actbio.2014.02.040

[84] Berry M V. The molecular mechanism of surface tension. Phys Educ 1971;6:001. https://doi.org/10.1088/0031-9120/6/2/001

[85] Gong X, Wang B, Li L. Spreading of Nanodroplets of Ionic Liquids on the Mica Surface. ACS Omega 2018;3:16398–402. https://doi.org/10.1021/acsomega.8b02423

[86] Guba S, Horváth B, Szalai I. Examination of contact angles of magnetic fluid droplets on different surfaces in uniform magnetic field. J Magn Magn Mater 2020;498:166181. https://doi.org/10.1016/j.jmmm.2019.166181

[87] De S, Malik S, Ghosh A, Saha R, Saha B. A review on natural surfactants. RSC Adv 2015;5:65757–67. https://doi.org/10.1039/C5RA11101C

[88] Yao Y, Wei M, Kang W. A review of wettability alteration using surfactants in carbonate reservoirs. Adv Colloid Interface Sci 2021;294:102477. https://doi.org/10.1016/j.cis.2021.102477

[89] Liu S, Liu J, Liu G, Liu Y, Zhong H. Modulation of the morphology, surface energy and wettability of malachite through a S,O,O-ligand surfactant: Mechanism and hydrophobization. Appl Surf Sci 2020;505:144467. https://doi.org/10.1016/j.apsusc.2019.144467

[90] Wang X, Yuan S, Jiang B. Wetting Process and Adsorption Mechanism of Surfactant Solutions on Coal Dust Surface. J Chem 2019;2019:1–9. https://doi.org/10.1155/2019/9085310

[91] Surfactant Adsorption at Solid Surfaces. Surf. Chem. Surfactants Polym., Chichester, UK: John Wiley & Sons, Ltd; 2014, p. 153–73. https://doi.org/10.1002/9781118695968.ch8

[92] Al-Wahaibi Y, Al-Hashmi A-A, Joshi S, Mosavat N, Rudyk S, Al-Khamisi S, et al. Mechanistic Study of Surfactant/Polymer Adsorption and Its Effect on Surface Morphology and Wettability. Day 2 Wed, April 05, 2017, SPE; 2017. https://doi.org/10.2118/185327-MS

[93] Wang R, Hashimoto K, Fujishima A, Chikuni M, Kojima E, Kitamura A, et al. Light-induced amphiphilic surfaces. Nature 1997;388:431–2. https://doi.org/10.1038/41233

[94] Madeira DMF, Vieira O, Pinheiro LA, de Melo Carvalho B. Correlation between Surface Energy and Adhesion Force of Polyethylene/Paperboard: A Predictive Tool for Quality Control in Laminated Packaging. Int J Chem Eng 2018;2018:1–7. https://doi.org/10.1155/2018/2709037

[95] ZISMAN WA. Relation of the Equilibrium Contact Angle to Liquid and Solid Constitution, 1964, p. 1–51. https://doi.org/10.1021/ba-1964-0043.ch001

[96] Annamalai M, Gopinadhan K, Han SA, Saha S, Park HJ, Cho EB, et al. Surface energy and wettability of van der Waals structures. Nanoscale 2016;8:5764–70. https://doi.org/10.1039/C5NR06705G

[97] Wu S. Calculation of interfacial tension in polymer systems. J Polym Sci Part C Polym Symp 2007;34:19–30. https://doi.org/10.1002/polc.5070340105

[98] Chibowski E. Surface free energy of a solid from contact angle hysteresis. Adv Colloid Interface Sci 2003;103:149–72. https://doi.org/10.1016/S0001-8686(02)00093-3

[99] Bedford MS, Yang X, Jolly KM, Binnicker RL, Cramer SB, Keen CE, et al. Tetraarylphosphonium polyelectrolyte chromophores: synthesis, stability, photophysics, film morphology and critical surface energy. Polym Chem 2015;6:900–8. https://doi.org/10.1039/C4PY01483A

[100] Fowkes FM. Determination of interfacial tensions, contact angles, and dispersion forces in surfaces by assumingadditivity of intermolecular interactions in surfaces. J Phys Chem 1962;66:382–382. https://doi.org/10.1021/j100808a524

[101] Kozbial A, Li Z, Conaway C, McGinley R, Dhingra S, Vahdat V, et al. Study on the Surface Energy of Graphene by Contact Angle Measurements. Langmuir 2014;30:8598–606. https://doi.org/10.1021/la5018328

[102] Owens DK, Wendt RC. Estimation of the surface free energy of polymers. J Appl Polym Sci 1969;13:1741–7. https://doi.org/10.1002/app.1969.070130815

[103] Jie-Rong C, Wakida T. Studies on the surface free energy and surface structure of PTFE film treated with low temperature plasma. J Appl Polym Sci 1997;63:1733–9. https://doi.org/10.1002/(SICI)1097-4628(19970328)63:13<1733::AID-APP4>3.0.CO;2-H

[104] Park S-M, Roy R, Kweon J-H, Nam Y. Strength and failure modes of surface treated CFRP secondary bonded single-lap joints in static and fatigue tensile loading regimes. Compos Part A Appl Sci Manuf 2020;134:105897. https://doi.org/10.1016/j.compositesa.2020.105897

[105] Kaelble DH. Dispersion-Polar Surface Tension Properties of Organic Solids. J Adhes 1970;2:66–81. https://doi.org/10.1080/0021846708544582

[106] Rabel W. Einige Aspekte der Benetzungstheorie un ihre Anwendung auf die Untersuchung und Veränderung der Oberflächeneigenschaften von Polymeren. Farbe und Lack 1971;77:997–1005.

[107] Wu S. Polar and Nonpolar Interactions in Adhesion. J Adhes 1973;5:39–55. https://doi.org/10.1080/00218467308078437

[108] van Oss CJ, Chaudhury MK, Good RJ. Monopolar surfaces. Adv Colloid Interface Sci 1987;28:35–64. https://doi.org/10.1016/0001-8686(87)80008-8

[109] Della Volpe C, Siboni S. Acid–base surface free energies of solids and the definition of scales in the Good–van Oss–Chaudhury theory. J Adhes Sci Technol 2000;14:235–72. https://doi.org/10.1163/156856100742546

[110] Schultz J, Nardin M. Determination of the Surface Energy of Solids by the Two-Liquid-Phase Method. Mod. Approaches to Wettability, Boston, MA: Springer US; 1992, p. 73–100. https://doi.org/10.1007/978-1-4899-1176-6_4

[111] Shi B, Wang Y, Jia L. Comparison of Dorris–Gray and Schultz methods for the calculation of surface dispersive free energy by inverse gas chromatography. J Chromatogr A 2011;1218:860–2. https://doi.org/10.1016/j.chroma.2010.12.050

[112] Girifalco LA, Good RJ. A Theory for the Estimation of Surface and Interfacial Energies. I. Derivation and Application to Interfacial Tension. J Phys Chem 1957;61:904–9. https://doi.org/10.1021/j150553a013

[113] Altay BN, Ma R, Fleming PD, Joyce MJ, Anand A, Chen T, et al. Surface Free Energy Estimation: A New Methodology for Solid Surfaces. Adv Mater Interfaces 2020;7:1901570. https://doi.org/10.1002/admi.201901570

[114] Li D, Neumann A. Contact angles on hydrophobic solid surfaces and their interpretation. J Colloid Interface Sci 1992;148:190–200. https://doi.org/10.1016/0021-9797(92)90127-8

[115] Zhang D. An Equation-of-State approach to measure the surface free energy (SFE) of bituminous binders. Measurement 2020;158:107715. https://doi.org/10.1016/j.measurement.2020.107715

[116] Mrinalini M, Prasanthkumar S. Recent Advances on Stimuli- Responsive Smart Materials and their Applications. Chempluschem 2019;84:1103–21. https://doi.org/10.1002/cplu.201900365

[117] Bratek-Skicki A. Towards a new class of stimuli-responsive polymer-based materials – Recent advances and challenges. Appl Surf Sci Adv 2021;4:100068. https://doi.org/10.1016/j.apsadv.2021.100068

[118] Brzezicki M. A Systematic Review of the Most Recent Concepts in Smart Windows Technologies with a Focus on Electrochromics. Sustainability 2021;13:9604. https://doi.org/10.3390/su13179604

[119] Zhang Y, Wang C, Zhao W, Li M, Wang X, Yang X, et al. Polymer Stabilized Liquid Crystal Smart Window with Flexible Substrates Based on Low-Temperature Treatment of Polyamide Acid Technology. Polymers (Basel) 2019;11:1869. https://doi.org/10.3390/polym11111869

[120] Abdo GG, Zagho MM, Khalil A. Recent advances in stimuli-responsive drug release and targeting concepts using mesoporous silica nanoparticles. Emergent Mater 2020;3:407–25. https://doi.org/10.1007/s42247-020-00109-x

[121] Jiang H, Ochoa M, Waimin JF, Rahimi R, Ziaie B. A pH-regulated drug delivery dermal patch for targeting infected regions in chronic wounds. Lab Chip 2019;19:2265–74. https://doi.org/10.1039/C9LC00206E

[122] Zahn D, Weidner A, Saatchi K, Häfeli UO, Dutz S. Biodegradable magnetic microspheres for drug targeting, temperature controlled drug release, and hyperthermia. Curr Dir Biomed Eng 2019;5:161–4. https://doi.org/10.1515/cdbme-2019-0041

[123] Seo J, Song M, Jeong J, Nam S, Heo I, Park S-Y, et al. Broadband pH-Sensing Organic Transistors with Polymeric Sensing Layers Featuring Liquid Crystal Microdomains Encapsulated by Di-Block Copolymer Chains. ACS Appl Mater Interfaces 2016;8:23862–7. https://doi.org/10.1021/acsami.6b08257

[124] Saitoh T, Suzuki Y, Hiraide M. Preparation of Poly(N-isopropylacrylamide)-Modified Glass Surface for Flow Control in Microfluidics. Anal Sci 2002;18:203–5. https://doi.org/10.2116/analsci.18.203

[125] Bakarich SE, Gorkin R, Panhuis M in het, Spinks GM. 4D Printing with Mechanically Robust, Thermally Actuating Hydrogels. Macromol Rapid Commun 2015;36:1211–7. https://doi.org/10.1002/marc.201500079

[126] Wang Y, Song C, Yu X, Liu L, Han Y, Chen J, et al. Thermo-responsive hydrogels with tunable transition temperature crosslinked by multifunctional graphene oxide nanosheets. Compos Sci Technol 2017;151:139–46. https://doi.org/10.1016/j.compscitech.2017.08.016

[127] Fu Q, Rama Rao G V., Basame SB, Keller DJ, Artyushkova K, Fulghum JE, et al. Reversible Control of Free Energy and Topography of Nanostructured Surfaces. J Am Chem Soc 2004;126:8904–5. https://doi.org/10.1021/ja047895q

[128] Zhang D, Cheng Z, Kang H, Yu J, Liu Y, Jiang L. A Smart Superwetting Surface with Responsivity in Both Surface Chemistry and Microstructure. Angew Chemie Int Ed 2018;57:3701–5. https://doi.org/10.1002/anie.201800416

[129] Li C, Li M, Ni Z, Guan Q, Blackman BRK, Saiz E. Stimuli-responsive surfaces for switchable wettability and adhesion. J R Soc Interface 2021;18. https://doi.org/10.1098/rsif.2021.0162

[130] Yang X, Huang Y, Zhao Y, Zhang X, Wang J, Sann EE, et al. Bioinspired Slippery Lubricant-Infused Surfaces With External Stimuli Responsive Wettability: A Mini Review. Front Chem 2019;7. https://doi.org/10.3389/fchem.2019.00826

[131] Etha SA, Desai PR, Sachar HS, Das S. Wetting Dynamics on Solvophilic, Soft, Porous, and Responsive Surfaces. Macromolecules 2021;54:584–96. https://doi.org/10.1021/acs.macromol.0c02234

[132] Chemin J-B, Bulou S, Baba K, Fontaine C, Sindzingre T, Boscher ND, et al. Transparent anti-fogging and self-cleaning TiO2/SiO2 thin films on polymer substrates using atmospheric plasma. Sci Rep 2018;8:9603. https://doi.org/10.1038/s41598-018-27526-7

[133] Zorba V, Chen X, Mao SS. Superhydrophilic TiO2 surface without photocatalytic activation. Appl Phys Lett 2010;96:093702. https://doi.org/10.1063/1.3291667

[134] Goulet- Hanssens A, Eisenreich F, Hecht S. Enlightening Materials with Photoswitches. Adv Mater 2020;32:1905966. https://doi.org/10.1002/adma.201905966

[135] Volarić J, Szymanski W, Simeth NA, Feringa BL. Molecular photoswitches in aqueous environments. Chem Soc Rev 2021;50:12377–449. https://doi.org/10.1039/D0CS00547A

[136] Dorel R, Feringa BL. Photoswitchable catalysis based on the isomerisation of double bonds. Chem Commun 2019;55:6477–86. https://doi.org/10.1039/C9CC01891C

[137] Rapp TL, DeForest CA. Targeting drug delivery with light: A highly focused approach. Adv Drug Deliv Rev 2021;171:94–107. https://doi.org/10.1016/j.addr.2021.01.009

[138] Wu Z, Li X, Jiang X, Xie T, Li H, Zhang G, et al. Photoswitchable de/adsorption of an azobenzene-derived surfactant on a silica surface. Phys Chem Chem Phys 2019;21:21030–7. https://doi.org/10.1039/C9CP01940E

[139] Frath D, Yokoyama S, Hirose T, Matsuda K. Photoresponsive supramolecular self-assemblies at the liquid/solid interface. J Photochem Photobiol C Photochem Rev 2018;34:29–40. https://doi.org/10.1016/j.jphotochemrev.2017.12.005

[140] Wu Z, Li X, Jiang X, Xie T, Li H, Zhang G, et al. Photoswitchable de/adsorption of an azobenzene-derived surfactant on a silica surface. Phys Chem Chem Phys 2019;21:21030–7. https://doi.org/10.1039/C9CP01940E

[141] Kunfi A, Bernadett Vlocskó R, Keresztes Z, Mohai M, Bertóti I, Ábrahám Á, et al. Photoswitchable Macroscopic Solid Surfaces Based On Azobenzene- Functionalized Polydopamine/Gold Nanoparticle Composite Materials: Formation, Isomerization and Ligand Exchange. Chempluschem 2020;85:797–805. https://doi.org/10.1002/cplu.201900674

[142] Dworak L, Reuss AJ, Zastrow M, Rück-Braun K, Wachtveitl J. Discrimination between FRET and non-FRET quenching in a photochromic CdSe quantum dot/dithienylethene dye system. Nanoscale 2014;6:14200–3. https://doi.org/10.1039/C4NR05144K

[143] Stubing DB, Heng S, Monro TM, Abell AD. A comparative study of the fluorescence and photostability of common photoswitches in microstructured optical fibre. Sensors Actuators B Chem 2017;239:474–80. https://doi.org/10.1016/j.snb.2016.07.172

[144] Doberenz F, Zeng K, Willems C, Zhang K, Groth T. Thermoresponsive polymers and their biomedical application in tissue engineering – a review. J Mater Chem B 2020;8:607–28. https://doi.org/10.1039/C9TB02052G

[145] Kotsuchibashi Y. Recent advances in multi-temperature-responsive polymeric materials. Polym J 2020;52:681–9. https://doi.org/10.1038/s41428-020-0330-0

[146] Zhang S, Wang J, Zhang X, Song W, Wang S. Tunable multi-stage wettability and adhesion force on polymer brushes triggered by temperature and pH. Sci China Mater 2019;62:597–603. https://doi.org/10.1007/s40843-018-9357-9

[147] Shivapooja P, Ista LK, Canavan HE, Lopez GP. ARGET–ATRP Synthesis and Characterization of PNIPAAm Brushes for Quantitative Cell Detachment Studies. Biointerphases 2012;7:32. https://doi.org/10.1007/s13758-012-0032-z

[148] Xiong X, Wu Z, Pan J, Xue L, Xu Y, Chen H. A facile approach to modify poly(dimethylsiloxane) surfaces via visible light-induced grafting polymerization. J Mater Chem B 2015;3:629–34. https://doi.org/10.1039/C4TB01600A

[149] Spasojević M, Vorenkamp J, Jansen M, de Vos P, Schouten A. Synthesis and Phase Behavior of Poly(N-isopropylacrylamide)-b- Poly(L-Lysine Hydrochloride) and Poly(N-Isopropylacrylamide- co-Acrylamide)-b-Poly(L-Lysine Hydrochloride). Materials (Basel) 2014;7:5305–26. https://doi.org/10.3390/ma7075305

[150] Kim YS, Kim MA, Lee C-M. Controlled drug release from PNIPAM-incorporated melanin nanovesicles by photo-stimulation. Mater Technol 2019;34:639–44. https://doi.org/10.1080/10667857.2019.1611055

[151] Choe A, Yeom J, Shanker R, Kim MP, Kang S, Ko H. Stretchable and wearable colorimetric patches based on thermoresponsive plasmonic microgels embedded in a hydrogel film. NPG Asia Mater 2018;10:912–22. https://doi.org/10.1038/s41427-018-0086-6

[152] Yu W, Lou L-L, Li S, Ma T, Ouyang L, Feng L, et al. Highly efficient and durable platinum nanocatalysts stabilized by thiol-terminated poly(N-isopropyl acrylomide) for

selective hydrogenation of halonitrobenzene to haloaniline. RSC Adv 2017;7:751–7. https://doi.org/10.1039/C6RA24773C

[153] Zhang L, Zhang S, He B, Wu Z, Zhang Z. TiO 2 Nanoparticles Functionalized by a Temperature-sensitive Poly(N-isopropylacrylamide) (PNIPAM): Synthesis and Characterization. Zeitschrift Für Naturforsch B 2008;63:973–6. https://doi.org/10.1515/znb-2008-0809

[154] Lou L-L, Qu H, Yu W, Wang B, Ouyang L, Liu S, et al. Covalently Immobilized Lipase on a Thermoresponsive Polymer with an Upper Critical Solution Temperature as an Efficient and Recyclable Asymmetric Catalyst in Aqueous Media. ChemCatChem 2018;10:1166–72. https://doi.org/10.1002/cctc.201701512

[155] Jia H, Roa R, Angioletti-Uberti S, Henzler K, Ott A, Lin X, et al. Thermosensitive Cu 2 O–PNIPAM core–shell nanoreactors with tunable photocatalytic activity. J Mater Chem A 2016;4:9677–84. https://doi.org/10.1039/C6TA03528K

[156] Merai L, Deak A, Szalai B, Samu GF, Katona G, Janovak L. Visible light-photoreactive composite surfaces with thermoresponsive wetting and photocatalytic properties. Express Polym Lett 2022;16:34–51. https://doi.org/10.3144/expresspolymlett.2022.4

[157] Arotçaréna M, Heise B, Ishaya S, Laschewsky A. Switching the Inside and the Outside of Aggregates of Water-Soluble Block Copolymers with Double Thermoresponsivity. J Am Chem Soc 2002;124:3787–93. https://doi.org/10.1021/ja012167d

[158] Li M, Chen Z. Thermo- responsive polymers for thermal regulation in electrochemical energy devices. J Polym Sci 2021;59:2230–45. https://doi.org/10.1002/pol.20210433

[159] Sarwan T, Kumar P, Choonara YE, Pillay V. Hybrid Thermo-Responsive Polymer Systems and Their Biomedical Applications. Front Mater 2020;7. https://doi.org/10.3389/fmats.2020.00073

[160] Ma W, Wang H. Magnetically driven motile superhydrophobic sponges for efficient oil removal. Appl Mater Today 2019;15:263–6. https://doi.org/10.1016/j.apmt.2019.02.004

[161] Sedlacik M, Mrlik M, Babayan V, Pavlinek V. Magnetorheological elastomers with efficient electromagnetic shielding. Compos Struct 2016;135:199–204. https://doi.org/10.1016/j.compstruct.2015.09.037

[162] Tian D, Zhang N, Zheng X, Hou G, Tian Y, Du Y, et al. Fast Responsive and Controllable Liquid Transport on a Magnetic Fluid/Nanoarray Composite Interface. ACS Nano 2016;10:6220–6. https://doi.org/10.1021/acsnano.6b02318

[163] Lee S, Yim C, Kim W, Jeon S. Magnetorheological Elastomer Films with Tunable Wetting and Adhesion Properties. ACS Appl Mater Interfaces 2015;7:19853–6. https://doi.org/10.1021/acsami.5b06273

[164] Huang Y, Stogin BB, Sun N, Wang J, Yang S, Wong T. A Switchable Cross- Species Liquid Repellent Surface. Adv Mater 2017;29:1604641. https://doi.org/10.1002/adma.201604641

[165] Sorokin V V., Sokolov BO, Stepanov G V., Kramarenko EY. Controllable hydrophobicity of magnetoactive elastomer coatings. J Magn Magn Mater 2018;459:268–71. https://doi.org/10.1016/j.jmmm.2017.10.074

[166] Yang C, Wu L, Li G. Magnetically Responsive Superhydrophobic Surface: In Situ Reversible Switching of Water Droplet Wettability and Adhesion for Droplet Manipulation. ACS Appl Mater Interfaces 2018;10:20150–8. https://doi.org/10.1021/acsami.8b04190

[167] Mérai L, Deák Á, Sebők D, Kukovecz Á, Dékány I, Janovák L. A Stimulus-Responsive Polymer Composite Surface with Magnetic Field-Governed Wetting and Photocatalytic Properties. Polymers (Basel) 2020;12:1890. https://doi.org/10.3390/polym12091890

[168] Zhao Y-P, Wang Y. Fundamentals and Applications of Electrowetting. Rev Adhes Adhes 2013;1:114–74. https://doi.org/10.7569/RAA.2013.097304

[169] Teng P, Tian D, Fu H, Wang S. Recent progress of electrowetting for droplet manipulation: from wetting to superwetting systems. Mater Chem Front 2020;4:140–54. https://doi.org/10.1039/C9QM00458K

[170] Yi Z, Feng H, Zhou X, Shui L. Design of an Open Electrowetting on Dielectric Device Based on Printed Circuit Board by Using a Parafilm M. Front Phys 2020;8. https://doi.org/10.3389/fphy.2020.00193

[171] Kim J-H, Lee J-H, Kim J-Y, Mirzaei A, Wu P, Kim HW, et al. Electrowetting on dielectric (EWOD) properties of Teflon-coated electrosprayed silica layers in air and oil media and the influence of electric leakage. J Mater Chem C 2018;6:6808–15. https://doi.org/10.1039/C8TC01284A

[172] Fouillet Y, Jary D, Brachet AG, Berthier J, Blervaque R, Davous L, et al. EWOD Digital Microfluidics for Lab on a Chip. ASME 4th Int. Conf. Nanochannels, Microchannels, Minichannels, Parts A B, ASMEDC; 2006, p. 1255–64. https://doi.org/10.1115/ICNMM2006-96020

[173] Song X, Zhang H, Li D, Jia D, Liu T. Electrowetting lens with large aperture and focal length tunability. Sci Rep 2020;10:16318. https://doi.org/10.1038/s41598-020-73260-4

[174] Zhang T, Deng Y. Driving Waveform Design of Electrowetting Displays Based on a Reset Signal for Suppressing Charge Trapping Effect. Front Phys 2021;9. https://doi.org/10.3389/fphy.2021.672541

[175] Xiao K, Chen X, Wu C-X. Electric field-triggered Cassie-Baxter-Wenzel wetting transition on textured surface. Phys Rev Res 2021;3:033277. https://doi.org/10.1103/PhysRevResearch.3.033277

[176] Kocak G, Tuncer C, Bütün V. pH-Responsive polymers. Polym Chem 2017;8:144–76. https://doi.org/10.1039/C6PY01872F

[177] Pant R, Dattatreya S, Barman J, Khare K. pH Responsive Reversibly Tunable Wetting Surfaces, 2018, p. 57–80. https://doi.org/10.1007/978-3-319-92654-4_3

[178] Wang Y, Jin L, Xue T, Shao F, Yao Y, Li X. Mussel inspired durable pH-responsive mesh for high-efficient oil/water separation. SN Appl Sci 2020;2:2138. https://doi.org/10.1007/s42452-020-03915-4

[179] Liu X, Hsieh Y-L. Tunable surface wettability and pH-responsive 2D structures from amphiphilic and amphoteric protein microfibrils. RSC Adv 2020;10:33033–9. https://doi.org/10.1039/D0RA05067A

[180] Jiang S, Zhou S. A method for preparing the pH-responsive superhydrophobic paper with high stability. Mater Res Express 2021;8:065306. https://doi.org/10.1088/2053-1591/ac08cf

[181] Chi H, Xu Z, Zhang T, Li X, Wu Z, Zhao Y. Randomly heterogeneous oleophobic/pH-responsive polymer coatings with reversible wettability transition for multifunctional fabrics and controllable oil–water separation. J Colloid Interface Sci 2021;594:122–30. https://doi.org/10.1016/j.jcis.2021.02.097

[182] Song Y, Zhang L, Dong L, Li H, Yu Z, Liu Y, et al. pH-Responsive Smart Wettability Surface with Dual Bactericidal and Releasing Properties. ACS Appl Mater Interfaces 2021;13:46065–75. https://doi.org/10.1021/acsami.1c08263

[183] Kwon D, Wooh S, Yoon H, Char K. Mechanoresponsive Tuning of Anisotropic Wetting on Hierarchically Structured Patterns. Langmuir 2018;34:4732–8. https://doi.org/10.1021/acs.langmuir.8b00496

[184] Parra-Barranco J, Lopez-Santos C, Sánchez-Valencia JR, Borras A, Gonzalez-Elipe AR, Barranco A. Mechanically Switchable Wetting Petal Effect in Self-Patterned Nanocolumnar Films on Poly(dimethylsiloxane). Nanomaterials 2021;11:2566. https://doi.org/10.3390/nano11102566

[185] Park JK, Yang Z, Kim S. Black Silicon/Elastomer Composite Surface with Switchable Wettability and Adhesion between Lotus and Rose Petal Effects by Mechanical Strain. ACS Appl Mater Interfaces 2017;9:33333–40. https://doi.org/10.1021/acsami.7b11143

[186] Rhee D, Lee W, Odom TW. Crack- Free, Soft Wrinkles Enable Switchable Anisotropic Wetting. Angew Chemie Int Ed 2017;56:6523–7. https://doi.org/10.1002/anie.201701968

[187] Zhao S, Xia H, Wu D, Lv C, Chen Q-D, Ariga K, et al. Mechanical stretch for tunable wetting from topological PDMS film. Soft Matter 2013;9:4236. https://doi.org/10.1039/c3sm27871a

[188] Yao X, Hu Y, Grinthal A, Wong T-S, Mahadevan L, Aizenberg J. Adaptive fluid-infused porous films with tunable transparency and wettability. Nat Mater 2013;12:529–34. https://doi.org/10.1038/nmat3598

[189] Jingcheng L, Reddy VS, Jayathilaka WADM, Chinnappan A, Ramakrishna S, Ghosh R. Intelligent Polymers, Fibers and Applications. Polymers (Basel) 2021;13:1427. https://doi.org/10.3390/polym13091427

[190] Zhou Y, Zheng Y, Wei T, Qu Y, Wang Y, Zhan W, et al. Multistimulus Responsive Biointerfaces with Switchable Bioadhesion and Surface Functions. ACS Appl Mater Interfaces 2020;12:5447–55. https://doi.org/10.1021/acsami.9b18505

[191] Jia R, Teng L, Gao L, Su T, Fu L, Qiu Z, et al. Advances in Multiple Stimuli-Responsive Drug-Delivery Systems for Cancer Therapy. Int J Nanomedicine 2021;Volume 16:1525–51. https://doi.org/10.2147/IJN.S293427

[192] Chatterjee S, Chi-leung Hui P. Stimuli-Responsive Hydrogels: An Interdisciplinary Overview. Hydrogels - Smart Mater. Biomed. Appl., IntechOpen; 2019. https://doi.org/10.5772/intechopen.80536

[193] Nau M, Seelinger D, Biesalski M. Independent Two Way Switching of the Wetting Behavior of Cellulose- Derived Nanoparticle Surface Coatings by Light and by Temperature. Adv Mater Interfaces 2019;6:1900378. https://doi.org/10.1002/admi.201900378

[194] Alkan A, Steinmetz C, Landfester K, Wurm FR. Triple-Stimuli-Responsive Ferrocene-Containing PEGs in Water and on the Surface. ACS Appl Mater Interfaces 2015;7:26137–44. https://doi.org/10.1021/acsami.5b07945

[195] Cao Z-Q, Wang G-J. Multi-Stimuli-Responsive Polymer Materials: Particles, Films, and Bulk Gels. Chem Rec 2016;16:1398–435. https://doi.org/10.1002/tcr.201500281

[196] Bowen JJ, Rose MA, Morin SA. Surface molding of multi-stimuli-responsive microgel actuators. MRS Bull 2021;46:337–44. https://doi.org/10.1557/s43577-021-00077-5

[197] Dong Y, Wang J, Guo X, Yang S, Ozen MO, Chen P, et al. Multi-stimuli-responsive programmable biomimetic actuator. Nat Commun 2019;10:4087. https://doi.org/10.1038/s41467-019-12044-5

[198] Wan S, Pu J, Zhang X, Wang L, Xue Q. The tunable wettability in multistimuli-responsive smart graphene surfaces. Appl Phys Lett 2013;102:011603. https://doi.org/10.1063/1.4775360

[199] Wang H, Zhang Z, Wang Z, Liang Y, Cui Z, Zhao J, et al. Multistimuli-Responsive Microstructured Superamphiphobic Surfaces with Large-Range, Reversible Switchable Wettability for Oil. ACS Appl Mater Interfaces 2019;11:28478–86. https://doi.org/10.1021/acsami.9b07941

[200] Zhang D, Xia Q, Lai H, Cheng Z, Liu P, Zhang H, et al. Dual-responsive shape memory polymer arrays with smart and precise multiple-wetting controllability. Sci China Mater 2021;64:1801–12. https://doi.org/10.1007/s40843-020-1554-y

[201] Yang H, Liang F, Chen Y, Wang Q, Qu X, Yang Z. Lotus leaf inspired robust superhydrophobic coating from strawberry-like Janus particles. NPG Asia Mater 2015;7:e176–e176. https://doi.org/10.1038/am.2015.33

[202] Wang F, Wang L, Wu H, Pang J, Gu D, Li S. A lotus-leaf-like SiO2 superhydrophobic bamboo surface based on soft lithography. Colloids Surfaces A Physicochem Eng Asp 2017;520:834–40. https://doi.org/10.1016/j.colsurfa.2017.02.043

[203] Yun X, Xiong Z, He Y, Wang X. Superhydrophobic lotus-leaf-like surface made from reduced graphene oxide through soft-lithographic duplication. RSC Adv 2020;10:5478–86. https://doi.org/10.1039/C9RA10373B

[204] Vanithakumari SC, Yadavalli P, George RP, Kamachi Mudali UM. Lotus effect-based coatings on marine steels to inhibit biofouling. Surf Innov 2015;3:115–26. https://doi.org/10.1680/si.14.00009

[205] Yang J, Long F, Wang R, Zhang X, Yang Y, Hu W, et al. Design of mechanical robust superhydrophobic Cu coatings with excellent corrosion resistance and self-cleaning performance inspired by lotus leaf. Colloids Surfaces A Physicochem Eng Asp 2021;627:127154. https://doi.org/10.1016/j.colsurfa.2021.127154

[206] Lin Y, Chen H, Wang G, Liu A. Recent Progress in Preparation and Anti-Icing Applications of Superhydrophobic Coatings. Coatings 2018;8:208. https://doi.org/10.3390/coatings8060208

[207] Son J, Kundu S, Verma LK, Sakhuja M, Danner AJ, Bhatia CS, et al. A practical superhydrophilic self cleaning and antireflective surface for outdoor photovoltaic applications. Sol Energy Mater Sol Cells 2012;98:46–51. https://doi.org/10.1016/j.solmat.2011.10.011

[208] Syafiq A, Vengadaesvaran B, Pandey AK, Rahim NA. Superhydrophilic Smart Coating for Self-Cleaning Application on Glass Substrate. J Nanomater 2018;2018:1–10. https://doi.org/10.1155/2018/6412601

[209] Topçu Kaya AS, Cengiz U. Fabrication and application of superhydrophilic antifog surface by sol-gel method. Prog Org Coatings 2019;126:75–82. https://doi.org/10.1016/j.porgcoat.2018.10.021

[210] Attri P, Kim YH, Park DH, Park JH, Hong YJ, Uhm HS, et al. Generation mechanism of hydroxyl radical species and its lifetime prediction during the plasma-initiated ultraviolet (UV) photolysis. Sci Rep 2015;5:9332. https://doi.org/10.1038/srep09332

[211] Merai L, Deak A, Sebok D, Csapo E, Kolumban TS, Hopp B, et al. Photoreactive composite coating with composition dependent wetting properties. Express Polym Lett 2018;12:1061–71. https://doi.org/10.3144/expresspolymlett.2018.93

[212] Byrne J, Dunlop P, Hamilton J, Fernández-Ibáñez P, Polo-López I, Sharma P, et al. A Review of Heterogeneous Photocatalysis for Water and Surface Disinfection. Molecules 2015;20:5574–615. https://doi.org/10.3390/molecules20045574

[213] Ahmed SN, Haider W. Heterogeneous photocatalysis and its potential applications in water and wastewater treatment: a review. Nanotechnology 2018;29:342001. https://doi.org/10.1088/1361-6528/aac6ea

[214] Garg S, Chandra A (editors) Green Photocatalytic Semiconductors – Recent Advance and Applications, Vol. 1. Springer; 2021. Chapter 2. https://doi.org/10.1007/978-3-030-77371-7_8.

[215] Deák Á, Janovák L, Csapó E, Ungor D, Pálinkó I, Puskás S, et al. Layered double oxide (LDO) particle containing photoreactive hybrid layers with tunable superhydrophobic and photocatalytic properties. Appl Surf Sci 2016;389:294–302. https://doi.org/10.1016/j.apsusc.2016.07.127

[216] Merai L, Deak A, Szalai B, Samu GF, Katona G, Janovak L. Visible light-photoreactive composite surfaces with thermoresponsive wetting and photocatalytic properties. Express Polym Lett 2022;16:34–51. https://doi.org/10.3144/expresspolymlett.2022.4

[217] Mérai L, Deák Á, Sebők D, Kukovecz Á, Dékány I, Janovák L. A Stimulus-Responsive Polymer Composite Surface with Magnetic Field-Governed Wetting and Photocatalytic Properties. Polymers (Basel) 2020;12:1890. https://doi.org/10.3390/polym12091890

[218] Lantos E, Mérai L, Deák Á, Gómez- Pérez J, Sebők D, Dékány I, et al. Preparation of sulfur hydrophobized plasmonic photocatalyst towards durable superhydrophobic coating material. J Mater Sci Technol 2020;41:159–67. https://doi.org/10.1016/j.jmst.2019.04.046

[219] Lai Y, Huang J, Gong J, Huang Y, Wang C, Chen Z, et al. Superhydrophilic–Superhydrophobic Template: A Simple Approach to Micro- and Nanostructure Patterning of TiO[sub 2] Films. J Electrochem Soc 2009;156:D480. https://doi.org/10.1149/1.3216032

[220] Xiong J, Sarkar DK, Chen XG. Ultraviolet-Durable Superhydrophobic Nanocomposite Thin Films Based on Cobalt Stearate-Coated TiO 2 Nanoparticles Combined with Polymethylhydrosiloxane. ACS Omega 2017;2:8198–204. https://doi.org/10.1021/acsomega.7b01579

[221] Liu J, Ye L, Wooh S, Kappl M, Steffen W, Butt H-J. Optimizing Hydrophobicity and Photocatalytic Activity of PDMS-Coated Titanium Dioxide. ACS Appl Mater Interfaces 2019;11:27422–5. https://doi.org/10.1021/acsami.9b07490

[222] Zhang X, Jin M, Liu Z, Tryk DA, Nishimoto S, Murakami T, et al. Superhydrophobic TiO 2 Surfaces: Preparation, Photocatalytic Wettability Conversion, and Superhydrophobic−Superhydrophilic Patterning. J Phys Chem C 2007;111:14521–9. https://doi.org/10.1021/jp0744432

[223] He F, Weon S, Jeon W, Chung MW, Choi W. Self-wetting triphase photocatalysis for effective and selective removal of hydrophilic volatile organic compounds in air. Nat Commun 2021;12:6259. https://doi.org/10.1038/s41467-021-26541-z

[224] Basso A, Battisti AP, Moreira R de FPM, José HJ. Photocatalytic effect of addition of TiO 2 to acrylic-based paint for passive toluene degradation. Environ Technol 2020;41:1568–79. https://doi.org/10.1080/09593330.2018.1542034

[225] Wu Y, Feng J, Gao H, Feng X, Jiang L. Superwettability-Based Interfacial Chemical Reactions. Adv Mater 2019;31:1800718. https://doi.org/10.1002/adma.201800718

[226] Fu G, Vary PS, Lin C-T. Anatase TiO 2 Nanocomposites for Antimicrobial Coatings. J Phys Chem B 2005;109:8889–98. https://doi.org/10.1021/jp0502196

[227] Peng C-C, Yang M-H, Chiu W-T, Chiu C-H, Yang C-S, Chen Y-W, et al. Composite Nano-Titanium Oxide-Chitosan Artificial Skin Exhibits Strong Wound-Healing Effect-An Approach with Anti-Inflammatory and Bactericidal Kinetics. Macromol Biosci 2008;8:316–27. https://doi.org/10.1002/mabi.200700188

[228] Ye L, Pelton R, Brook MA, Filipe CDM, Wang H, Brovko L, et al. Targeted Disinfection of E. coli via Bioconjugation to Photoreactive TiO 2. Bioconjug Chem 2013;24:448–55. https://doi.org/10.1021/bc300581t

[229] Adlhart C, Verran J, Azevedo NF, Olmez H, Keinänen-Toivola MM, Gouveia I, et al. Surface modifications for antimicrobial effects in the healthcare setting: a critical overview. J Hosp Infect 2018;99:239–49. https://doi.org/10.1016/j.jhin.2018.01.018

[230] Li W, Thian ES, Wang M, Wang Z, Ren L. Surface Design for Antibacterial Materials: From Fundamentals to Advanced Strategies. Adv Sci 2021;8:2100368. https://doi.org/10.1002/advs.202100368

[231] Mahanta U, Khandelwal M, Deshpande AS. Antimicrobial surfaces: a review of synthetic approaches, applicability and outlook. J Mater Sci 2021;56:17915–41. https://doi.org/10.1007/s10853-021-06404-0

[232] Luo L, Zhou Y, Xu X, Shi W, Hu J, Li G, et al. Progress in construction of bio-inspired physico-antimicrobial surfaces. Nanotechnol Rev 2020;9:1562–75. https://doi.org/10.1515/ntrev-2020-0089

[233] Encinas N, Yang C-Y, Geyer F, Kaltbeitzel A, Baumli P, Reinholz J, et al. Submicrometer-Sized Roughness Suppresses Bacteria Adhesion. ACS Appl Mater Interfaces 2020;12:21192–200. https://doi.org/10.1021/acsami.9b22621

[234] Bao Q, Nishimura N, Kamata H, Furue K, Ono Y, Hosomi M, et al. Antibacterial and anti-biofilm efficacy of fluoropolymer coating by a 2,3,5,6-tetrafluoro-p-phenylenedimethanol structure. Colloids Surfaces B Biointerfaces 2017;151:363–71. https://doi.org/10.1016/j.colsurfb.2016.12.020

[235] Tallósy SP, Janovák L, Nagy E, Deák Á, Juhász Á, Csapó E, et al. Adhesion and inactivation of Gram-negative and Gram-positive bacteria on photoreactive TiO 2

/polymer and Ag-TiO 2 /polymer nanohybrid films. Appl Surf Sci 2016;371:139–50. https://doi.org/10.1016/j.apsusc.2016.02.202

[236] Encinas N, Yang C-Y, Geyer F, Kaltbeitzel A, Baumli P, Reinholz J, et al. Submicrometer-Sized Roughness Suppresses Bacteria Adhesion. ACS Appl Mater Interfaces 2020;12:21192–200. https://doi.org/10.1021/acsami.9b22621

[237] Yang WJ, Cai T, Neoh K-G, Kang E-T, Teo SL-M, Rittschof D. Barnacle Cement as Surface Anchor for "Clicking" of Antifouling and Antimicrobial Polymer Brushes on Stainless Steel. Biomacromolecules 2013;14:2041–51. https://doi.org/10.1021/bm400382e

[238] Li M, Liu X, Liu N, Guo Z, Singh PK, Fu S. Effect of surface wettability on the antibacterial activity of nanocellulose-based material with quaternary ammonium groups. Colloids Surfaces A Physicochem Eng Asp 2018;554:122–8. https://doi.org/10.1016/j.colsurfa.2018.06.031

[239] Nguyen DT, Pham LT, Le HTT, Vu MX, Le HTM, Le HTM, et al. Synthesis and antibacterial properties of a novel magnetic nanocomposite prepared from spent pickling liquors and polyguanidine. RSC Adv 2018;8:19707–12. https://doi.org/10.1039/C8RA03096K

[240] Leong J, Yang C, Tan J, Tan BQ, Hor S, Hedrick JL, et al. Combination of guanidinium and quaternary ammonium polymers with distinctive antimicrobial mechanisms achieving a synergistic antimicrobial effect. Biomater Sci 2020;8:6920–9. https://doi.org/10.1039/D0BM00752H

[241] Yasir M, Dutta D, Hossain KR, Chen R, Ho KKK, Kuppusamy R, et al. Mechanism of Action of Surface Immobilized Antimicrobial Peptides Against Pseudomonas aeruginosa. Front Microbiol 2020;10. https://doi.org/10.3389/fmicb.2019.03053

[242] Boldogkői Z, Csabai Z, Tombácz D, Janovák L, Balassa L, Deák Á, et al. Visible Light-Generated Antiviral Effect on Plasmonic Ag-TiO2-Based Reactive Nanocomposite Thin Film. Front Bioeng Biotechnol 2021;9. https://doi.org/10.3389/fbioe.2021.709462.

[243] Endo-Kimura M, Kowalska E. Plasmonic photocatalysts for microbiological applications. Catalysts 2020;10:824. https://doi.org/10.3390/catal10080824

[244] Yang L, Ning X, Xiao Q, Chen K, Zhou H. Development and characterization of porous silver-incorporated hydroxyapatite ceramic for separation and elimination of microorganisms. J Biomed Mater Res Part B Appl Biomater 2007;81B:50–6. https://doi.org/10.1002/jbm.b.30635

[245] Galdiero S, Falanga A, Vitiello M, Cantisani M, Marra V, Galdiero M. Silver Nanoparticles as Potential Antiviral Agents. Molecules 2011;16:8894–918. https://doi.org/10.3390/molecules16108894

[246] Lorenz K, Bauer S, Gutbrod K, Guggenbichler JP, Schmuki P, Zollfrank C. Anodic TiO 2 nanotube layers electrochemically filled with MoO 3 and their antimicrobial properties. Biointerphases 2011;6:16–21. https://doi.org/10.1116/1.3566544

[247] Zollfrank C, Gutbrod K, Wechsler P, Guggenbichler JP. Antimicrobial activity of transition metal acid MoO3 prevents microbial growth on material surfaces. Mater Sci Eng C 2012;32:47–54. https://doi.org/10.1016/j.msec.2011.09.010

[248] Plumridge A, Hesse SJA, Watson AJ, Lowe KC, Stratford M, Archer DB. The Weak Acid Preservative Sorbic Acid Inhibits Conidial Germination and Mycelial Growth of Aspergillus niger through Intracellular Acidification. Appl Environ Microbiol 2004;70:3506–11. https://doi.org/10.1128/AEM.70.6.3506-3511.2004

[249] Lutey AHA, Gemini L, Romoli L, Lazzini G, Fuso F, Faucon M, et al. Towards Laser-Textured Antibacterial Surfaces. Sci Rep 2018;8:10112. https://doi.org/10.1038/s41598-018-28454-2

[250] Nascimbén Santos É, László Z, Hodúr C, Arthanareeswaran G, Veréb G. Photocatalytic membrane filtration and its advantages over conventional approaches in the treatment of oily wastewater: A review. Asia-Pacific J Chem Eng 2020;15. https://doi.org/10.1002/apj.2533

[251] Cerff B, Key D, Bladergroen B. A Review of the Processes Associated with the Removal of Oil in Water Pollution. Sustainability 2021;13:12339. https://doi.org/10.3390/su132212339

[252] Gupta RK, Dunderdale GJ, England MW, Hozumi A. Oil/water separation techniques: a review of recent progresses and future directions. J Mater Chem A 2017;5:16025–58. https://doi.org/10.1039/C7TA02070H

[253] Mogensen K, Masalmeh S. A review of EOR techniques for carbonate reservoirs in challenging geological settings. J Pet Sci Eng 2020;195:107889. https://doi.org/10.1016/j.petrol.2020.107889

[254] Abdulredha MM, Siti Aslina H, Luqman CA. Overview on petroleum emulsions, formation, influence and demulsification treatment techniques. Arab J Chem 2020;13:3403–28. https://doi.org/10.1016/j.arabjc.2018.11.014

[255] Wang H, Hu X, Ke Z, Du CZ, Zheng L, Wang C, et al. Review: Porous Metal Filters and Membranes for Oil–Water Separation. Nanoscale Res Lett 2018;13:284. https://doi.org/10.1186/s11671-018-2693-0

[256] Zhang J, Ge D, Wang X, Wang W, Cui D, Yuan G, et al. Influence of Surfactant and Weak-Alkali Concentrations on the Stability of O/W Emulsion in an Alkali-Surfactant–Polymer Compound System. ACS Omega 2021;6:5001–8. https://doi.org/10.1021/acsomega.0c06142

[257] Boussu K, Kindts C, Vandecasteele C, Van der Bruggen B. Surfactant Fouling of Nanofiltration Membranes: Measurements and Mechanisms. ChemPhysChem 2007;8:1836–45. https://doi.org/10.1002/cphc.200700236

[258] Kishimoto N, Kimura H. Fouling behaviour of a reverse osmosis membrane by three types of surfactants. J Water Reuse Desalin 2012;2:40–6. https://doi.org/10.2166/wrd.2012.065

[259] Chen Q, de Leon A, Advincula RC. Inorganic–Organic Thiol–ene Coated Mesh for Oil/Water Separation. ACS Appl Mater Interfaces 2015;7:18566–73. https://doi.org/10.1021/acsami.5b04980

[260] Xue Z, Wang S, Lin L, Chen L, Liu M, Feng L, et al. A Novel Superhydrophilic and Underwater Superoleophobic Hydrogel-Coated Mesh for Oil/Water Separation. Adv Mater 2011;23:4270–3. https://doi.org/10.1002/adma.201102616

[261] Li Y, Feng Z, He Y, Fan Y, Ma J, Yin X. Facile way in fabricating a cotton fabric membrane for switchable oil/water separation and water purification. Appl Surf Sci 2018;441:500–7. https://doi.org/10.1016/j.apsusc.2018.02.060

[262] Lin Y, Salem MS, Zhang L, Shen Q, El-shazly AH, Nady N, et al. Development of Janus membrane with controllable asymmetric wettability for highly-efficient oil/water emulsions separation. J Memb Sci 2020;606:118141. https://doi.org/10.1016/j.memsci.2020.118141

[263] Lin J, Lin F, Liu R, Li P, Fang S, Ye W, et al. Scalable fabrication of robust superhydrophobic membranes by one-step spray-coating for gravitational water-in-oil emulsion separation. Sep Purif Technol 2020;231:115898. https://doi.org/10.1016/j.seppur.2019.115898

[264] Jiang Y-H, Zhang Y-Q, Gao C, An Q-D, Xiao Z-Y, Zhai S-R. Superhydrophobic aerogel membrane with integrated functions of biopolymers for efficient oil/water separation. Sep Purif Technol 2022;282:120138. https://doi.org/10.1016/j.seppur.2021.120138

[265] Yang C, Han N, Wang W, Zhang W, Han C, Cui Z, et al. Fabrication of a PPS Microporous Membrane for Efficient Water-in-Oil Emulsion Separation. Langmuir 2018;34:10580–90. https://doi.org/10.1021/acs.langmuir.8b02393

[266] Lin X, Choi M, Heo J, Jeong H, Park S, Hong J. Cobweb-Inspired Superhydrophobic Multiscaled Gating Membrane with Embedded Network Structure for Robust Water-in-Oil Emulsion Separation. ACS Sustain Chem Eng 2017;5:3448–55. https://doi.org/10.1021/acssuschemeng.7b00124

[267] Huang H, Li Y, Zhao L, Yu Y, Xu J, Yin X, et al. A facile fabrication of chitosan modified PPS-based microfiber membrane for effective antibacterial activity and oil-in-water emulsion separation. Cellulose 2019;26:2599–611. https://doi.org/10.1007/s10570-019-02274-7

[268] Zhang S, Lu F, Tao L, Liu N, Gao C, Feng L, et al. Bio-Inspired Anti-Oil-Fouling Chitosan-Coated Mesh for Oil/Water Separation Suitable for Broad pH Range and Hyper-Saline Environments. ACS Appl Mater Interfaces 2013;5:11971–6. https://doi.org/10.1021/am403203q

[269] Halim A, Xu Y, Lin K-H, Kobayashi M, Kajiyama M, Enomae T. Fabrication of cellulose nanofiber-deposited cellulose sponge as an oil-water separation membrane. Sep Purif Technol 2019;224:322–31. https://doi.org/10.1016/j.seppur.2019.05.005

[270] Zhang L, Lin Y, Wu H, Cheng L, Sun Y, Yasui T, et al. An ultrathin in situ silicification layer developed by an electrostatic attraction force strategy for ultrahigh-performance oil–water emulsion separation. J Mater Chem A 2019;7:24569–82. https://doi.org/10.1039/C9TA07988B

[271] Liu S, Zhou Z, Zhou S, Cui J, Wang Q, Zhang Y, et al. Fabrication of acrylamide decorated superhydrophilic and underwater superoleophobic poly(vinylidene fluoride) membranes for oil/water emulsion separation. J Taiwan Inst Chem Eng 2019;95:300–7. https://doi.org/10.1016/j.jtice.2018.07.015

[272] Gondal MA, Sadullah MS, Dastageer MA, McKinley GH, Panchanathan D, Varanasi KK. Study of Factors Governing Oil–Water Separation Process Using TiO 2 Films Prepared by Spray Deposition of Nanoparticle Dispersions. ACS Appl Mater Interfaces 2014;6:13422–9. https://doi.org/10.1021/am501867b

[273] Ngang HP, Ahmad AL, Low SC, Ooi BS. Preparation of thermoresponsive PVDF/SiO2-PNIPAM mixed matrix membrane for saline oil emulsion separation and its cleaning efficiency. Desalination 2017;408:1–12. https://doi.org/10.1016/j.desal.2017.01.005

[274] Chen Y, Wang N, Guo F, Hou L, Liu J, Liu J, et al. A Co 3 O 4 nano-needle mesh for highly efficient, high-flux emulsion separation. J Mater Chem A 2016;4:12014–9. https://doi.org/10.1039/C6TA02579J

[275] Cao Y, Zhang X, Tao L, Li K, Xue Z, Feng L, et al. Mussel-Inspired Chemistry and Michael Addition Reaction for Efficient Oil/Water Separation. ACS Appl Mater Interfaces 2013;5:4438–42. https://doi.org/10.1021/am4008598

[276] Zhang W, Li X, Qu R, Liu Y, Wei Y, Feng L. Janus membrane decorated via a versatile immersion-spray route: controllable stabilized oil/water emulsion separation satisfying industrial emission and purification criteria. J Mater Chem A 2019;7:4941–9. https://doi.org/10.1039/C8TA11452H

[277] Wang Y, Lai C, Wang X, Liu Y, Hu H, Guo Y, et al. Beads-on-String Structured Nanofibers for Smart and Reversible Oil/Water Separation with Outstanding Antifouling Property. ACS Appl Mater Interfaces 2016;8:25612–20. https://doi.org/10.1021/acsami.6b08747

[278] Li H-N, Yang J, Xu Z-K. Hollow fiber membranes with Janus surfaces for continuous deemulsification and separation of oil-in-water emulsions. J Memb Sci 2020;602:117964. https://doi.org/10.1016/j.memsci.2020.117964

[279] Wang Y-X, Li Y-J, Yang H, Xu Z-L. Super-wetting, photoactive TiO2 coating on amino-silane modified PAN nanofiber membranes for high efficient oil-water emulsion separation application. J Memb Sci 2019;580:40–8. https://doi.org/10.1016/j.memsci.2019.02.062

[280] Uhlmann P, Varnik F, Truman P, Zikos G, Moulin J-F, Müller-Buschbaum P, et al. Microfluidic emulsion separation—simultaneous separation and sensing by multilayer nanofilm structures. J Phys Condens Matter 2011;23:184123. https://doi.org/10.1088/0953-8984/23/18/184123

[281] Wu S-T, Huang C-Y, Weng C-C, Chang C-C, Li B-R, Hsu C-S. Rapid Prototyping of an Open-Surface Microfluidic Platform Using Wettability-Patterned Surfaces Prepared by an Atmospheric-Pressure Plasma Jet. ACS Omega 2019;4:16292–9. https://doi.org/10.1021/acsomega.9b01317

[282] Alazzam A, Alamoodi N. Microfluidic Devices with Patterned Wettability Using Graphene Oxide for Continuous Liquid–Liquid Two-Phase Separation. ACS Appl Nano Mater 2020;3:3471–7. https://doi.org/10.1021/acsanm.0c00200

[283] Francesko A, Cardoso VF, Lanceros-Méndez S. Lab-on-a-chip technology and microfluidics. Microfluid. Pharm. Appl., Elsevier; 2019, p. 3–36. https://doi.org/10.1016/B978-0-12-812659-2.00001-6

[284] Männel MJ, Weigel N, Hauck N, Heida T, Thiele J. Combining Hydrophilic and Hydrophobic Materials in 3D Printing for Fabricating Microfluidic Devices with Spatial Wettability. Adv Mater Technol 2021;6:2100094. https://doi.org/10.1002/admt.202100094

[285] Trojanowicz M. Flow Chemistry in Contemporary Chemical Sciences: A Real Variety of Its Applications. Molecules 2020;25:1434. https://doi.org/10.3390/molecules25061434

[286] Olanrewaju A, Beaugrand M, Yafia M, Juncker D. Capillary microfluidics in microchannels: from microfluidic networks to capillaric circuits. Lab Chip 2018;18:2323–47. https://doi.org/10.1039/C8LC00458G

[287] Wang S, Zhang X, Ma C, Yan S, Inglis D, Feng S. A Review of Capillary Pressure Control Valves in Microfluidics. Biosensors 2021;11:405. https://doi.org/10.3390/bios11100405

[288] Pascual M, Kerdraon M, Rezard Q, Jullien M-C, Champougny L. Wettability patterning in microfluidic devices using thermally-enhanced hydrophobic recovery of PDMS. Soft Matter 2019;15:9253–60. https://doi.org/10.1039/C9SM01792E

[289] Wang S, Wang T, Ge P, Xue P, Ye S, Chen H, et al. Controlling Flow Behavior of Water in Microfluidics with a Chemically Patterned Anisotropic Wetting Surface. Langmuir 2015;31:4032–9. https://doi.org/10.1021/acs.langmuir.5b00328.

[290] Li C, Boban M, Snyder SA, Kobaku SPR, Kwon G, Mehta G, et al. Paper-Based Surfaces with Extreme Wettabilities for Novel, Open-Channel Microfluidic Devices. Adv Funct Mater 2016;26:6121–31. https://doi.org/10.1002/adfm.201601821

[291] Hecht L, Philipp J, Mattern K, Dietzel A, Klages C-P. Controlling wettability in paper by atmospheric-pressure microplasma processes to be used in μPAD fabrication. Microfluid Nanofluidics 2016;20:25. https://doi.org/10.1007/s10404-015-1682-1

[292] Yadav S, Sharma NN, Akhtar J. Paper for microfluidics: Selection criteria, 2020, p. 030002. https://doi.org/10.1063/5.0031966

[293] Sachdeva S, Davis RW, Saha AK. Microfluidic Point-of-Care Testing: Commercial Landscape and Future Directions. Front Bioeng Biotechnol 2021;8. https://doi.org/10.3389/fbioe.2020.602659

[294] Nishat S, Jafry AT, Martinez AW, Awan FR. Paper-based microfluidics: Simplified fabrication and assay methods. Sensors Actuators B Chem 2021;336:129681. https://doi.org/10.1016/j.snb.2021.129681

[295] Shchedrina NN, Kudryashov SI, Moskvin MK, Odintsova G V., Krylach I V., Danilov PA, et al. Elementary autonomous surface microfluidic devices based on laser-fabricated wetting gradient microtextures that drive directional water flows. Opt Express 2021;29:12616. https://doi.org/10.1364/OE.418173

[296] Loo J, Pei SN, Wu MC. Co-planar light-actuated optoelectrowetting microfluidic device for droplet manipulation. J Opt Microsystems 2021;1. https://doi.org/10.1117/1.JOM.1.3.034001

[297] Naik AR, Warren B, Burns A, Lenigk R, Morse J, Alizadeh A, et al. Electrowetting valves for sweat-based microfluidics. Microfluid Nanofluidics 2021;25:2. https://doi.org/10.1007/s10404-020-02403-w

[298] De Jong E, Kremer R, Liu L, Den Toonder JMJ, Onck PR. Mechanowetting drives droplet and fluid transport on traveling surface waves generated by light-responsive liquid crystal polymers. Phys Fluids 2021;33:063307. https://doi.org/10.1063/5.0050864

[299] Zhao B, MacMinn CW, Juanes R. Wettability control on multiphase flow in patterned microfluidics. Proc Natl Acad Sci 2016;113:10251–6. https://doi.org/10.1073/pnas.1603387113

[300] Ma Y, Sun M, Duan X, van den Berg A, Eijkel JCT, Xie Y. Dimension-reconfigurable bubble film nanochannel for wetting based sensing. Nat Commun 2020;11:814. https://doi.org/10.1038/s41467-020-14580-x

[301] Zhu H, Huang Y, Lou X, Xia F. Bioinspired superwetting surfaces for biosensing. View 2021;2:20200053. https://doi.org/10.1002/VIW.20200053

[302] Erzuah S, Fjelde I, Voke Omekeh A. Wettability Estimation by Oil Adsorption Using Quartz Crystal Microbalance with Dissipation QCM-D. Day 3 Wed, June 13, 2018, SPE; 2018. https://doi.org/10.2118/190882-MS

[303] Murray B, Narayanan S. The Role of Wettability on the Response of a Quartz Crystal Microbalance Loaded with a Sessile Droplet. Sci Rep 2019;9:17289. https://doi.org/10.1038/s41598-019-53233-y

[304] Sakti SP, Khusnah NF, Santjojo DJDH, Masruroh, Sabarudin A. Surface Modification of Polystyrene Coating on QCM Sensor using Ambient Air Plasma at Low Pressure. Mater Today Proc 2018;5:15149–54. https://doi.org/10.1016/j.matpr.2018.04.073

[305] Su J, Esmaeilzadeh H, Wang P, Ji S, Inalpolat M, Charmchi M, et al. Effect of wetting states on frequency response of a micropillar-based quartz crystal microbalance. Sensors Actuators A Phys 2019;286:115–22. https://doi.org/10.1016/j.sna.2018.12.012

[306] Esmeryan KD, Chaushev TA. Complex characterization of human urine using super-nonwettable soot coated quartz crystal microbalance sensors. Sensors Actuators A Phys 2021;317:112480. https://doi.org/10.1016/j.sna.2020.112480

[307] Hu S, Shi Z, Zheng R, Ye W, Gao X, Zhao W, et al. Superhydrophobic Liquid–Solid Contact Triboelectric Nanogenerator as a Droplet Sensor for Biomedical Applications. ACS Appl Mater Interfaces 2020;12:40021–30. https://doi.org/10.1021/acsami.0c10097

[308] He X, Xu T, Gao W, Xu L-P, Pan T, Zhang X. Flexible Superwettable Tapes for On-Site Detection of Heavy Metals. Anal Chem 2018;90:14105–10. https://doi.org/10.1021/acs.analchem.8b04536

[309] Lin P-H, Li B-R. Antifouling strategies in advanced electrochemical sensors and biosensors. Analyst 2020;145:1110–20. https://doi.org/10.1039/C9AN02017A

[310] Lin J, Cai X, Liu Z, Liu N, Xie M, Zhou B, et al. Anti- liquid- Interfering and Bacterially Antiadhesive Strategy for Highly Stretchable and Ultrasensitive Strain Sensors Based on Cassie- Baxter Wetting State. Adv Funct Mater 2020;30:2000398. https://doi.org/10.1002/adfm.202000398

[311] Melnikov P V., Aleksandrovskaya AY, Safonov A V., Popova NM, Spitsin B V., Naumova AO, et al. Tuning the wetting angle of fluorinated polymer with modified nanodiamonds: towards new type of biosensors. Mendeleev Commun 2020;30:453–5. https://doi.org/10.1016/j.mencom.2020.07.015

[312] Gao ZF, Sann EE, Lou X, Liu R, Dai J, Zuo X, et al. Naked-eye point-of-care testing platform based on a pH-responsive superwetting surface: toward the non-invasive detection of glucose. NPG Asia Mater 2018;10:177–89. https://doi.org/10.1038/s41427-018-0024-7

[313] Gao ZF, Liu R, Wang J, Dai J, Huang W-H, Liu M, et al. Controlling Droplet Motion on an Organogel Surface by Tuning the Chain Length of DNA and Its Biosensing Application. Chem 2018;4:2929–43. https://doi.org/10.1016/j.chempr.2018.09.028

[314] Sharma V, Yiannacou K, Karjalainen M, Lahtonen K, Valden M, Sariola V. Large-scale efficient water harvesting using bioinspired micro-patterned copper oxide nanoneedle surfaces and guided droplet transport. Nanoscale Adv 2019;1:4025–40. https://doi.org/10.1039/C9NA00405J

[315] Lei J, Guo Z. A fog-collecting surface mimicking the Namib beetle: its water collection efficiency and influencing factors. Nanoscale 2020;12:6921–36. https://doi.org/10.1039/C9NR10808D

[316] Nioras D, Ellinas K, Constantoudis V, Gogolides E. How Different Are Fog Collection and Dew Water Harvesting on Surfaces with Different Wetting Behaviors? ACS Appl Mater Interfaces 2021;13:48322–32. https://doi.org/10.1021/acsami.1c16609

[317] Bai H, Wang L, Ju J, Sun R, Zheng Y, Jiang L. Efficient Water Collection on Integrative Bioinspired Surfaces with Star-Shaped Wettability Patterns. Adv Mater 2014;26:5025–30. https://doi.org/10.1002/adma.201400262

[318] Zhang Y, Wang T, Wu M, Wei W. Durable superhydrophobic surface with hierarchical microstructures for efficient water collection. Surf Coatings Technol 2021;419:127279. https://doi.org/10.1016/j.surfcoat.2021.127279

[319] Han S, Sung J, So H. Simple Fabrication of Water Harvesting Surfaces Using Three-Dimensional Printing Technology. Int J Precis Eng Manuf Technol 2021;8:1449–59. https://doi.org/10.1007/s40684-020-00263-x

[320] Seo D, Lee J, Lee C, Nam Y. The effects of surface wettability on the fog and dew moisture harvesting performance on tubular surfaces. Sci Rep 2016;6:24276. https://doi.org/10.1038/srep24276

[321] Jin Y, Zhang L, Wang P. Atmospheric Water Harvesting: Role of Surface Wettability and Edge Effect. Glob Challenges 2017;1:1700019. https://doi.org/10.1002/gch2.201700019

[322] Kang JH, Lee J-W, Kim JY, Moon JW, Jang HS, Jung SY. Effect of Mesh Wettability Modification on Atmospheric and Industrial Fog Harvesting. Front Phys 2021;9. https://doi.org/10.3389/fphy.2021.680641

[323] Knapczyk-Korczak J, Szewczyk PK, Ura DP, Berent K, Stachewicz U. Hydrophilic nanofibers in fog collectors for increased water harvesting efficiency. RSC Adv 2020;10:22335–42. https://doi.org/10.1039/D0RA03939J

[324] Jarimi H, Powell R, Riffat S. Review of sustainable methods for atmospheric water harvesting. Int J Low-Carbon Technol 2020;15:253–76. https://doi.org/10.1093/ijlct/ctz072

[325] Bhushan B. Design of water harvesting towers and projections for water collection from fog and condensation. Philos Trans R Soc A Math Phys Eng Sci 2020;378:20190440. https://doi.org/10.1098/rsta.2019.0440

[326] Dai X, Sun N, Nielsen SO, Stogin BB, Wang J, Yang S, et al. Hydrophilic directional slippery rough surfaces for water harvesting. Sci Adv 2018;4. https://doi.org/10.1126/sciadv.aaq0919

[327] Guo Z, Zhang L, Monga D, Stone HA, Dai X. Hydrophilic slippery surface enabled coarsening effect for rapid water harvesting. Cell Reports Phys Sci 2021;2:100387. https://doi.org/10.1016/j.xcrp.2021.100387

[328] Gurera D, Bhushan B. Designing bioinspired surfaces for water collection from fog. Philos Trans R Soc A Math Phys Eng Sci 2019;377:20180269. https://doi.org/10.1098/rsta.2018.0269

[329] Liu X, Trosseille J, Mongruel A, Marty F, Basset P, Laurent J, et al. Tailoring silicon for dew water harvesting panels. IScience 2021;24:102814. https://doi.org/10.1016/j.isci.2021.102814

[330] Zhou X, Lu H, Zhao F, Yu G. Atmospheric Water Harvesting: A Review of Material and Structural Designs. ACS Mater Lett 2020;2:671–84. https://doi.org/10.1021/acsmaterialslett.0c00130

[331] Sharma V, Balaji R, Krishnan V. Fog-Harvesting Properties of Dryopteris marginata: Role of Interscalar Microchannels in Water-Channeling. Biomimetics 2018;3:7. https://doi.org/10.3390/biomimetics3020007

Tables

Model	Information	Minimum no. of liquids	Application	Related references
Zisman	Critical surface tension	2	Non-polar solids	[95,99]
Fowkes	Disperse parts of surface free energy	2	Non-polar systems	[100,101]
Extended Fowkes (Owens-Wendt)	Disperse, polar and hydrogen parts of surface free energy	3	Specific questions of surface properties	[102-104]
OWRK	Disperse and polar parts	2	universal	[96,102,105,106]
Wu1 (harmonic mean)	Disperse and polar parts of surface free energy	2 (at least 1 polar liquid)	low energy systems	[79,97]
Wu2 (geometric harmonic mean)	Disperse and polar parts of surface free energy	2 (at least 1 polar liquid)	high energy systems	[107]
Acid-Base Theory (Good-van Oss-Chaudhury)	Disperse, acid and base parts of surface free energy	3	Specific questions of surface properties	[108,109]
Schultz	Disperse and polar parts of surface free energy	2 (at least 1 polar liquid)	High or low energy systems	[110,111]
Good and Girifalco	surface free energy	1	Low energy systems	[112,113]
Equation of State (Neumann)	surface free energy	1	universal	[101,114,115]
Chibowsky	surface free energy	1	universal	[73,98]

Table 1. Popular surface free energy determination methods and their scope of application

Figure captions

Figure 1. Different wetting characteristics of smooth solid surfaces, categorized according to contact angle values **a)** visual representation of the Young-equation **b)** and representation of the sliding angle **c)**

Figure 2. Schematic representation of nine wetting scenarios for a surface with hierarchical roughness [32] **a)** SEM images of a natural [34] **b) c)** and a biomimetic artificial superhydrophobic surface [34] **d) e)**

Figure 3. Schematic representation of the wetting and photocatalytic efficiency of pNIPAAM-grafted Ag-TiO_2/PDMS composite coatings; methylene-blue (c_0= 6.25 μM) relative concentration vs. illumination time (λ=405 nm) **A** and the calculated surface free energy values of the composites as a function of temperature and grafting NIPAAm monomer concentration **B** [156]

Figure 4. CCD images of water droplet catch and release from a superhydrophobic surface by magnetic pillar coatings with 16.7 wt.% Ag-TiO_2 content (top) and SEM images of the magnetic pillars with 0 and 16.7 wt.% nominal Ag-TiO_2 content) (bottom) [167]

Figure 5. Measured Θ-values on Ag-TiO_2/pPFDAc hybrid layers as a function of Ag-TiO_2 content (the dashed line is a guide to the eyes) [73] and SEM images of the prepared smooth pPFDAc fluoropolymer layer (top) and the 80 wt% Ag-TiO_2 containing pPFDAc thin layers with different magnifications (bottom) [211] **A** measured apparent static initial water contact angles on pure polyacrylate thin films and Ag-TiO_2 photocatalyst-roughened polyacrylate hybrid layers (r-) as a function of the hydrophobic pPFDAc content of the copolymer matrix (T = 25±0.5 °C) [211] beside the determined total apparent surface free energy (γ^s_{tot}) values of initial (smooth) and roughened (r-) polyacrylate thin layers [211] **B**

Figure 6. Evolution of ROS on roughened (r-) pPFDAc and pHEA hybrid layers upon blue LED illumination (λ = 405 nm), the measured maximum H_2O_2-equivalent radical concentrations as a function of the pPFDAc content of the polymer matrix **A** [214] and characterization of EtOH (g) (c_0=0.36 mM) decomposition on Ag-TiO_2/polyarcrylate hybrid

layers under LED light illumination (λ = 405 nm) as the function of illumination time (the legends refer to the composition of the polymer matrix) [211]

Figure 7. Determination of the specific surface charge values for TiO_2 **A**, for *E. coli* bacteria **B** and the amount of the adhered TiO_2 on the surface of *E. coli* at the electrostatic charge compensation point **C**. In all cases the pH was 4.5 and the standard error is 2.0%. [235]

Figure 8. Schematic of a double emulsion device made via printing from two different materials with individual wettability. By manufacturing a surface pattern that is hydrophobic–hydrophilic–hydrophobic, O/W/O double emulsions can be formed inside the planar microchannels. In the lower row, a bright-field microscopy image of both junctions is shown. The hydrophobic material is colored in light-yellow and the hydrophilic material in reddish. The successful formation of double emulsions is followed inside the tubing of the outflow port (bottom right: Bright-field microscopy image of two double emulsion droplets). The scale bar denotes 300 μm. [284]

Figure 9. Working principle of the switching of the pH-responsive superwetting surface properties is shown, where a CA of water droplet decreased to ∼0° at pH 1 and increased to 161.4° ± 6.2° at pH 13. **A** Wetting states of droplets with different concentrations of glucose within the linear range. **B** Corresponding to hydrophobicity, and those from patients with diabetes decreased to nearly 50°, indicating the hydrophilicity of the surface. **C** Non-invasive detection of saliva and urine obtained from nine patients with diabetes and six normal people illustrating that the CA can be employed to distinguish between samples of people with diabetes and normal people. **D** [301]

Figure 10. Schematic illustration of the fabrication process of bioinspired surfaces with star-shaped wettability patterns. **a)** Superhydrophilic surface composed of TiO_2 nanoparticles, where fog droplets spread (the bottom). **b)** Superhydrophobic surface modified with FAS showing non-wetting property to fog droplets (the bottom). **c)** Bioinspired gradient surface with a star-shaped wettability pattern. It is realized by illuminating the FAS-modified film under UV light with a photomask. The fog droplets would be collected directionally toward the star-shape region, which is more wettable (the bottom). [317]

Figures

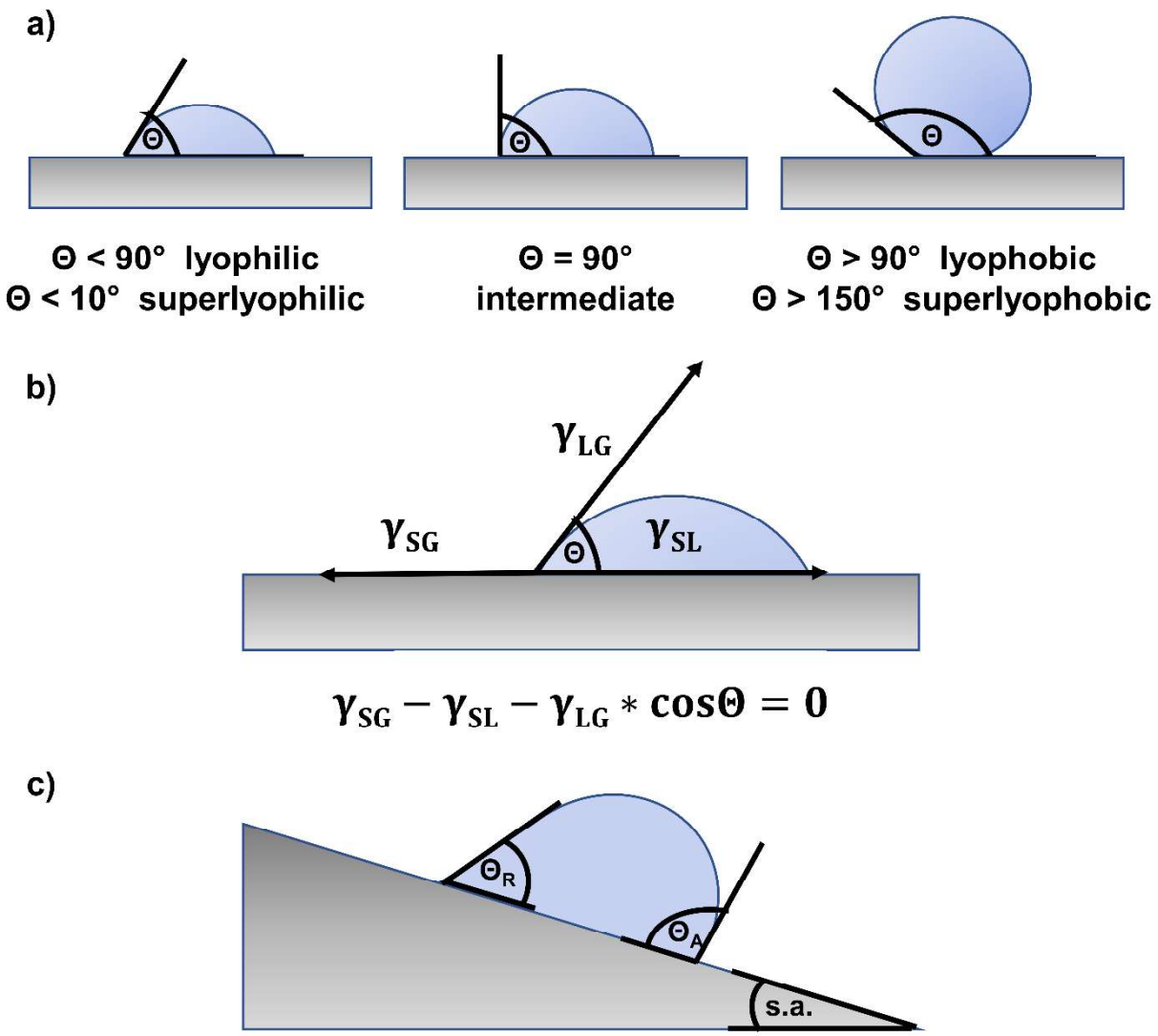

Figure 1.

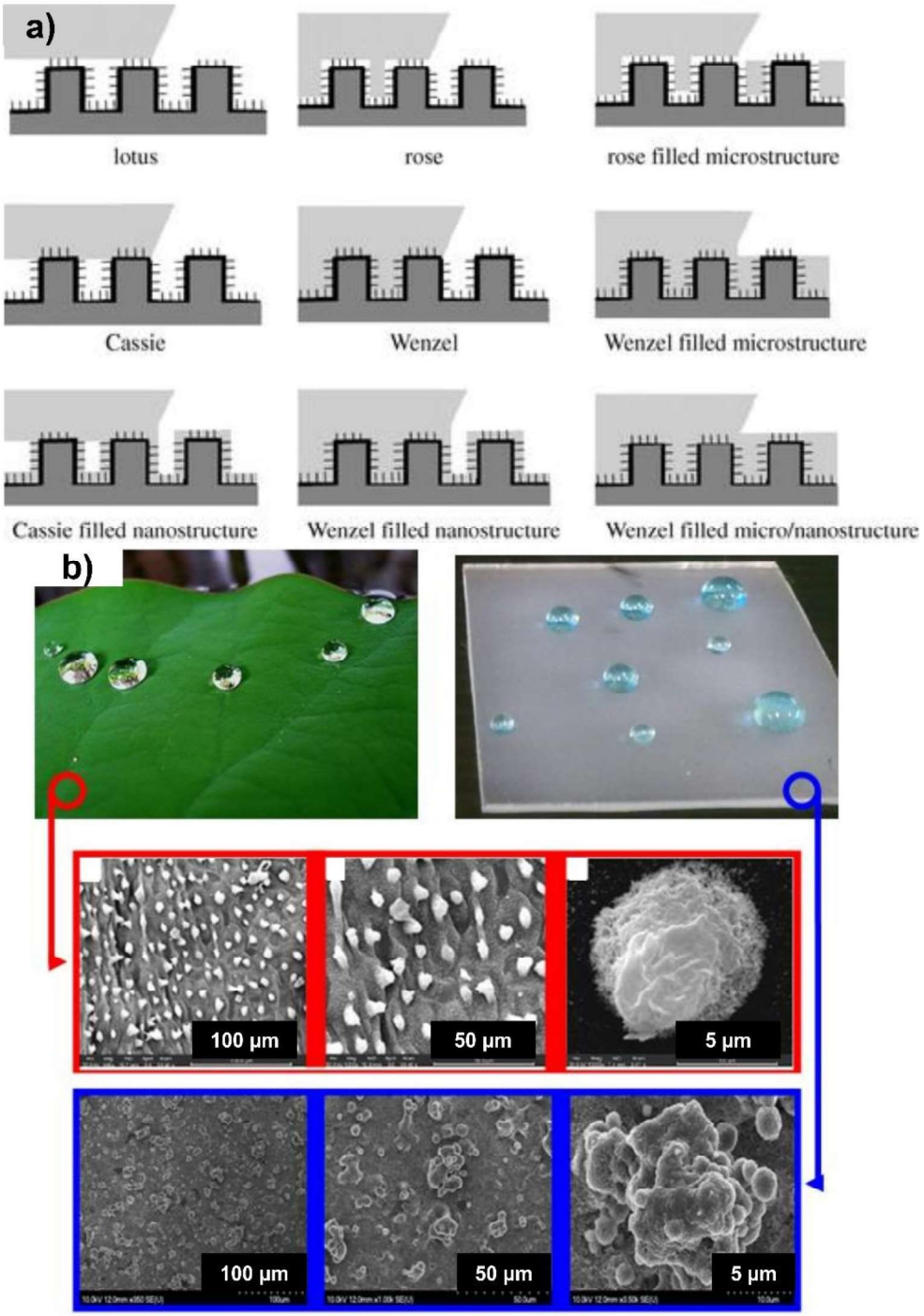
a)
lotus
rose
rose filled microstructure
Cassie
Wenzel
Wenzel filled microstructure
Cassie filled nanostructure
Wenzel filled nanostructure
Wenzel filled micro/nanostructure
b)
100 µm
50 µm
5 µm
100 µm
50 µm
5 µm

Figure 2.

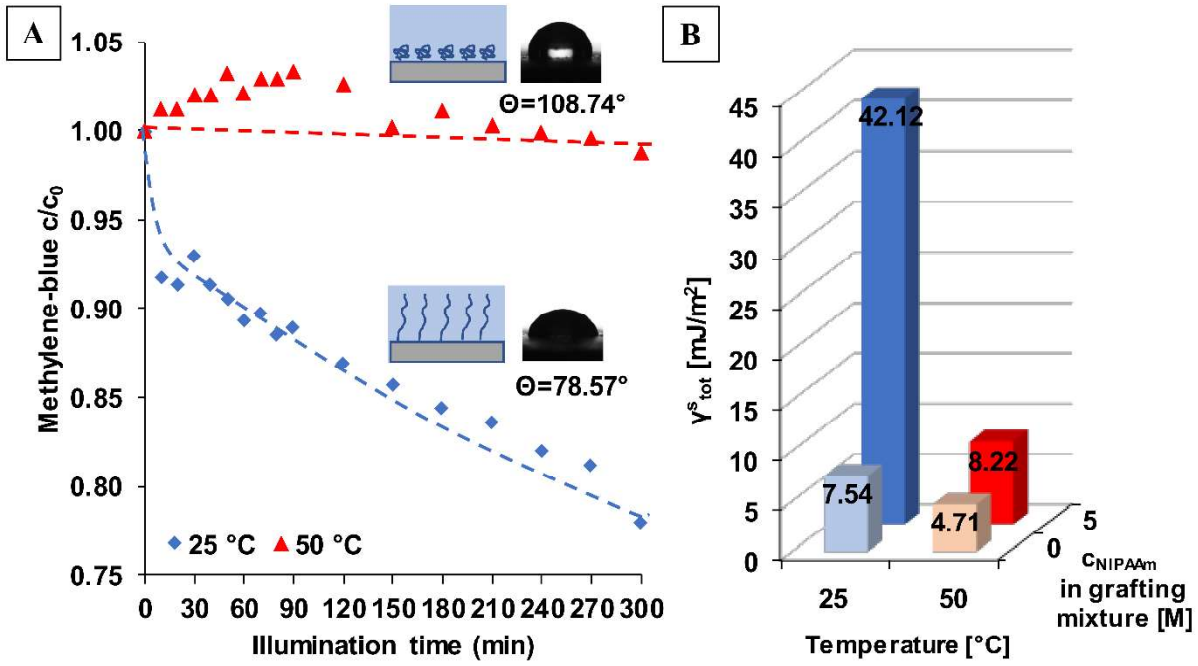
A
1.05
1.00
0.95
0.90
0.85
0.80
0.75
Methylene-blue c/c0
Θ=108.74°
Θ=78.57°
25 °C
50 °C
0 30 60 90 120 150 180 210 240 270 300
Illumination time (min)
B
45
40
35
30
25
20
15
10
5
0
γs tot [mJ/m2]
42.12
7.54
8.22
4.71
25
50
Temperature [°C]
0
5
cNIPAAm in grafting mixture [M]

Figure 3.

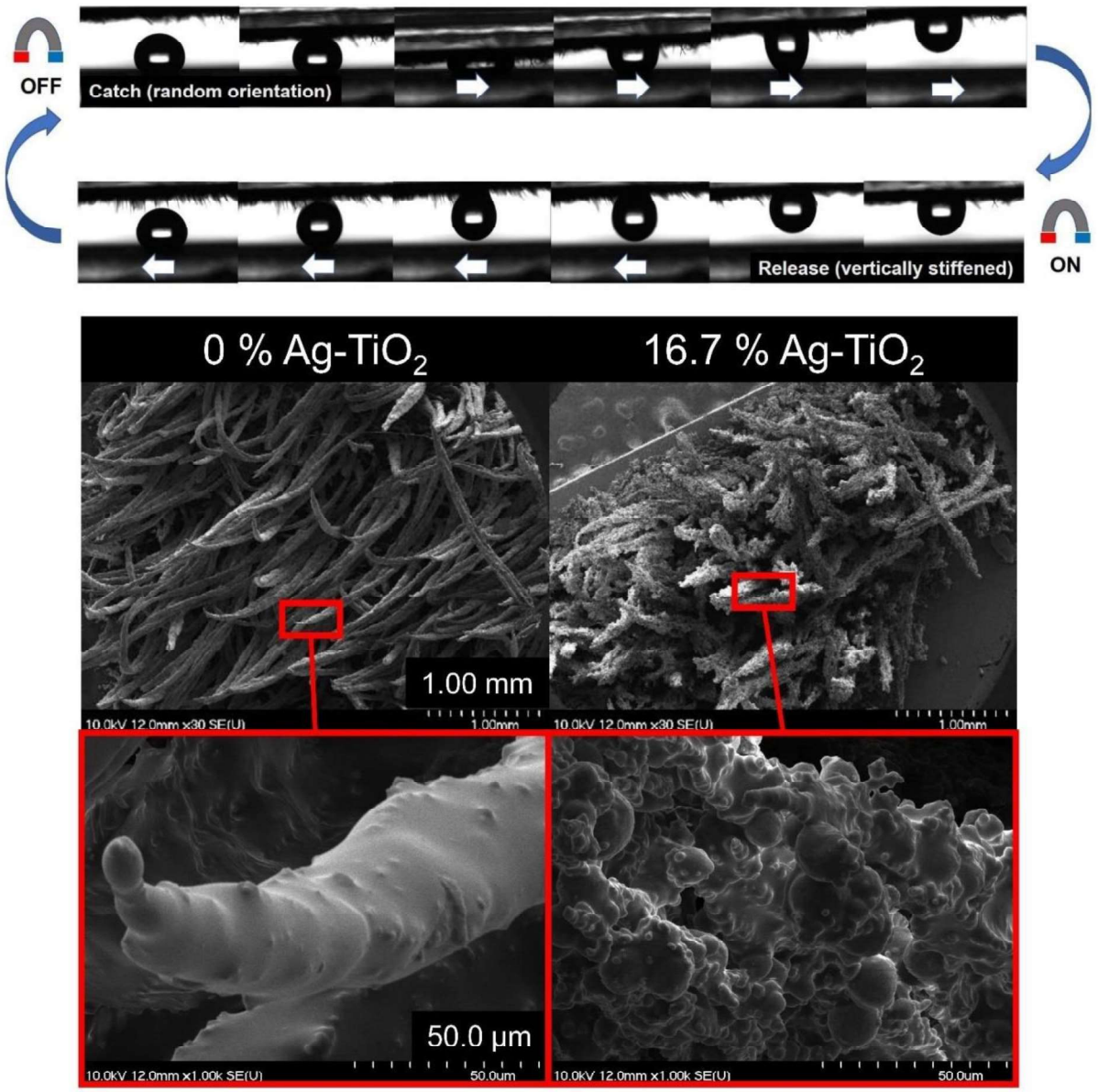
OFF
Catch (random orientation)
Release (vertically stiffened)
ON
0 % Ag-TiO2
16.7 % Ag-TiO2
1.00 mm
10.0kV 12.0mm x30 SE(U)
1.00mm
50.0 µm
10.0kV 12.0mm x1.00k SE(U)
50.0um

Figure 4.

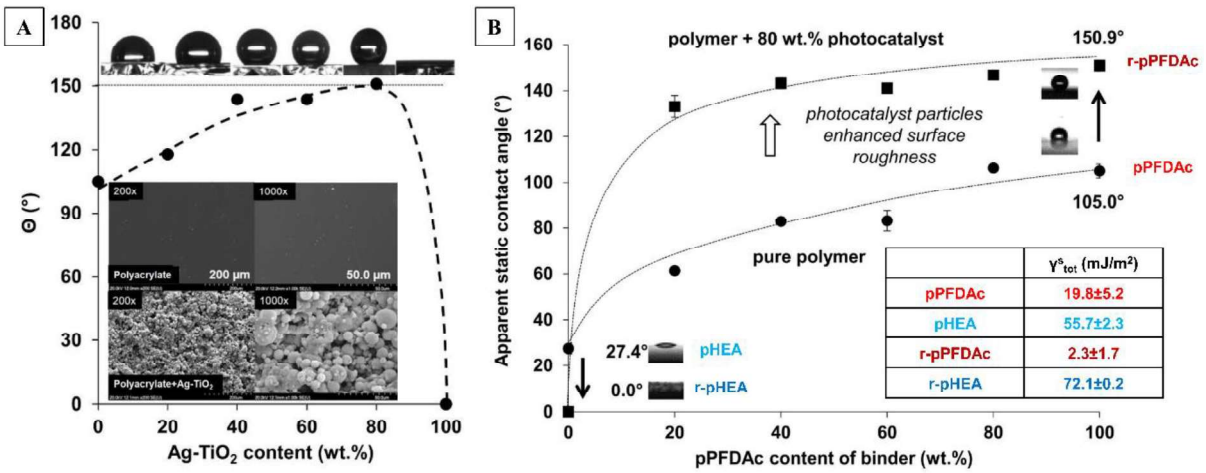

Figure 5.

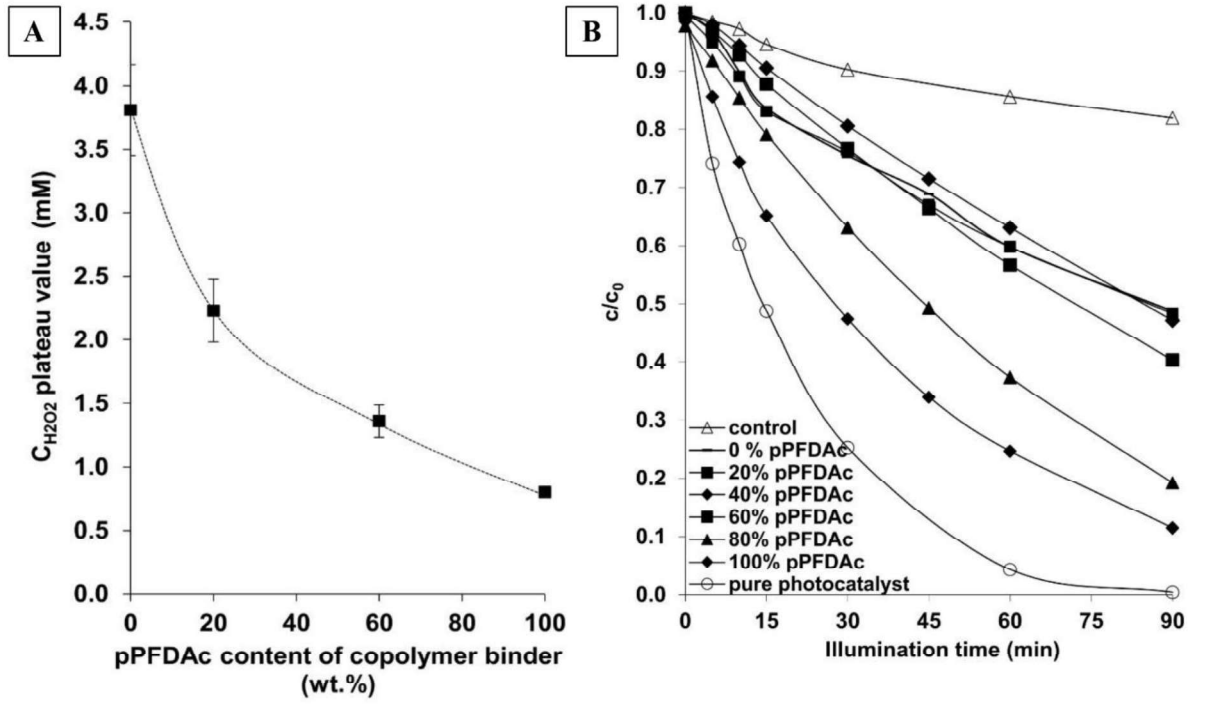

Figure 6.

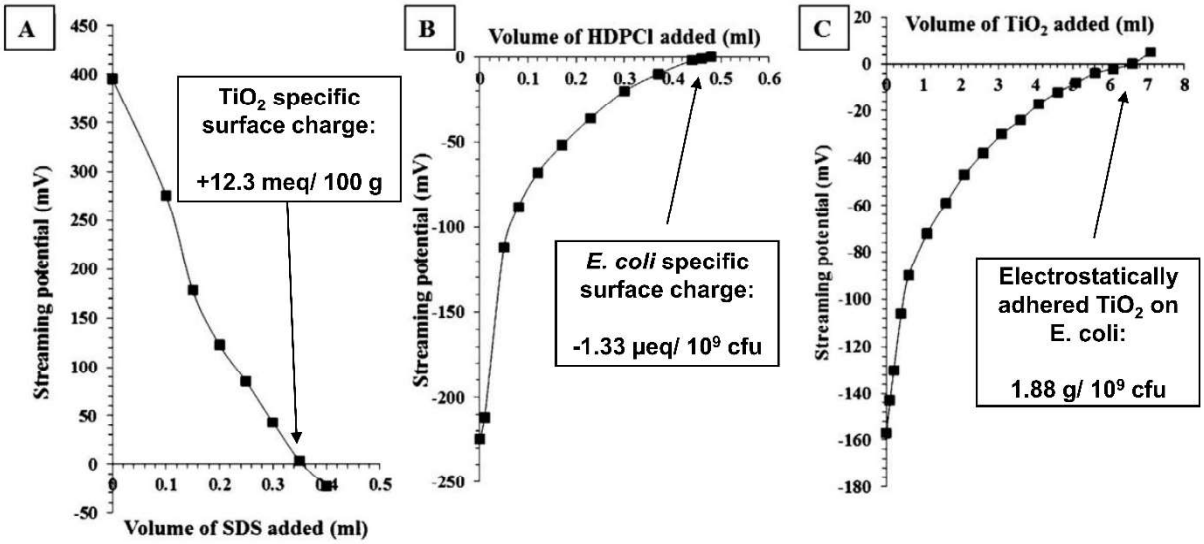

Figure 7.

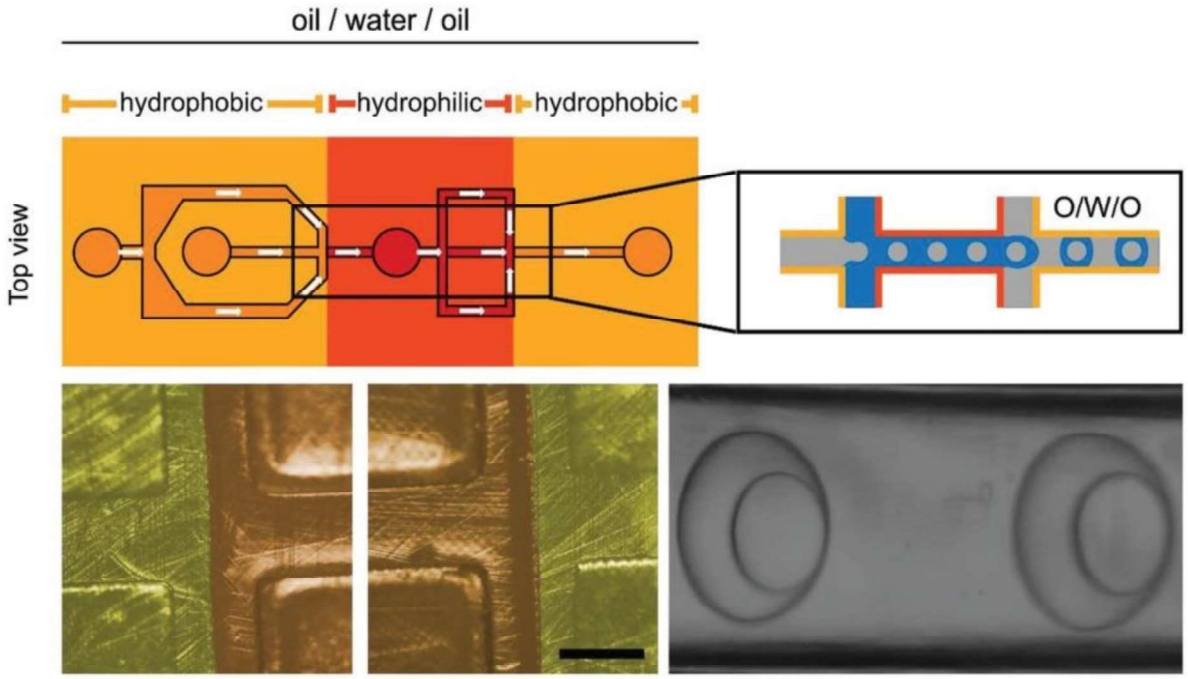

Figure 8.

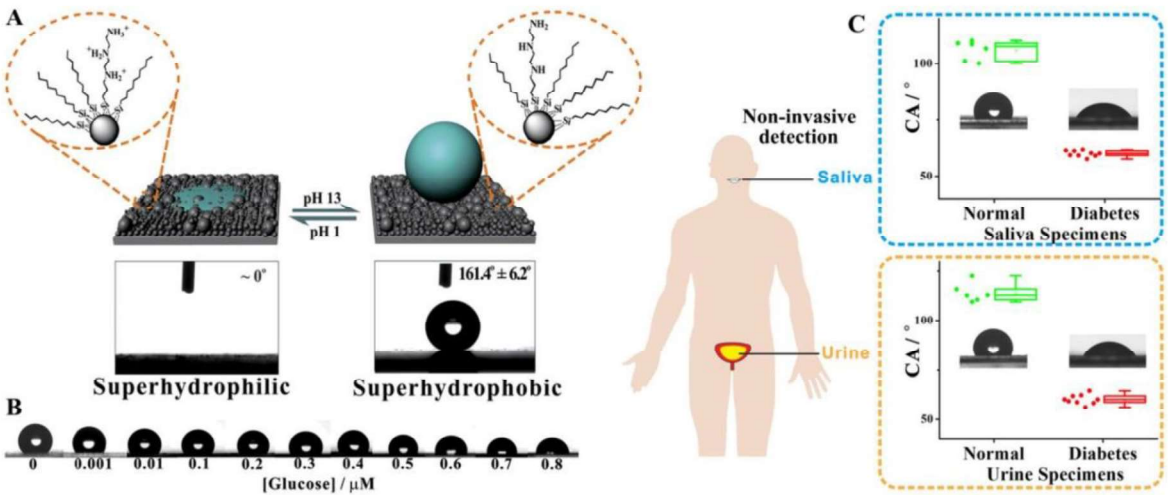

Figure 9.

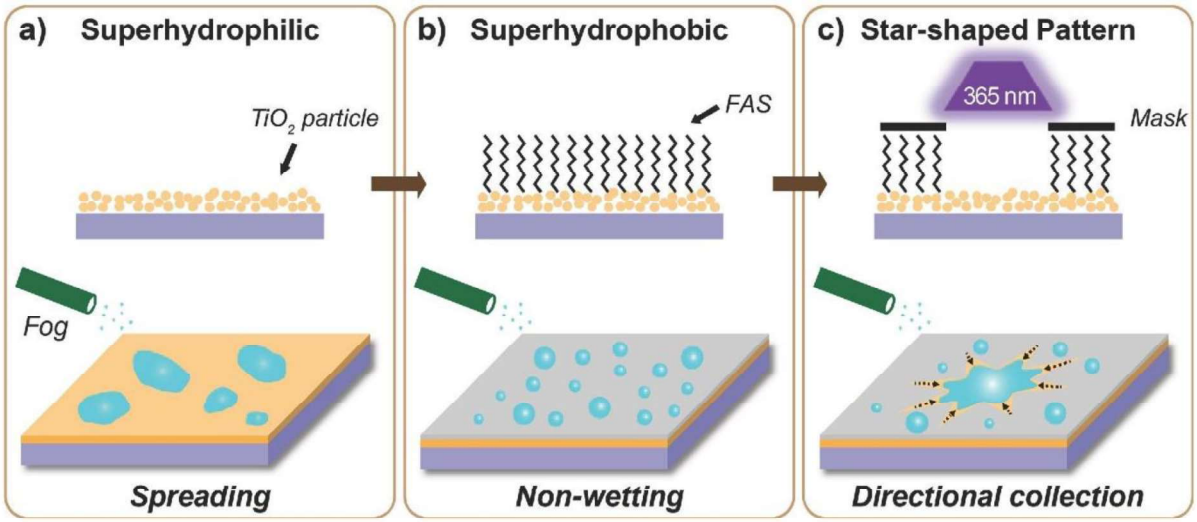

Figure 9.

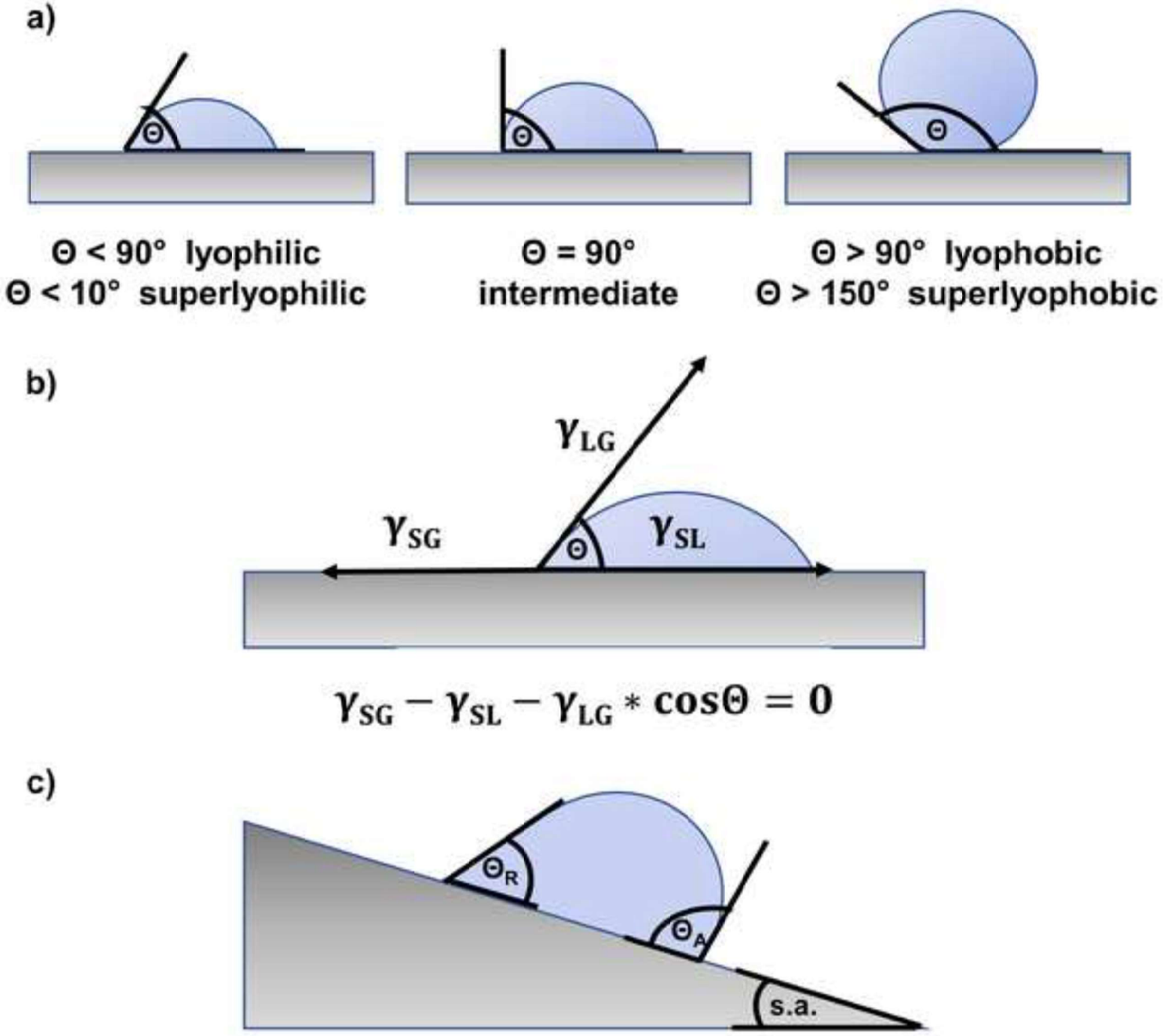

Figure 2

Click here to access/download;Figure;Fig 2_v3.tif

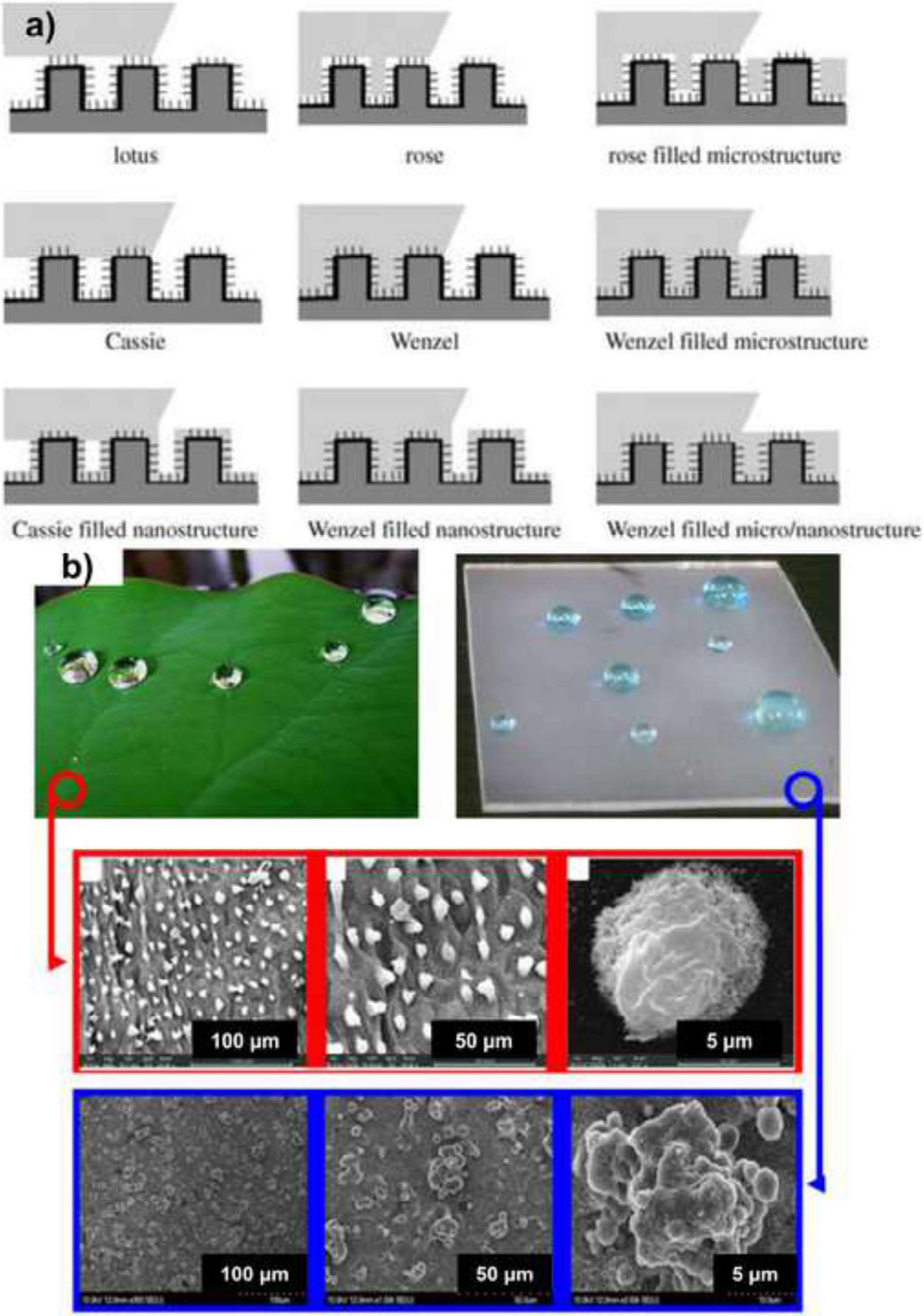

Figure 3

Click here to access/download;Figure;Fig 3.tif

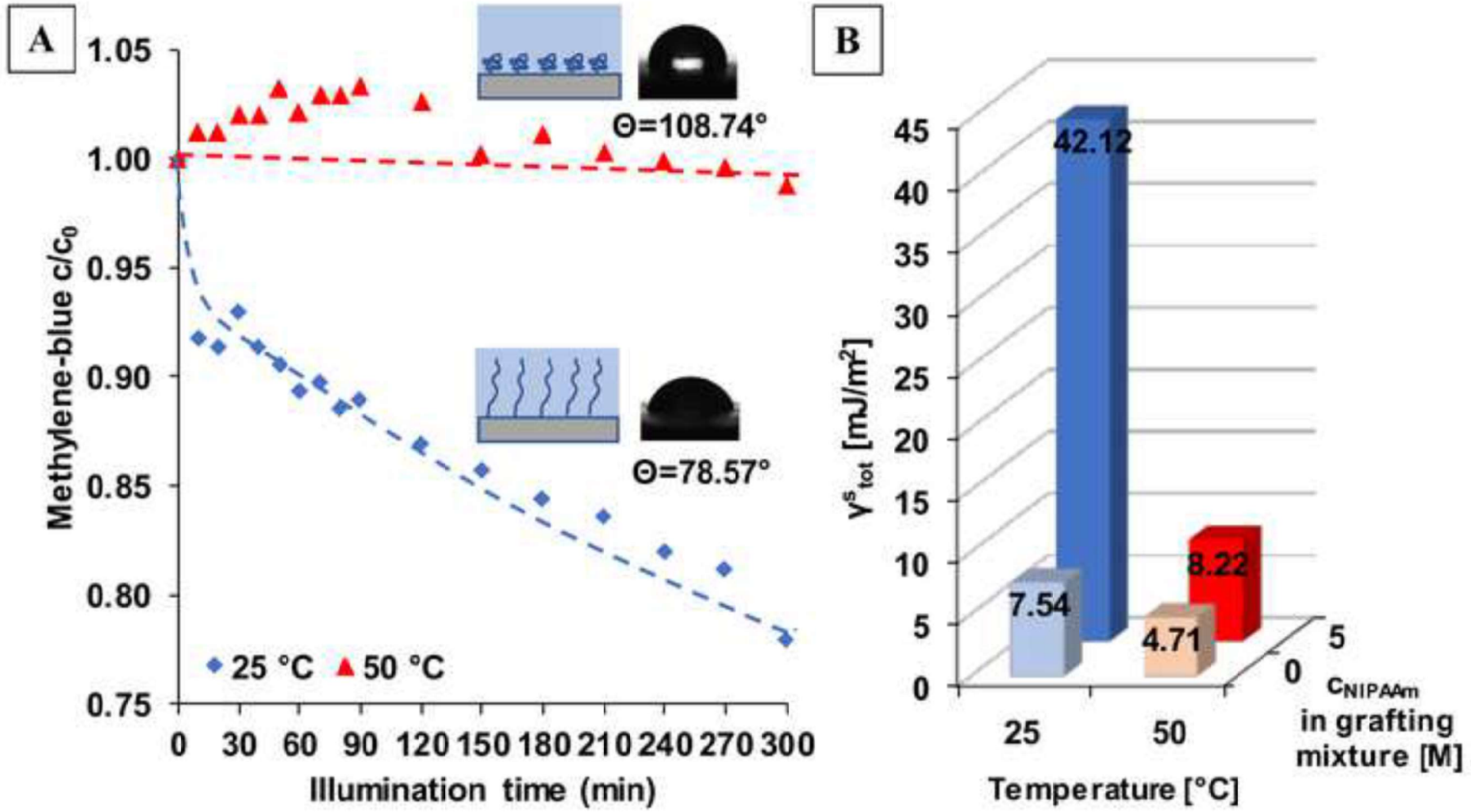

Figure 4

Click here to access/download;Figure;Fig 4.tif

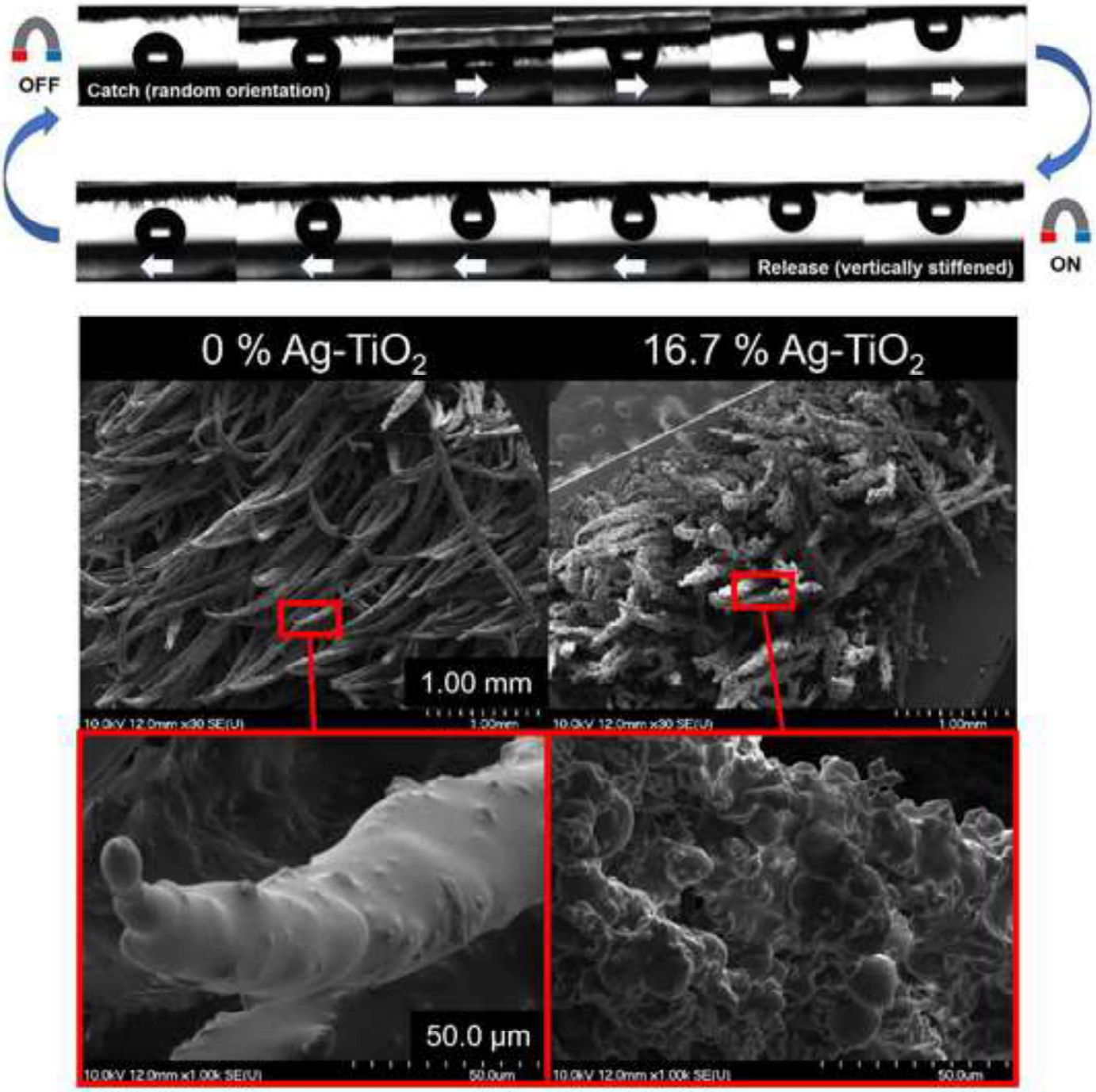

Figure 5

Click here to access/download;Figure;Fig 5_v2.tif

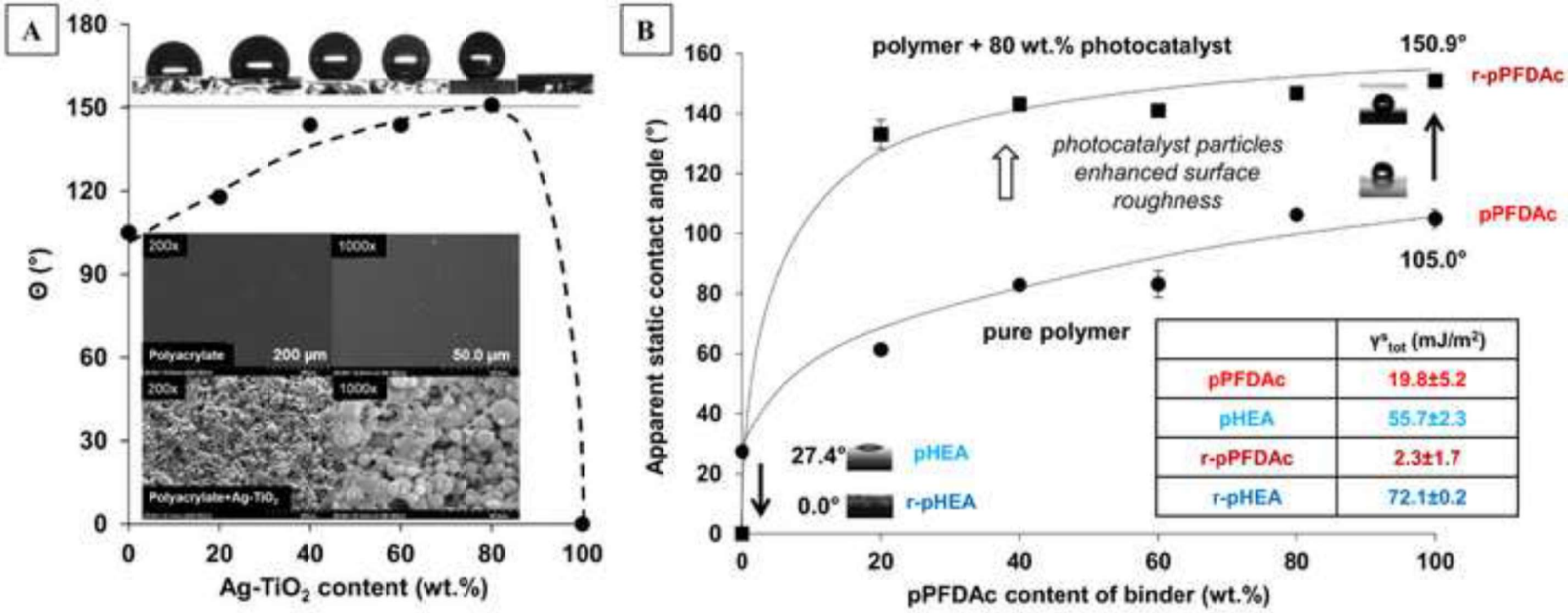

Figure 6

Click here to access/download;Figure;Fig 6.tif

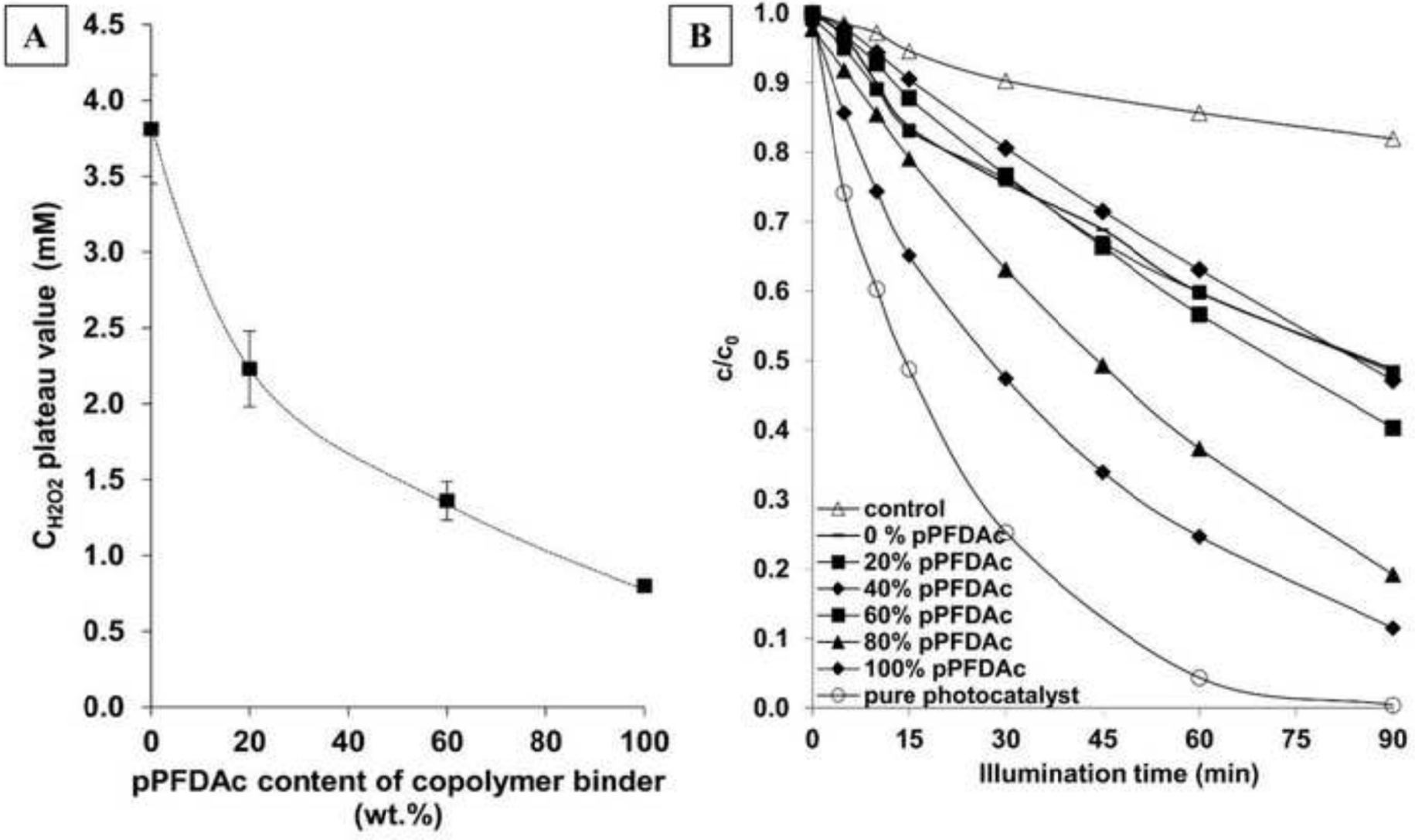

Figure 7

Click here to access/download;Figure;Fig 7_v2.tif

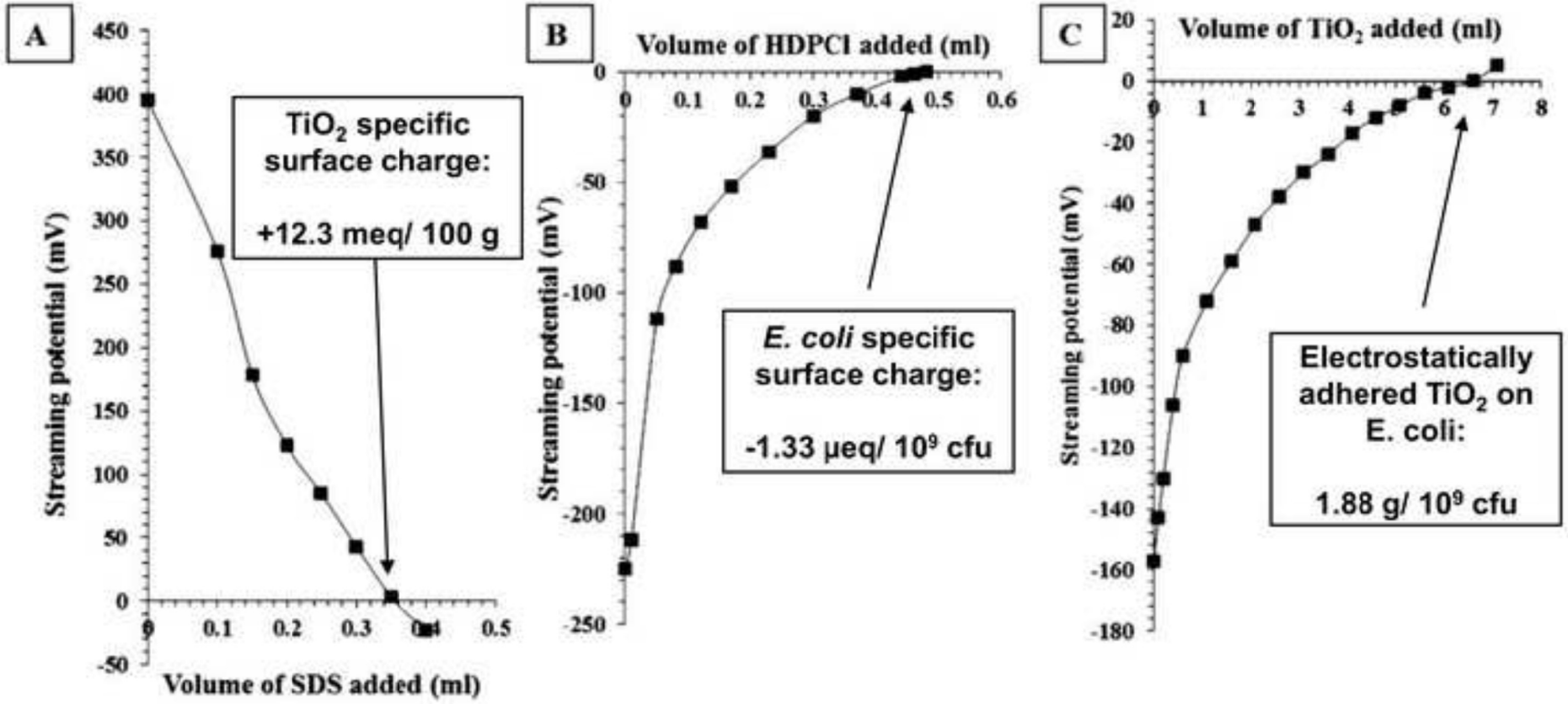

Figure 8

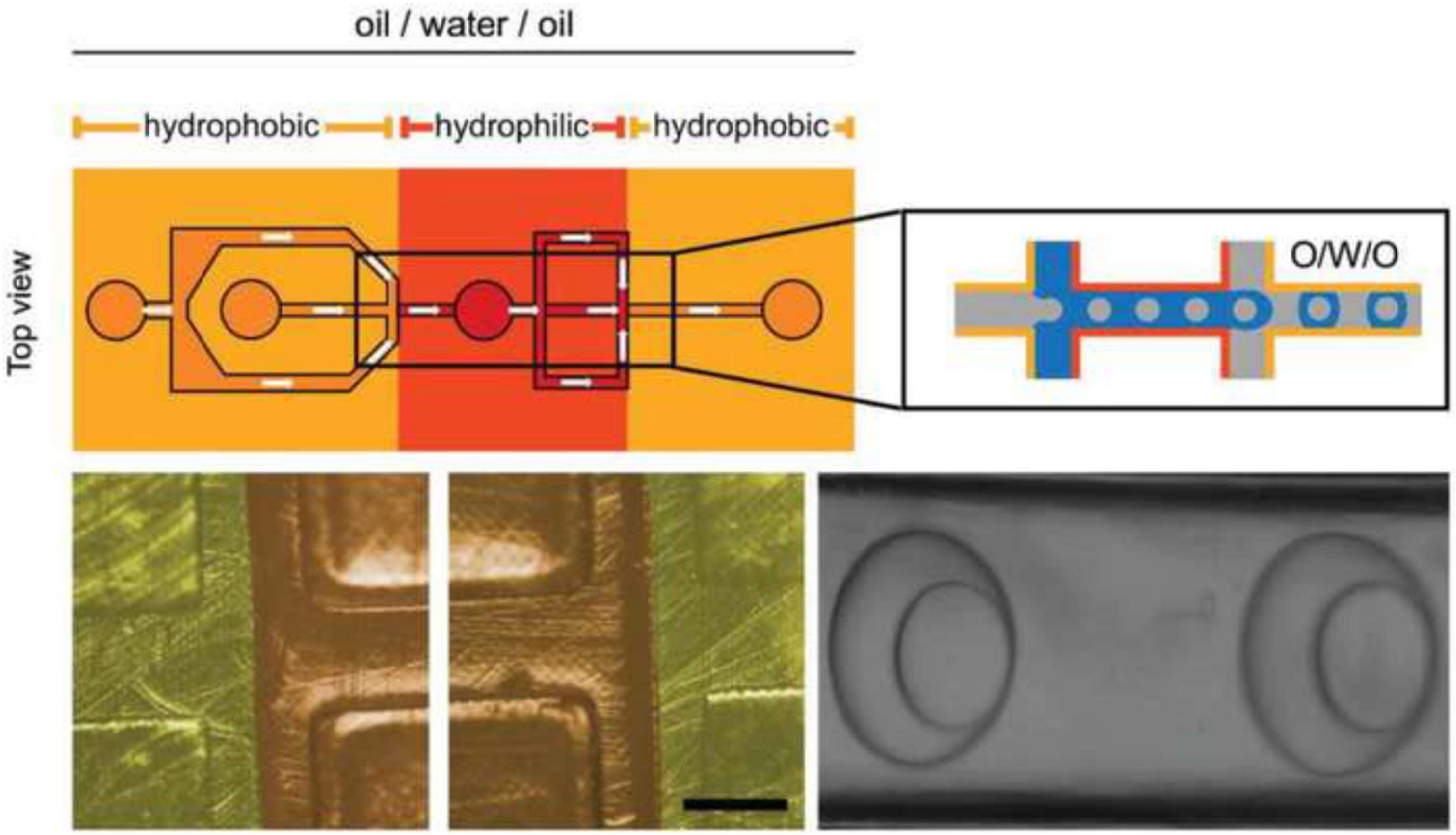

Figure 9

Click here to access/download;Figure;Fig 9.tif

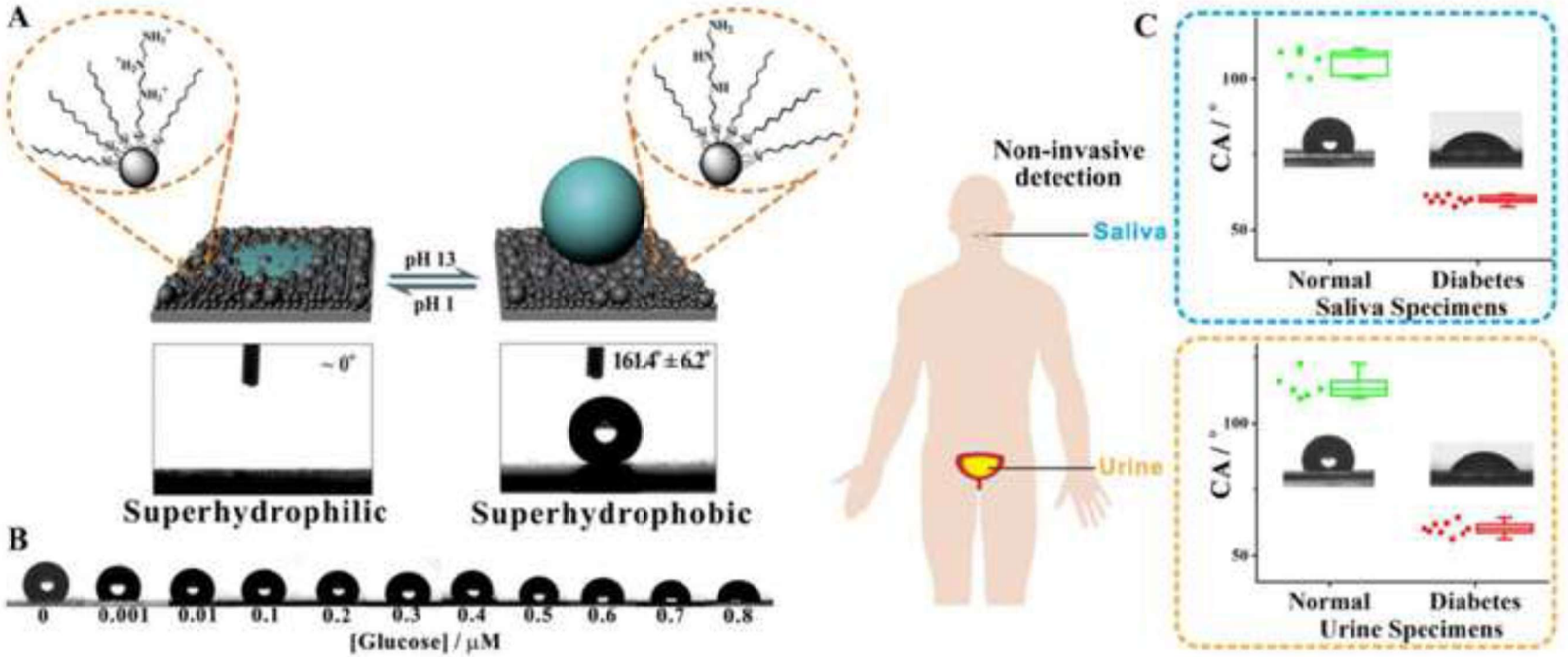

Figure 10

Click here to access/download;Figure;Fig 10.tif